The sushi domains and their role in $GABA_B$ receptor compartmentalization

Inauguraldissertation

Zur Erlangung der Würde eines Doktors der Philosophie
vorgelegt der
Philosophisch-Naturwissenschaftlichen Fakultät
der Universität Basel

von

Barbara Biermann
aus Münster (Deutschland)

Institut für Physiologie / Pharmazentrum, Universität Basel

Basel, 2010

UNI
BASEL

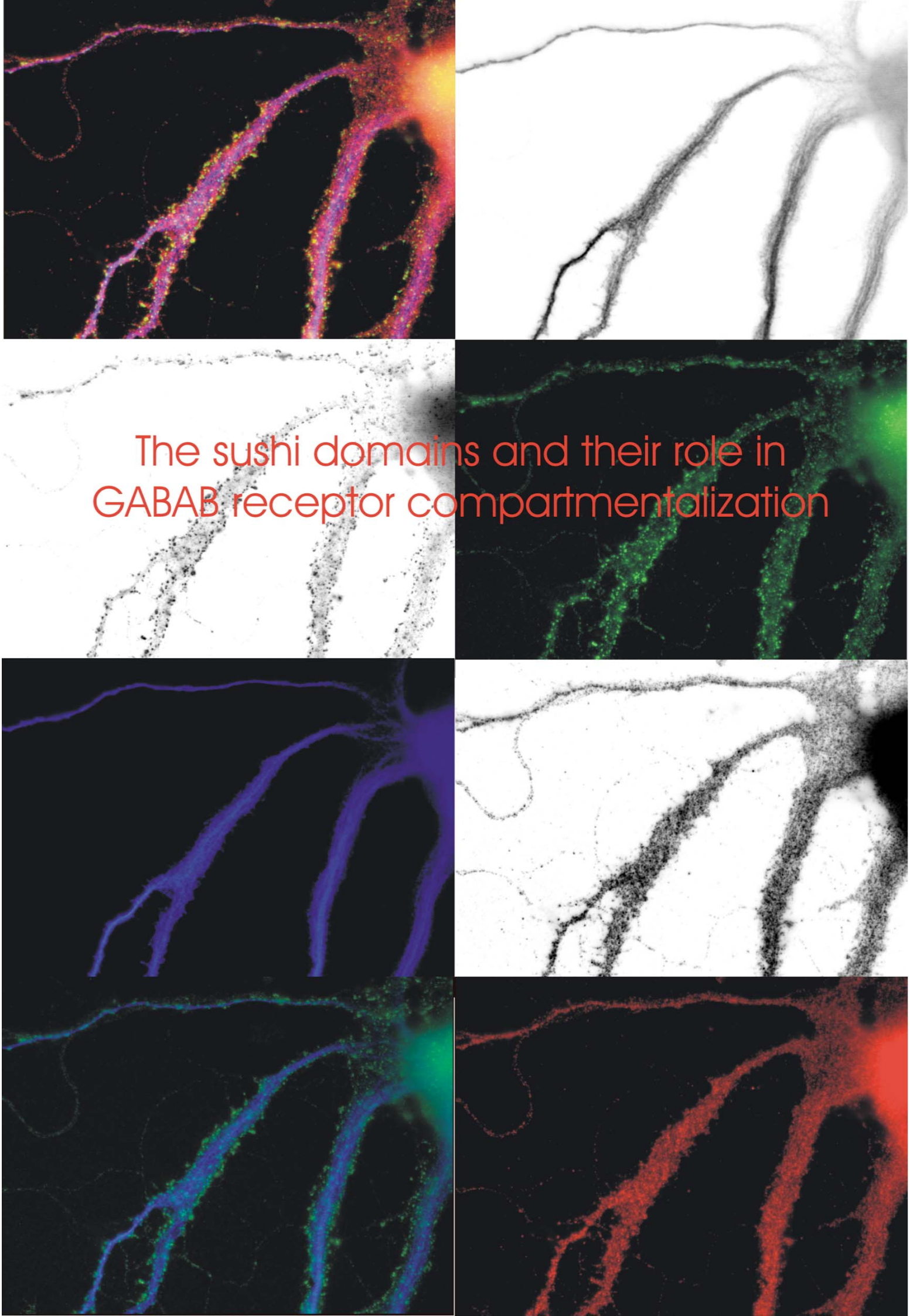

The sushi domains and their role in GABAB receptor compartmentalization

Genehmigt von der Philosophisch-Naturwissenschaftlichen Fakultät auf Antrag von

Prof. Dr. Bernhard Bettler

(Dissertationsleitung)

Prof. Dr. Markus A. Rüegg

(Fakultätsverantwortlicher)

Prof. Dr. Thomas G. Oertner

(Korreferat)

Basel, den 27. November 2007

Prof. Dr. Hans-Peter Hauri

(Dekan)

“Adieu, dit le renard. Voici mon secret. Il est très simple: on ne voit bien qu’avec le coeur. L’essentiel est invisible pour les yeux!”

Antoine de Saint-Exupéry (1900-1944)

In tiefer Liebe und Dankbarkeit meinen Eltern, dass sie Mich die Bedeutung dieser Zeilen lehrten und meinen Brüder für ihre stete Hilfe auch in schwierigen Zeiten diese Zeilen nicht zu vergessen.

Table of contents

Explanation of the cover image

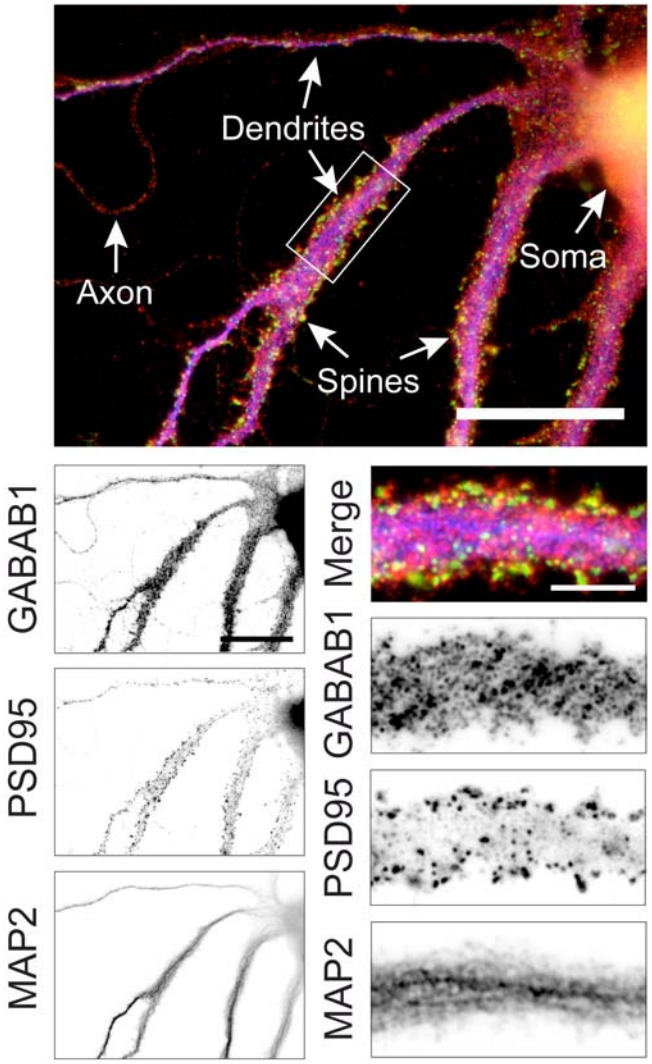

$GABA_{B1}$ protein in cultured hippocampal neurons

Low-density cultured hippocampal neurons from WT mouse embryos were fixed at DIV23, permeabilized and triple-stained with a C-terminal antibody against $GABA_{B1}$ (red), the dendritic marker MAP2 (blue) and the postsynaptic density protein PSD95 (green). The upper panel shows merged pictures from a triple staining (scale bar 25 µm). The lower panels on the left represent separately the inverted images from the picture above (scale bar 25 µm). The panels on the right show a dendritic section (scale bar 5 µm). $GABA_{B1}$ punctae are rarely co-localizing with PSD95, indicating that most dendritic $GABA_{B1}$ protein is present at extrasynaptic sites. A weak punctuate $GABA_{B1}$ labeling is further visible in the axon (MAP2 negative; for more details about materials and methods see chapter 3).

List of publications

During my PhD, I contributed to the following publications:

Paper 1

Vigot R, Barbieri S, Brauner-Osborne H, Turecek R, Shigemoto R, Zhang YP, Lujan R, Jacobson LH, Biermann B, Fritschy JM, Vacher CM, Muller M, Sansig G, Guetg N, Cryan JF, Kaupmann K, Gassmann M, Oertner TG, Bettler B

Differential compartmentalization and distinct functions of $GABA_B$ receptor variants

Neuron. 2006 May 18;50(4):589-601.

Paper 2

Biermann B, Bradaia A, Ivankova-Susankova K, Besseyrias V, Abdel Aziz S, Kapfhammer JP, Gassmann M, Bettler B

The N-terminal sushi domains of $GABA_B$ receptors function as a dominant axonal targeting signal

In preparation.

Paper 3

Tiao JY, Bradaia A, Biermann B (co-first author), Kaupmann K, Pless E, Barlow PN, Gassmann M, Bettler B

The sushi domains of secreted $GABA_{B1}$ isoforms selectively impair $GABA_B$ heteroreceptors

In preparation.

Paper 4

Gassmann M, Haller C, Stoll Y, Abdel Aziz S, Biermann B, Mosbacher J, Kaupmann K, Bettler B

The RXR-type endoplasmic reticulum-retention/retrieval signal of $GABA_{B1}$ requires distant spacing from the membrane to function

Mol Pharmacol. 2005 Jul; 68(1):137-44. Epub 2005 Apr 1.

Paper 5

Bradaia A, Jensen A, Haller C, Abdel Aziz S, Biermann B, Barbieri S, Kaupmann K, Brenner HR and Bettler B

A molecular switch regulates tonic $GABA_B$ receptor activity

In preparation.

List of abbreviations

aa	amino acids
ACSF	artificial cerebrospinal fluid
A:D ratio	axon-to-dendrite ratio
C-	carboxyl-
DIV	days in vitro
DTT	dithiothreitol
ECM	extracellular matrix
EPSC	excitatory postsynaptic current
ER	endoplasmatic reticulum
GABA	γ-aminobutyric acid
GPCR	G protein-coupled receptor
LL-motif	dileucine motif
mEPSC	miniature excitatory postsynaptic current
mGluR	metabotropic glutamate receptor
mIPSC	miniature inhibitory postsynaptic current
n	number
N-	amino-
NgCAM	neuron-glia cell adhesion molecule
RFP	red fluorescent protein
RSDP	recombinant sushi-domain protein
SD	sushi domain
SEM	standard error of the mean
SP	signal peptide
TGN	trans-Golgi network
VAMP2	vesicle-associated membrane protein 2
WT	wild-type

Summary

$GABA_B$ receptors are G protein-coupled receptors for γ-aminobutyric acid (GABA), the main inhibitory neurotransmitter in the CNS. As such they mediate the late phase of GABAergic inhibitory neurotransmission and are promising drug targets for neurological and mental health disorders. Molecular diversity in the $GABA_B$ system arises from the $GABA_{B1a}$ and $GABA_{B1b}$ subunit isoforms, both of which assemble with the $GABA_{B2}$ subunit to form functional heteromeric receptors. Structurally, $GABA_{B1a}$ differs from $GABA_{B1b}$ by a pair of evolutionary conserved protein interaction motifs, the sushi domains (SDs). It is now generally accepted that two $GABA_B$ receptor subtypes, $GABA_{B(1a,2)}$ and $GABA_{B(1b,2)}$, are co-expressed in most if not all neurons. Drug development in the $GABA_B$ field has been hampered by the fact that receptor subtypes have indistinguishable pharmacological properties. Thus, any progress in the understanding of a differential distribution or functional regulation of receptor subtypes harbors high potential for therapeutic interference.

Using genetically modified mice we were the first to demonstrate that the two $GABA_B$ receptor subtypes engage in non-redundant functions owing to their differing pre- versus postsynaptic localization. Most strikingly, it was observed that selectively $GABA_{B1a}$ assembles heteroreceptors controlling glutamate release, while predominantly $GABA_{B1b}$ mediates postsynaptic inhibition. To further unravel the molecular mechanism underlying $GABA_B$ receptor compartmentalization I aimed at identifying sequence determinants accounting for the selective occurrence of $GABA_{B(1a,2)}$ receptors at glutamatergic terminals. I analyzed the axonal versus dendritic distribution of diverse epitope-tagged expression constructs of individual $GABA_B$ receptor subunits in cultured hippocampal neurons. Thereby, I demonstrate that the $GABA_{B1a}$-specific SDs engage in axonal targeting. Disruption of disulfide bond formation in the SDs abolishes $GABA_{B1a}$ axonal localization indicating that proper folding of the SDs is important for specific interaction with axon targeting proteins. Furthermore, the SDs are able to redirect a typical somatodendritic receptor to axons, thus dominating over dendritic targeting information. In addition, I provide evidence that somatodendritic targeting of $GABA_B$ receptors is mediated by sequences in the cytoplasmic C-terminal domain of the $GABA_{B2}$ subunit. Thus a combination of distinct signals compartmentalizes $GABA_B$ receptors to pre- and

postsynaptic sites. Last, I demonstrate that exogenous application of a soluble recombinant SD protein to cultured hippocampal neurons completely abolishes heteroreceptor function. A likely mechanism involves scavenging of auxiliary cell surface proteins that normally bind to the SDs. This indicates that the SDs in $GABA_{B1a}$ not only mediate axonal targeting but further engage in a specific protein interaction at the cell surface, which is subject to modulation thereby regulating heteroreceptor function.

It thus appears that the SDs interact with (diverse) intracellular and extracellular proteins important for the localization and proper function of $GABA_{B(1a,2)}$ receptors at glutamatergic terminals. This finding further provides a first potential tool for a selective therapeutic interference within the $GABA_B$ field.

Outline of the thesis

Chapter I: Introduction

This chapter briefly introduces the field of $GABA_B$ receptors and provides a short overview about axonal versus dendritic protein segregation in polarized neurons. It further explains the topic of this doctoral thesis.

Chapter II: Differential compartmentalization and distinct functions of $GABA_B$ receptor variants

By morphological and electrophysiological analysis of genetically modified mice we initially demonstrated that $GABA_{B1}$ subunit isoforms localize to distinct synaptic sites and convey non-redundant functions.

Chapter III: The N-terminal sushi domains of $GABA_B$ receptors function as a dominant axonal targeting signal

In this second experimental approach, we address the role of the $GABA_{B1a}$-specific SDs in the axonal targeting of $GABA_{B(1a,2)}$ receptors in glutamatergic neurons.

Chapter IV: The sushi domains of secreted $GABA_{B1}$ isoforms selectively impair $GABA_B$ heteroreceptors

This study identifies $GABA_{B1j}$, a soluble $GABA_{B1}$ subunit isoform encoding the two SDs. Soluble recombinant SD protein (RSDP) mimicking $GABA_{B1j}$, impaired $GABA_B$ heteroreceptor function, while leaving auto- and postsynaptic receptors unaffected. This provides a first tool for a selective interference with the $GABA_B$ receptor system.

Chapter V: Discussion and Perspectives

This last chapter summarizes the main findings described in chapter 2, 3 and 4 and discusses them with respect to the current understanding of $GABA_B$ receptor signalling.

Chapter I

INTRODUCTION

$GABA_B$ receptors

GABA is the main inhibitory neurotransmitter in the mammalian brain and modulates neuronal excitability by activating ionotropic $GABA_{A/C}$ receptors as well as metabotropic $GABA_B$ receptors. $GABA_B$ receptors were first identified based on their distinct pharmacological profile compared to ionotropic $GABA_{A/C}$ receptors (Hill & Bowery, 1981) and only subsequently were shown to function as G protein-coupled receptors (Hill, 1985). As such $GABA_B$ receptors mediate the late phase of GABAergic inhibitory neurotransmission in the CNS and are promising drug targets for neurological and mental health disorders like epilepsy, pain, spasticity, addiction, schizophrenia, depression and anxiety (Enna & Bowery, 2004; Bettler et al., 2004; Cryan & Kaupmann, 2005; Bowery, 2006).

Pre- versus postsynaptic localization and physiological function

$GABA_B$ receptors are expressed on pre- and, more abundantly, on postsynaptic elements of GABAergic and glutamatergic neurons (Kaupmann et al., 1998; Kulik et al., 2002; Lopez-Bendito et al., 2002; Kulik et al., 2003; Koyrakh et al., 2005). Presynaptic $GABA_B$ receptors are mainly detected in the extrasynaptic membrane and occasionally over presynaptic membrane specializations, while postsynaptic $GABA_B$ receptors are predominantly distributed to dendritic shafts and the extrasynaptic plasma membrane of spines (Drake et al., 1997; Kulik et al., 2003). Activation of presynaptic $GABA_B$ receptors located on GABAergic terminals (autoreceptors) or other nerve terminals (heteroreceptors) suppresses neurotransmitter release by inhibiting voltage-sensitive Ca^{2+} channels (Mintz & Bean, 1993; Thompson et al., 1993; Poncer et al., 1997) and modulating synaptic vesicle priming (Sakaba & Neher, 2003). Stimulation of postsynaptic $GABA_B$ receptors produces a prolonged neuronal hyperpolarization through activation of inwardly rectifying Kir3-type K^+ channels, which induce a slow inhibitory postsynaptic current (sIPSC) (Lüscher et al., 1997). Both pre- and postsynaptic effector channels are regulated by the βγ-subunit of the activated G-protein (Bowery et al., 2002; Calver et al., 2002; Bettler et al., 2004), while the $G_{\alpha i/o}$-subunit inhibits adenylate cyclase (Hill, 1985) with putative effects on transcription factors (Steiger et al., 2004) and kinases (Diverse-Pierluissi et al., 1997; Couve et al., 2002;

Ren & Mody et al., 2003). $GABA_B$ receptors further modulate synaptic plasticity (Davies et al., 1991; Patenaude et al., 2003; Huang et al., 2005), heterosynaptic depression (Vogt & Nicoll, 1999), population burst firing and inhibit backpropagating action potentials (Zilberter et al., 1999; Leung & Peloquin, 2006).

Heteromer formation

Biochemical and pharmacological studies in various *in vivo* preparations initially suggested the existence of a multitude of $GABA_B$ receptor subtypes with specific subcellular distribution and effector systems, analogous to the metabotropic glutamate receptors (Kerr & Ong, 1995; Conn & Pin, 1997). Molecular cloning, however, has only identified two genes encoding for $GABA_B$ receptors, namely *GABA$_{B1}$* and *GABA$_{B2}$* (Kaupmann et al., 1997, 1998; Bettler et al., 2004), disproving the predicted diversity of native $GABA_B$ receptors based on pharmacological studies. The present dogma stipulates that functional $GABA_B$ receptors are heteromers assembled from $GABA_{B1}$ and $GABA_{B2}$ subunits (Kaupmann et al., 1998; Marshall et al., 1999; Mohler & Fritschy, 1999; Bettler et al., 2004). The two subunits are functionally unique in that $GABA_{B1}$ binds GABA with high affinity, whereas $GABA_{B2}$ mediates coupling to G proteins (Pin et al., 2004).

Surface trafficking

The C-terminal domain of the $GABA_{B1}$ subunit harbours an arginine-based ER retention/retrieval signal, RSRR, which retains unassembled $GABA_{B1}$ subunits in the ER and restricts surface expression only to correctly assembled heteromeric receptors (Couve et al., 1998; Margeta-Mitrovic et al., 2000; Pagano et al., 2001). Presumably, the $GABA_{B2}$ subunit triggers forward trafficking by masking the RSRR motif. Monomeric $GABA_{B1}$ subunits that escape from the ER to the cis-Golgi compartment bind to COPI via the RSRR signal and are probably transported back to the ER via COPI - coated vesicles (Brock et al., 2005). Scaffolding proteins of the 14-3-3 family compete with COPI for RSRR binding, however, their function remains elusive (Couve et al., 2001; Brock et al., 2005). The coiled-coil domain of $GABA_{B1}$ contains an LL-motif involved in the association with msec7-1, a guanine-nucleotide-exchange factor (GEF) for ADP-ribosylation factor (ARF)

family of GTPases (Restitutio et al., 2005). msec7-1 acts at the level of the trans-Golgi network (TGN) and probably controls $GABA_B$ receptor export from this organelle. Moreover, the γ2S subunit of $GABA_A$ receptors has been shown to associate with $GABA_{B1}$ subunits and promotes their cell surface expression in the absence of $GABA_{B2}$. This interaction further enhances agonist-induced internalization of heteromeric $GABA_B$ receptors (Balasubramanian et al., 2004).

Molecular diversity

Molecular diversity in the $GABA_B$ system arises from the $GABA_{B1a}$ and $GABA_{B1b}$ isoforms (Kaupmann et al., 1997), which are both generated from the *$GABA_{B1}$* gene by alternative promoter usage (Bischoff et al., 1999; Steiger et al., 2004). Structurally, the two subunit isoforms differ in their extracellular N-terminal domain by a pair of tandemly arranged SDs that are unique to $GABA_{B1a}$ and replaced by a short 18 amino acid sequence in $GABA_{B1b}$ (Hawrot et al., 1998; Blein et al., 2004). It is now generally accepted that two $GABA_B$ receptor subtypes, $GABA_{B(1a,2)}$ and $GABA_{B(1b,2)}$ are co-expressed in most if not all neurons of the central nervous system, and are pharmacologically and biophysically indistinguishable *in vitro* (Brauner-Osborne and Krogsgaard-Larsen, 1999).

Indirect evidence had long anticipated a differential segregation of $GABA_{B1a}$ and $GABA_{B1b}$ to pre- and postsynaptic structures (Benke et al., 1999; Billinton et al., 1999; Bischoff et al., 1999), but until recently no solid evidence was available. Of note, a differential distribution together with separate transcriptional control would allow for a high degree of plasticity permiting dynamically adjustable $GABA_B$ signalling in subcellular compartments. Classical compounds interfering with the $GABA_B$ system, like the $GABA_B$ receptor agonist baclofen, activate both $GABA_B$ receptor subtypes and cause the rapid development of tolerance and adverse effects in humans following systematic administration. Thus, differences in signalling between $GABA_{B1}$ isoforms would potentially open up new opportunities for therapeutic interference with the $GABA_B$ system (Bonanno & Raiteri, 1999; Gemignani et al., 1994; Cunningham & Enna, 1996; Deisz et al., 1997; Mohler & Fritschy, 1999; Yamada et al., 1999; Bowery et al., 2002). However, the lack of subunit specific antibodies and selective pharmacological tools has so far

hindered the visualization of individual $GABA_{B1}$ subunit isoforms in distinct subcellular compartments and prevented to study the individual contributions of $GABA_{B1a}$ and $GABA_{B1b}$ to pre- and postsynaptic $GABA_B$ functions.

Sushi domains

SDs, also known as complement control protein (CCP) modules or short consensus repeats (SCR), are evolutionary conserved protein interaction motifs (Lehtinen et al., 2004) that were first identified in Factor B, a protein of the complement system (Morley and Campbell, 1984). The three-dimensional structure of a typical SD has a compact hydrophobic core containing conserved residues sandwiched between small antiparallel β-sheets (Blein et al., 2004). Often occurring in multiple copies, SDs are structural motifs of about 60 amino acids characterized by a consensus sequence that includes four invariant cysteines, an almost invariant tryptophan and highly conserved prolines, glycines and hydrophobic residues (Kirkitadze & Barlow, 2001; Blein et al., 2004). The four cysteines form two disulfide bridges in a 1-3 and 2-4 pattern, which are essential for the SDs to maintain their tertiary structure. Recently, a SD was identified as the structural fold in the N-terminal hormone-binding domain of corticotrophin-releasing factor receptors (Perrin et al., 2006) raising the possibility that SDs are more universally used for regulating GPCR function (Grace et al., 2004). The SDs in $GABA_{B1a}$ display strikingly different structural properties: the first, N-terminal SD exhibits conformational heterogeneity under a wide range of conditions and interacts with the extracellular matrix protein fibulin-2, whereas the second SD is more compactly folded and shows stronger structural similarity to SDs in regulators of complement activation (Blein et al., 2004). It is thus likely that the $GABA_{B1a}$-specific SDs interact with multiple partners, which could generate some of the heterogeneity in the $GABA_B$ system predicted by studies with native $GABA_B$ receptors.

Vectorial protein transport in polarized neurons

Polarity is a pivotal requirement for neuronal communication. On a basic level neurons are divided into two functionally and biochemically distinct domains: the axonal and

somatodendritic compartment (Craig & Banker, 1994; Winkler & Mellmann, 1999). However, there are important functional specializations within these two compartments, which exhibit plasma membrane regions with specific molecular compositions (Horton & Ehlers, 2003). Among such specializations are the axonal initial segment, the nodes of Ranvier in myelinated neurons, presynaptic active zones as well as postsynaptic densities. It is thus evident that lipids, organelles, mRNAs and proteins must be precisely distributed to these specific subcellular compartments. This is especially important for the pre- versus postsynaptic segregation of neurotransmitter receptors being directly responsible for information transmission. Lateral diffusion of plasma membrane components between the axonal and somatodendritic compartment is inhibited by a cytoskeleton-based fence at the axonal initial segment (Kobayashi et al., 1992; Winckler & Mellmann, 1999). Nevertheless, how membrane proteins are initially sorted to axons and dendrites is still poorly defined.

Protein targeting in epithelial and neuronal cells – a comparison

Polarized membrane traffic is best understood in epithelial cells, where the plasma membrane is separated into basolateral and apical surfaces (Mellman 1995; Mostov & Cardone, 1995; Folsch et al., 1999; Mostov et al., 2003). Epithelial Madin-Darby canine kidney (MDCK) cells use the trans-Golgi network (TGN) as the main sorting station for polarized cargo by selectively accumulating membrane proteins destined for different domains into distinct vesicle populations (Wandinger-Ness et al., 1990). In contrast, hepatocytes, another epithelial cell type, transport almost all membrane proteins first to the basolateral surface. Subsequently, proteins scheduled for the apical surface are internalized and resorted towards the apical domain via endosomes, a process referred to as “transcytosis” or “indirect route” (Tuma and Hubbard, 2003). Neurons develop from the primitive neuroepithelium and thus could share sorting mechanisms with epithelial cells. Based on experiments studying the vectorial trafficking of apical and basolateral proteins in cultured hippocampal neurons it was hypothesized that the somatodendritic compartment corresponds to the basolateral compartment, whereas the apical compartment is the equivalent of the axonal compartment (Dotti & Simons, 1990). Indeed, for some transmembrane proteins basolateral signals also determine somatodendritic targeting.

However, the signals that target proteins to the apical membrane do not always appear to work for axonal targeting (West et al., 1997a; Jareb and Banker, 1998).

Polarized protein transport in neurons

In neurons, the majority of functional membrane proteins is synthesized in the cell body and subsequently transported to their target destination in axons or dendrites. In addition, some specific mRNAs are delivered to dendrites, where so called Golgi outposts support local protein synthesis (Job & Eberwine 2001; Hirokawa, 2006; Gardiol A et al., 1999; Horton & Ehlers 2003a). The extent to which protein synthesis occurs at presynaptic sites remains elusive, but recent evidence suggests that mRNAs are also present and translated locally in axons (Alvarez et al., 2000; Guiditta et al., 2002; Piper & Holt, 2004).

Like in MDCK cells, most axonal and dendritic membrane proteins are sorted into specific post-Golgi carriers and transported by microtubuli-dependent motors to the appropriate domain (Hirokawa & Takemura, 2005). Microtubuli are dynamic polymers with intrinsic polarity (Desai & Mitchison 1997). In axons and distal dendrites microtubuli are unipolar, whereas proximal dendrites contain microtubuli of mixed polarity (Burton & Paige 1981; Baas et al., 1988; Hirokawa & Takemura, 2005). Selectivity is further provided by the kinesin-superfamily of molecular motor proteins. Fourty-five family-members were identified in neurons, each holding binding affinities for different cargos. Moreover, individual kinesins possess differential preference for axonal or dendritic microtubuli (Hirokawa 1998; Baas et al., 1999; Hirokawa & Takemura, 2005).

At the surface, the protein-laden vesicles fuse with the plasma membrane. Membrane proteins are thus inserted and subsequently linked to the submembranous cytoskeleton if they have reached the appropriate compartment. Otherwise, proteins are internalized and degraded or resorted towards the correct location. The information required for such directional transport is usually harboured in the amino acid sequence or tertiary structure of the given protein or provided by posttranslational modifications. Such structural motifs typically associate with specific molecules like molecular motors or clathrin adaptors. The two following sections state some examples for axonal and somatodendritic targeting signals.

Somatodendritic determinants

Somatodendritic targeting is mostly mediated by amino acid residues in the cytoplasmic domains of transmembrane proteins. The low-density lipoprotein receptor (Jareb and Banker, 1998) and the transferrin receptor (West et al., 1997; Jareb and Banker, 1998) are targeted to dendrites by a cytosolic tyrosine-based motif characterized by an essential tyrosine in the context of YXXΦ (where X represents any amino acid and Φ is a bulky hydrophobic residue). Dendritic targeting of glycine transporter 1b (Poyatos et al, 2000) and potassium channel Kv4.2 (Rivera et al., 2003) is mediated by dileucine-based motifs. Both tyrosine-based and dileucine-containing signals have been shown to bind to subunits of adaptor protein complexes (Ohno et al., 1995; Rapoport et al., 1998). It is possible that the interaction of such adaptors with the targeting motifs may either initialize clathrin-mediated endocytosis of the existing receptors or contribute to the loading of newly synthesized receptors into vesicles bound for specific localizations (Burack et al., 2000; Garrido et al., 2001; Bonifacino & Traub, 2003).

Axonal determinants

Much less is known about the signals that lead to the targeting of proteins towards the axonal compartment (Winckler & Mellman, 1999; Burack et al., 2000). The first identified discrete motif required for axonal targeting was a RRK-tripeptide in the membrane proximal region of mGluR1 receptors. It directs the shorter splice variant mGluR1b to axons of chick retinal cells. However, it is masked in mGluR1a by its longer C-terminal domain harbouring somatodendritic targeting information (Francesconi & Duvoisin, 2002). For mGluR5 the interaction with different splice variants of Homer1 protein regulates axonal versus dendritic targeting. In cerebellar granule cells, Homer1b/c translocates mGluR5 to dendrites, whereas Homer1a mediates distribution to both axons and dendrites (Ango et al., 2000). In contrast, a cytoplasmic 60 amino acid motif determines both dendritic targeting of mGluR2 and axonal targeting of mGluR7 (Stowell & Craig, 1999). Moreover, the voltage-gated Shaker K^+ channel $K_v1.2$ is targeted to the axonal compartment by a cytosolic T1 domain, a region of ~130 amino acid residues that mediates tetramerization (Gu et al., 2003). Interaction between the T1 domain and the auxiliary

Kvβ(2) subunit links $K_v1.2$ channels to EB1 (microtuble (MT) plus-end tracking protein (+TIP) end-binding-protein 1) and KIF3/kinesin II (Gu et al., 2006) and is thus mandatory for axonal trafficking. Furthermore, short peptide motifs that include palmitoylation signals specifically target intracellular proteins like GAP-43 and GAD-65 to the Golgi apparatus and subsequently to the axon (El-Husseini Ael et al., 2001; Kanaani et al., 2002).

Topic of the thesis

$GABA_B$ receptors mediate the late phase of GABAergic inhibitory neurotransmission and as such are promising drug targets for neurological and mental health disorders (Enna & Bowery, 2004; Bettler et al., 2004; Cryan & Kaupmann, 2005; Bowery, 2006). It is now generally accepted that two $GABA_B$ receptor subtypes, $GABA_{B(1a,2)}$ and $GABA_{B(1b,2)}$, are coexpressed in most if not all neurons. Nevertheless, drug development in the $GABA_B$ field has been hampered since receptor subtypes have indistinguishable pharmacological properties. A differential segregation of $GABA_{B1a}$ and $GABA_{B1b}$ isoforms to pre- and postsynaptic structures was expected based on earlier studies (Benke et al., 1999; Billinton et al., 1999; Bischoff et al., 1999), but solid evidence was lacking. To dissociate the native functions of $GABA_B$ receptor subtypes knock-in mice with point-mutations in the translation start codons of either the $GABA_{B1a}$ or $GABA_{B1b}$ transcript were generated. Morphological and electrophysiological analysis of these mice revealed that the two pharmacological indistinguishable $GABA_{B1}$ isoforms localize to distinct synaptic sites and convey non-redundant functions. Most strikingly it was observed that at CA3-to-CA1 synapses in the hippocampus $GABA_{B1a}$ assembles heteroreceptors controlling glutamate release, while postsynaptic inhibition is predominantly mediated by $GABA_{B1b}$. Moreover, transfected CA3 pyramidal neurons exhibited a remarkable expression of $GABA_{B1a}$, but not $GABA_{B1b}$ protein in axon, whereas both isoforms are present in dendrites. This was the first solid evidence for a differential compartmentalization of $GABA_{B1}$ isoforms. Since the $GABA_{B1a}$-specific SDs provide the only region of sequence divergence between the two $GABA_{B1}$ isoforms, they are likely engaged in their segregation. The molecular mechanism underlying $GABA_B$ receptor compartmentalization is still poorly defined. Within this doctoral thesis I thus aimed at deciphering the role of the SDs in the pre- versus postsynaptic distribution and functional segregation of $GABA_B$ receptor subtypes.

Chapter II

DIFFERENTIAL COMPARTMENTALIZATION AND DISTINCT FUNCTIONS OF $GABA_B$ RECEPTOR VARIANTS

Vigot R, Barbieri S, Brauner-Osborne H, Turecek R, Shigemoto R, Zhang YP, Lujan R, Jacobson LH, Biermann B, Fritschy JM, Vacher CM, Muller M, Sansig G, Guetg N, Cryan JF, Kaupmann K, Gassmann M, Oertner TG, Bettler B

Neuron 50(4), 589-601, 2006

My contribution to this paper

This PhD thesis is based on a study published by Bischoff et al. in 1999. They analyzed the spatial distribution of $GABA_{B1a}$ and $GABA_{B1b}$ transcripts as well as $GABA_B$ receptor binding sites in rat cerebellum. They found that $GABA_{B1a}$ transcripts are mainly present in the granule cell layer, whereas $GABA_{B1b}$ mRNA was predominantly localized in the Purkinje cell layer. In addition, $GABA_B$ receptor binding sites were basically detected in the molecular cell layer, where parallel fibers make synapses onto Purkinje cells (Figure S2.1). They therefore suggested that the $GABA_{B1a}$ subunit isoform assembles presynaptic

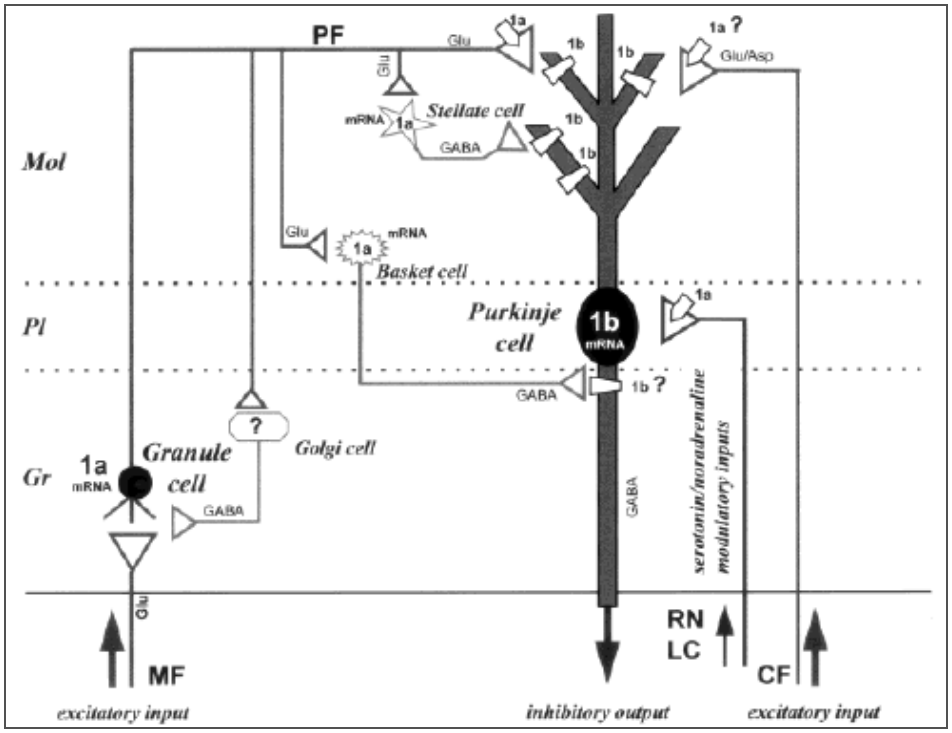

Figure S2.1: *Model of the possible localization of the $GABA_{B1a}$ and $GABA_{B1b}$ receptor subunits on the cerebellar circuitry. This hypothetical model is based on the data on the localization of the mRNA transcripts, the autoradiographic distribution of [^{3}H]CGP 54626-labeled binding sites, and the first immunohistochemical data with ultrastructural localization of antibodies in the molecular (Mol), Purkinje cell (Pl), and granular layers (Gr) of the cerebellum. The $GABA_{B1b}$ subunit, which is essentially expressed in Purkinje cells, might play a key role in the inhibitory output of the cerebellum. The $GABA_{B1a}$ subunit is expected to be located on presynaptic terminals of the glutamate-containing (Glu) parallel fibers (PF), the excitatory climbing fibers (CF) of glutamate and/or aspartate nature (Glu/Asp) and the serotonin/noradrenaline modulatory afferents from the raphe nucleus (RN) and locus coerulus (LC). In view of the low density of binding sites in the granular layer, few $GABA_{B1a}$ receptors might be localized in the granule or Golgi cells or on the terminals of the mossy fibers (MF) (adapted from Bischoff et al., 1999).*

receptors, whereas $GABA_{B1b}$ forms postsynaptic receptors. Nevertheless, solid evidence revealing a differential pre- versus postsynaptic segregation of $GABA_{B1a}$ and $GABA_{B1b}$ on the protein level was lacking. Since the $GABA_{B1a}$ -specific SDs constitute the only molecular difference between $GABA_{B1a}$ and $GABA_{B1b}$ it was hypothesized that the SDs are responsible for the axonal targeting of $GABA_B$ receptors.

To decipher the role of the SDs in the pre- versus postsynaptic distribution and functional segregation of $GABA_B$ receptor subtypes several different experimental approaches were undertaken in the Bettler lab and in collaboration. My task was to investigate the role of the SDs in axonal targeting at the molecular level in cell culture experiments. These experiments contributed to the different papers and paper drafts presented in this thesis (chapter II, III, IV and (VI)).

The SDs in the ectodomain of $GABA_{B1a}$ are part of the extracellular N-terminal protein sequence of the receptor. Therefore, the SDs are unable to interact directly with cytosolic molecular motor or adaptor proteins often responsible for axonal targeting (see chapter I). It was thus hypothesized that the SDs interact with membrane bound or ECM protein(s) at the cell surface thereby leading to the predominant axonal localization of $GABA_{B1a}$. Since organotypic slice cultures preserve the extracellular matrix I initially investigated the axonal versus dendritic distribution of eGFP-tagged $GABA_{B1a}$ and eCFP-tagged $GABA_{B1b}$ in organotypic slice cultures of mouse cerebellum. For this purpose, the corresponding cytomegalovirus-based expression plasmids were electroporated into organotypic cerebellar slices or transferred using Similiki-Forest-Virus. Unfortunately, the analysis of the axonal versus dendritic protein distribution was extremely difficult to perform in these slices. Distal neurites were often covered by neighboring cells on pictures obtained with a conventional epifluorescent microscope, whereas when using a confocal microscope to gain 3D stacks of the tissue the high laser intensity used at the time in such set ups bleached the eGFP, and especially the eCFP tags of the expression constructs. Unfortunately, a two-photon microscope circumventing these experimental problems was at that time yet not available at Basel.

I thus continued this study using dissociated hippocampal primary cultures, a culture system that is widely used for axonal versus dendritic targeting studies. In such monolayer

cultures the analysis of the axonal versus dendritic protein distribution is generally easier to perform. Nevertheless, the preparation of cultured hippocampal neurons involves a dissociation step partially disrupting the native cellular environment. It is thus possible that a surface protein potentially important for the proper localization of $GABA_{B1a}$ is missing in such cultures. I made cultures from $GABA_{B1a}^{-/-}$, $GABA_{B1b}^{-/-}$ and WT mouse embryos and analyzed the axonal versus dendritic distribution of $GABA_B$ receptors using a pan antibody. Both, endogenous $GABA_{B1a}$ and $GABA_{b1b}$ protein was present in the soma and dendrites, whereas selectively $GABA_{B1a}$ was found in axons. Nevertheless, I could not detect a differential distribution of transfected $GABA_{B1a}$-eGFP and $GABA_{B1b}$-eGFP expressed under the cytomegalovirus-based expression plasmids (Figure S2.2). For this reason

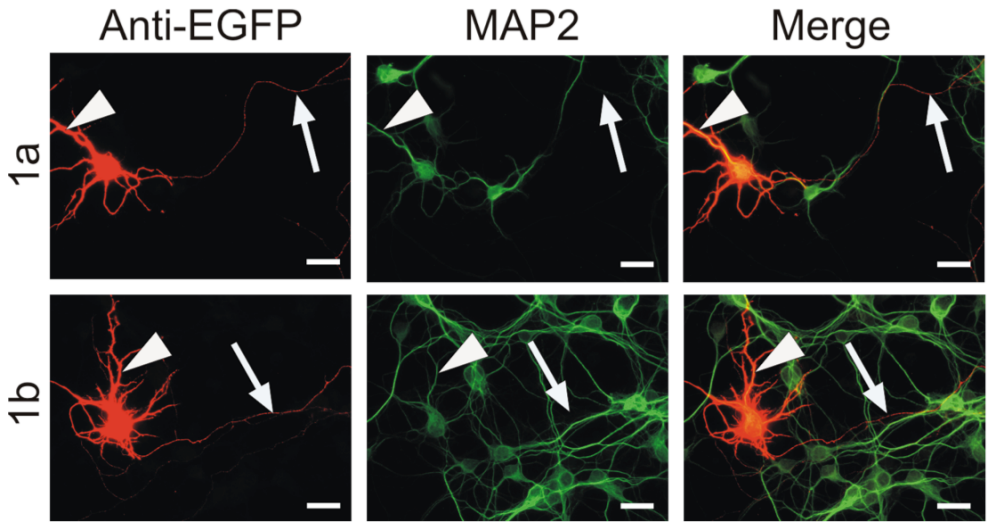

Figure S2.2: *Both $GABA_{B1a}$-eGFP (1a) and $GABA_{B1b}$-eGFP (1b) are localized to axons when expressed by the CMV promoter in cultured hippocampal neurons. Neurons were fixed at DIV6, permeabilzed and immunostained with the dendritic marker MAP2 and an antibody against the eGFP tag (Anti-EGFP). Axons are marked by arrows, dendrites by arrow heads. Scale bar 50 µm.*

the experiment was repeated by Yan-Ping Zhang and Thomas G. Oertner (FMI, Basel) in organotypic slice cultures of the hippocampus and analyzed with their newly established two-photon laser scanning microscope. Further, a neuron-specific synapsin-1 promoter was used. With this approach it was possible to show that transfected CA3 neurons selectively express $GABA_{B1a}$ in axons, whereas both isoforms are present in dendrites (Chapter II). I

subsequently investigated the distribution of these expression constructs in cultured hippocampal neurons and revealed a selective occurrence of $GABA_{B1a}$ in axons (Chapter III). This shows that the cytomegalovirus-based eukaryotic expression vector is not suitable for studying the axonal versus dendritic distribution of $GABA_B$ receptors. Nevertheless, it also appears that dissociated hippocampal neurons despite of their partially disrupted ECM preserve the native targeting of $GABA_B$ receptor subtypes and were thus used to further decipher the role of the SDs in axonal targeting (chapter III).

Summary

$GABA_B$ receptors are the G protein-coupled receptors for the main inhibitory neurotransmitter in the brain, γ-aminobutyric acid (GABA). Molecular diversity in the $GABA_B$ system arises from the $GABA_{B1a}$ and $GABA_{B1b}$ subunit isoforms that solely differ in their ectodomains by a pair of sushi repeats that is unique to $GABA_{B1a}$. Using a combined genetic, physiological, and morphological approach, we now demonstrate that $GABA_{B1}$ isoforms localize to distinct synaptic sites and convey separate functions in vivo. At hippocampal CA3-to-CA1 synapses, $GABA_{B1a}$ assembles heteroreceptors inhibiting glutamate release, while predominantly $GABA_{B1b}$ mediates postsynaptic inhibition. Electron microscopy reveals a synaptic distribution of $GABA_{B1}$ isoforms that agrees with the observed functional differences. Transfected CA3 neurons selectively express $GABA_{B1a}$ in distal axons, suggesting that the sushi repeats, a conserved protein interaction motif, specify heteroreceptor localization. The constitutive absence of $GABA_{B1a}$ but not $GABA_{B1b}$ results in impaired synaptic plasticity and hippocampus-dependent memory, emphasizing molecular differences in synaptic $GABA_B$ functions.

Introduction

$GABA_B$ receptors are considered promising drug targets for the treatment of neurological and mental health disorders (Bettler et al., 2004 and Cryan and Kaupmann, 2005). Presynaptic $GABA_B$ receptors are subdivided into auto- and heteroreceptors that control the release of GABA and other neurotransmitters, respectively. They restrict neurotransmitter release either by inhibiting voltage-sensitive Ca^{2+} channels or through a direct modulation of synaptic vesicle priming (Mintz and Bean, 1993, Poncer et al., 1997 and Sakaba and Neher, 2003). Postsynaptic $GABA_B$ receptors induce slow inhibitory potentials by gating Kir3-type K^+ channels (Lüscher et al., 1997). Considerable evidence has accumulated over the years, using a variety of preparations and techniques, to support the notion that multiple subtypes of $GABA_B$ receptors exist (Bonanno and Raiteri, 1993, Bowery et al., 2002, Cunningham and Enna, 1996, Deisz et al., 1997, Gemignani et al., 1994, Lei and McBain, 2003, Mohler and Fritschy, 1999, Pozza et al., 1999 and Yamada et al., 1999). The predicted receptor heterogeneity is not readily supported by molecular

studies (Bettler et al., 2004). $GABA_B$ receptors are heterodimers composed of $GABA_{B1}$ and $GABA_{B2}$ subunits, which are both required for normal receptor functioning (Marshall et al., 1999 and Mohler and Fritschy, 1999). Accordingly, mice lacking $GABA_{B1}$ (referred to as $1^{-/-}$ mice) or $GABA_{B2}$ subunits show a complete absence of typical $GABA_B$ responses (Gassmann et al., 2004, Prosser et al., 2001 and Schuler et al., 2001). The only firmly established molecular diversity in the $GABA_B$ system arises from the $GABA_{B1a}$ and $GABA_{B1b}$ subunit isoforms (Kaupmann et al., 1997). However, no unique pharmacological or functional properties could be assigned to $GABA_{B1a}$ or $GABA_{B1b}$. Most, if not all neurons coexpress $GABA_{B1a}$ and $GABA_{B1b}$, which are generated by differential promoter usage from the *$GABA_{B1}$* gene (Bischoff et al., 1999 and Steiger et al., 2004). *$GABA_{B1a}$* and *$GABA_{B1b}$* expression levels vary during development and across individual cells, suggestive of a functional specialization. Structurally, the isoforms differ in their N-terminal ectodomain by a pair of sushi repeats that is present in $GABA_{B1a}$ but not in $GABA_{B1b}$ (Blein et al., 2004). Sushi repeats, also known as complement control protein modules, or short consensus repeats, are found in other G protein-coupled receptors as well (Grace et al., 2004) and mediate protein interactions in a wide variety of adhesion proteins (Lehtinen et al., 2004). The presence of sushi repeats in $GABA_{B1a}$, together with the absence of functional or pharmacological differences in vitro, suggested the existence of auxiliary proteins that modify receptor activity, pharmacology, and localization (Marshall et al., 1999 and Mohler and Fritschy, 1999), precedence for which is found with other G protein-coupled receptors (McLatchie et al., 1998). So far, the lack of selective reagents has not allowed addressing the individual contributions of $GABA_{B1a}$ and $GABA_{B1b}$ to native $GABA_B$ functions. In the light of the proposed heterogeneity of native $GABA_B$ receptors, it therefore remains a key question whether $GABA_{B1}$ isoforms exhibit pharmacological and/or functional differences in vivo. Here, we have taken a genetic approach to dissociate the native functions of $GABA_{B1a}$ and $GABA_{B1b}$.

Results

Generation of Mice Selectively Expressing $GABA_{B1a}$ or $GABA_{B1b}$ Subunits

To selectively prevent translation of the $GABA_{B1a}$ and $GABA_{B1b}$ proteins, we converted their initiation codons in the *$GABA_{B1}$* gene into stop codons (Figure 1). Balb/c gene

targeting constructs with mutated initiation codons (Figure 1A) were electroporated into Balb/c embryonic stem cells (Dinkel et al., 1999) and homologous recombination events diagnosed with short-arm PCR and Southern blots (data not shown). Targeted embryonic stem cells were injected into C57BL/6 blastocysts. Founder mice were crossed with Balb/c mice expressing Cre-recombinase under control of the cytomegalus virus promoter to excise the neomycin cassette. Pups born from these matings were scored for Cre-mediated loss of the neomycin cassette and bred to homozygosity. Consequently, all mutant mice were on a pure inbred Balb/c genetic background, which was maintained throughout the experiments. Homozygous mice with mutations in the $GABA_{B1a}$ (referred to as $1a^{-/-}$ mice) or $GABA_{B1b}$ ($1b^{-/-}$ mice) initiation codon were viable, reproduced normally, and exhibited no overt phenotypic abnormalities. Mutant mice showed normal levels of $GABA_{B1a}$ and $GABA_{B1b}$ mRNA, indicating that the genetic manipulations do not influence mRNA expression or stability (Figure 1B). Immunoblot analysis revealed the total absence of $GABA_{B1a}$ and $GABA_{B1b}$ protein in $1a^{-/-}$ and $1b^{-/-}$ mice, respectively, confirming that mutation of the initiation codons prevents translation of the individual subunits (Figure 1C). $GABA_{B1a}$ and $GABA_{B1b}$ proteins appeared upregulated in total brain extracts of knockout mice (Figure 1C), possibly because of increased availability of complementary $GABA_{B2}$ protein, which is required for cross-stabilization (Gassmann et al., 2004). We analyzed whether $GABA_B$ protein is also upregulated in the CA1 region of the hippocampus, where the electrophysiological and morphological studies described below were carried out. Similar to those seen in total brain extracts, $GABA_{B1a}$ and $GABA_{B1b}$ protein levels in CA1 extracts were increased in the $1b^{-/-}$ (129% of wild-type) and $1a^{-/-}$ mice (115% of wild-type), respectively (Figure S1).

Immunohistochemical, Pharmacological, and Biochemical Characterization of $1a^{-/-}$ and $1b^{-/-}$ Mice

Immunohistochemistry in the CA1 and CA3 region of the hippocampus revealed completely overlapping expression patterns for the $GABA_{B1a}$ and $GABA_{B1b}$ proteins (Figure 2), consistent with an ubiquitous expression of the two proteins in brain neurons (Bischoff et al., 1999). The regional immunostaining in $1a^{-/-}$ and wild-type mice was similar, while the staining in $1b^{-/-}$ mice was more diffuse and lacked distinct laminar

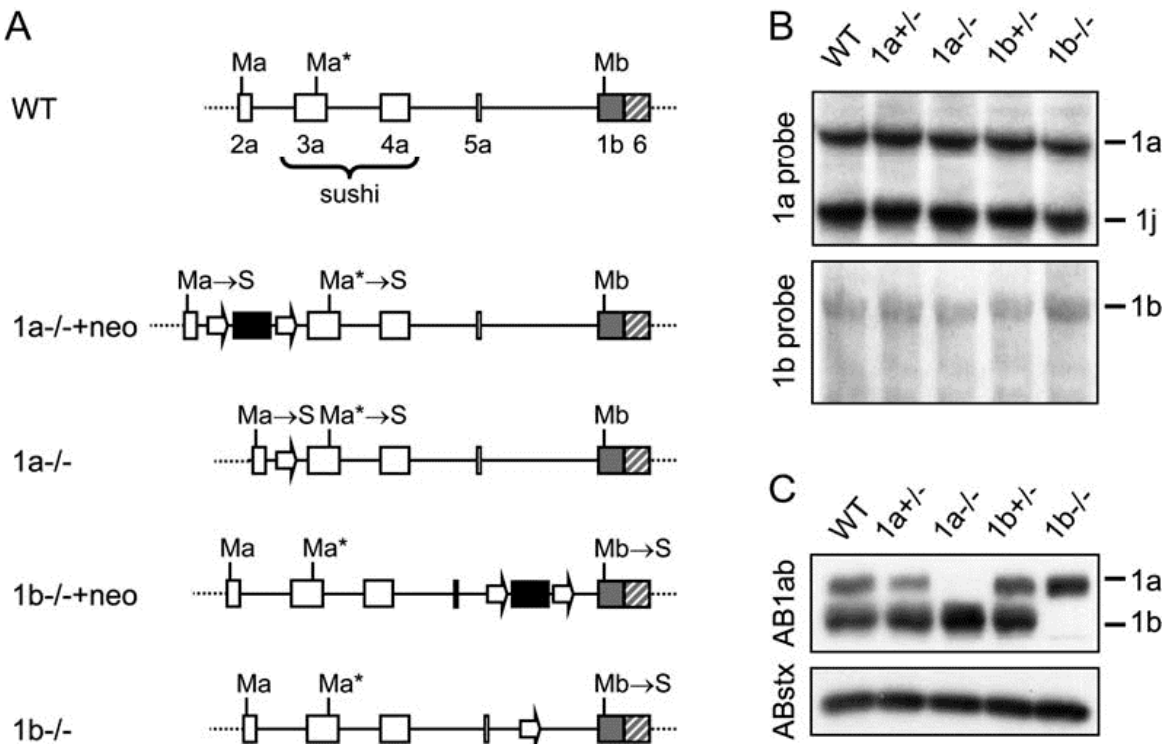

Figure.1. Generation of a 1a-/- and 1b-/- Mice

(A) *5′ region of wild-type (WT) (Martin et al., 2001) and mutated $GABA_{B1}$ alleles. Exons encoding the N terminus of $GABA_{B1a}$ are represented by white boxes and specify the signal peptide (exon 2a), a pair of sushi repeats of 75 amino acids each (exons 3a, 4a), and a linker of six amino acids (exon 5a). The exon specifying the N terminus of $GABA_{B1b}$ is represented by a gray box. All exons downstream of exon 1b are shared between the two isoforms (only exon 6 is shown; hatched box). Start codons for $GABA_{B1a}$ (Ma) and $GABA_{B1b}$ (Mb) transcripts were converted into stop codons (S) using a knockin approach. A putative alternative start site (Ma^*) in $GABA_{B1a}$ transcripts was mutated in addition. The floxed neomycin cassette (black bar) for selection of transfected embryonic stem cells was introduced in the introns between exons 2a/3a ($1a^{-/-}$neo) or exons 5a/1b ($1b^{-/-}$neo). A loxP site (arrow) is left behind after Cre-mediated excision of the neomycin cassette ($1a^{-/-}$, $1b^{-/-}$).*

(B) *Northern blot analysis of $GABA_{B1a}$ and $GABA_{B1b}$ mRNA expression in the brain of WT, heterozygous ($^{+/-}$), and homozygous ($^{-/-}$) knockout mice. The 1a hybridization probe (1a probe) corresponds to nucleotides 1–405 of the $GABA_{B1a}$ cDNA (Kaupmann et al., 1997) and detects $GABA_{B1a}$ as well as a truncated $GABA_{B1j}$ transcript (M.G., unpublished data) of ~1.6 kb (upper panel). The 1b probe corresponds to nucleotides 16–259 of the $GABA_{B1b}$ cDNA (Kaupmann et al., 1997) and detects 1b transcripts (lower panel).*

(C) *Immunoblot analysis of total brain lysates using antibodies recognizing the common C terminus of $GABA_{B1a}$ and $GABA_{B1b}$ (AB1ab) (Gassmann et al., 2004). Anti-syntaxin (ABstx) antibodies control for sample loading.*

boundaries. Immunohistochemistry therefore suggests differences in the relative abundance of the two isoform proteins at different subcellular sites. For example, intense immunoreactivity is evident in CA3 stratum lucidum of $1b^{-/-}$ mice, which may hint at a preferential expression of $GABA_{B1a}$ protein at presynaptic sites (arrowhead in Figure 2). The immunostainings obtained with antibodies directed at the $GABA_{B1}$ and $GABA_{B2}$ proteins are similar in the different strains of mice, suggesting that most of the $GABA_{B2}$ and $GABA_{B1}$ protein assembles into heterodimeric receptors.

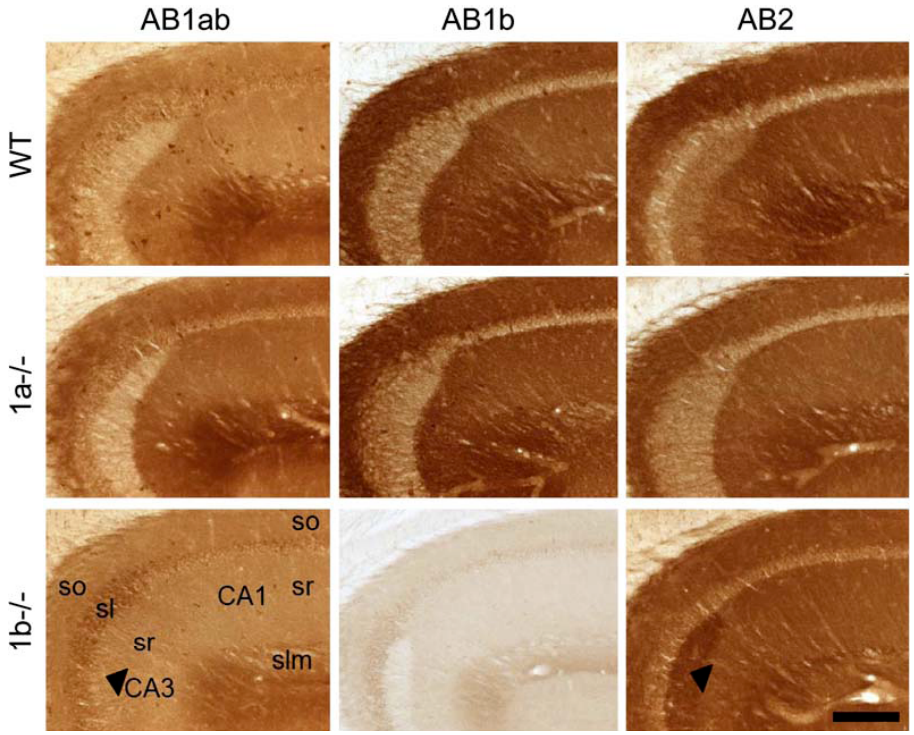

Figure 2. Distribution of $GABA_{B1a}$ and $GABA_{B1b}$ Protein in the Hippocampus of $1a^{-/-}$ and $1b^{-/-}$ Mice

Immunohistochemistry in the CA1/CA3 region using antibodies specific for $GABA_{B1}$ (AB1ab, recognizing an epitope shared by $GABA_{B1a}$ and $GABA_{B1b}$), $GABA_{B1b}$ (AB1b), and $GABA_{B2}$ (AB2). No $GABA_{B1a}$-specific antibody suitable for immunohistochemistry is available. The expression pattern of $GABA_{B1a}$ protein is revealed in $1b^{-/-}$ mice stained with AB1ab. No specific immunostaining is observed with AB1b in $1b^{-/-}$ mice, demonstrating the specificity of this antibody for $GABA_{B1b}$ protein. No specific immunostaining was obtained in control experiments with AB1ab/AB1b and AB2 antibodies in mice devoid of $GABA_{B1}$ and $GABA_{B2}$ subunits, respectively (Fritschy et al., 2004). Abbreviations: so, stratum oriens; sl, stratum lucidum; sr, stratum radiatum; slm, stratum lacunosum-moleculare. Scale bar, 200 µm. The WT mouse was a littermate of the $1a^{-/-}$ mouse.

To compare the pharmacology of $GABA_{B1a}$ and $GABA_{B1b}$ in native tissue, we analyzed the inhibition of [^{125}I]CGP64213 antagonist binding (Kaupmann et al., 1997) by GABA and L-baclofen in cortical membranes (Figure 3A). In agreement with recombinant data (Kaupmann et al., 1998), the inhibition curves for wild-type, $1a^{-/-}$, and $1b^{-/-}$ mice were almost identical (IC_{50} values for wild-type, $1a^{-/-}$, and $1b^{-/-}$ mice in μM are as follows: GABA: 0.7 ± 0.2, 0.4 ± 0.2, 0.6 ± 0.2; baclofen: 1.2 ± 0.3, 0.8 ± 0.3, 0.9 ± 0.3; n = 3 per genotype). [^{3}H]baclofen binding in $1a^{-/-}$ and $1b^{-/-}$ cortical membranes was similarly reduced compared to wild-type membranes (Figure 3B), in agreement with the relative abundance of the two isoform proteins in the cortex (Kaupmann et al., 1997). To determine functional $GABA_B$ receptor levels, we measured GTPγ[^{35}S] binding, which assesses the activation of Gαi/o-type G proteins, the main effectors of $GABA_B$ receptors (Figure 3C). Cortical membranes of $1a^{-/-}$ and $1b^{-/-}$ mice showed 52% ± 4% and 28% ± 8% of the maximal GTPγ[^{35}S] binding seen with wild-type mice. The sum of the maximal GTPγ[^{35}S] responses in knockout membranes is therefore 20% lower than expected. This suggests the absence of a compensatory upregulation of functional receptor levels, despite the upregulation of $GABA_{B1}$ isoforms seen at the protein level (Figure 1C and Figure S1 in the Supplemental Data available with this article online). Presumably, most of the extra $GABA_{B1}$ isoform protein is retained intracellularly and does not participate in functional responses.

Distinct Contributions of $GABA_{B1a}$ and $GABA_{B1b}$ to Pre- and Postsynaptic $GABA_B$ Functions

Using whole-cell patch-clamp recording in slice preparations, we examined whether wild-type and knockout mice differ in their hippocampal $GABA_B$ responses. We first checked for the presence of heteroreceptors on excitatory terminals. Stimulation of the Schaffer collateral-commissural fibers induces excitatory postsynaptic currents (EPSCs) in CA1 pyramidal neurons, which are reduced by blocking glutamate release through activation of $GABA_B$ heteroreceptors (Schuler et al., 2001). Baclofen, a $GABA_B$ agonist, was effective in reducing the EPSC amplitude in wild-type and $1b^{-/-}$ mice but not in $1a^{-/-}$ mice (Figures 4A and 4B). As a control, adenosine inhibited glutamate release in all three genotypes.

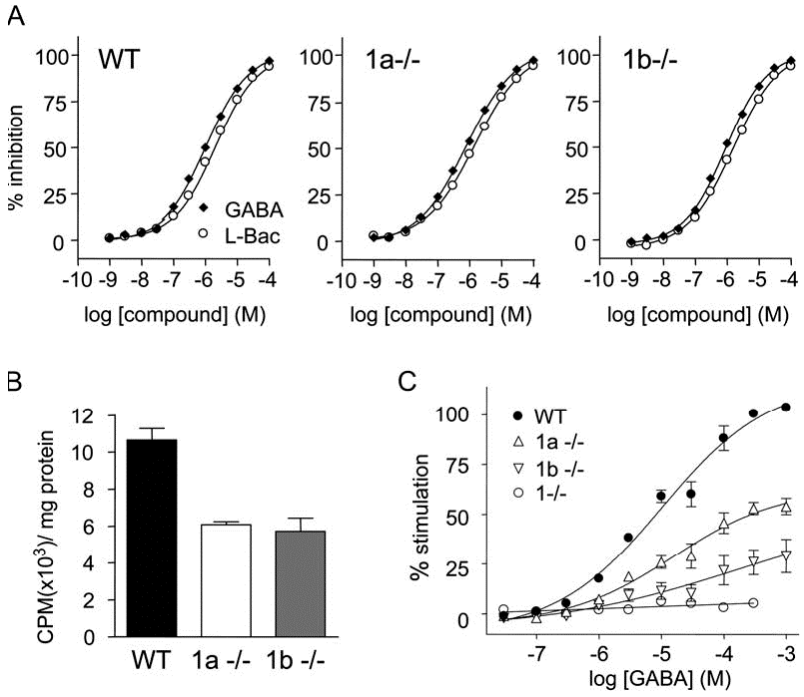

Figure 3. Pharmacological and Biochemical Analysis of Brain Membranes from Wild-Type, $1a^{-/-}$, and $1b^{-/-}$ Mice

(A) *Inhibition of [^{125}I]CGP64213 $GABA_B$ antagonist binding to cortical membranes by the agonists GABA and L-baclofen (L-Bac). The curves were fitted using nonlinear regression (Graph Pad PRISM program, Graph Pad software Inc., San Diego). Error bars (±SEM) are smaller than the symbols.*

(B) *Binding of [^{3}H]baclofen to cortical membranes of $1a^{-/-}$ and $1b^{-/-}$ mice was 57% ± 2% and 50% ± 7%, respectively, of the binding to WT membranes (±SEM of two independent experiments performed in triplicate).*

(C) *GABA-stimulated GTPγ[^{35}S] binding in cortical membranes. Data points are mean (±SEM) values calculated from five (WT) and four ($1a^{-/-}$, $1b^{-/-}$, $1^{-/-}$) mice.*

This indicates that $1a^{-/-}$ mice, in contrast to $1b^{-/-}$ mice, lack $GABA_B$ heteroreceptors on Schaffer collateral terminals. Small residual heteroreceptor activity in $1a^{-/-}$ mice suggests that minute amounts of $GABA_B$ receptors assembled with $GABA_{B1b}$ are localized at glutamatergic terminals. We next looked for the presence of autoreceptors on GABAergic terminals and recorded inhibitory postsynaptic currents (IPSCs) in the presence of the ionotropic glutamate receptor antagonist kynurenate. Baclofen reduced the amplitude of IPSCs in CA1 pyramidal neurons of all genotypes, suggesting that both $GABA_{B1a}$ and

$GABA_{B1b}$ can efficiently participate in autoreceptor function (Figures 4C and 4D). Postsynaptic $GABA_B$ receptors induce a late IPSC by activating Kir3-type K^+ channels (Lüscher et al., 1997). At a holding potential of −50 mV and in physiological extracellular [K^+], baclofen elicited similar outward currents in CA1 pyramidal cells of *1a*$^{-/-}$ and wild-type mice (Figures 4E and 4F). However, in CA1 pyramidal cells of *1b*$^{-/-}$ mice, the baclofen-induced outward current was reduced by ~60% compared to wild-type or *1a*$^{-/-}$ mice. This indicates that predominantly $GABA_{B1b}$ mediates postsynaptic inhibition. As a control, adenosine receptors, which converge on the same Kir3 channels (Lüscher et al., 1997), induced similar outward currents in all genotypes. It is formally possible that the upregulation of $GABA_{B1a}$ protein observed in the *1b*$^{-/-}$ mice (Figure 1C and Figure S1) compensates to some extent for the missing $GABA_{B1b}$ protein. We consider this unlikely because functional receptor levels in the *1b*$^{-/-}$ mice are lower than expected (Figure 3C). Moreover, GFP-tagged $GABA_{B1a}$ protein clearly distributes to the dendritic compartment of CA1 neurons when expressed in organotypic slice culture (Figure 6A). Likely, therefore, both $GABA_{B1a}$- and $GABA_{B1b}$-containing receptors address Kir3 channels under normal conditions.

Distinct Subcellular Compartmentalization of the $GABA_{B1a}$ and $GABA_{B1b}$ Proteins

The lack of suitable antibodies thus far prevented studying the distribution of $GABA_{B1}$ isoforms using electron microscopy. We now used the *1a*$^{-/-}$ and *1b*$^{-/-}$ mice to determine the subcellular localization of $GABA_{B1b}$ and $GABA_{B1a}$ protein, respectively. Preembedding immunogold labeling experiments in the CA1 stratum radiatum of wild-type mice confirmed that $GABA_{B1}$ protein is present in pre- and postsynaptic elements (Figure 5A), as reported for rat brain (Kulik et al., 2003). In *1a*$^{-/-}$ mice, $GABA_{B1b}$ was mostly found in spines opposite glutamate release sites (Figures 5B and 5C). In *1b*$^{-/-}$ mice, $GABA_{B1a}$ predominantly localized to glutamatergic terminals (Figures 5D and 5E). Quantitative analysis of $GABA_{B1}$ labeling showed that the ratio of pre- to postsynaptic immunoparticles in wild-type, *1a*$^{-/-}$, and *1b*$^{-/-}$ mice was 0.31, 0.17, and 1.61, respectively (Figure 5F). Thus, the electron microscopy data support the electrophysiological data (Figure 4) and confirm that $GABA_{B1a}$ preferentially localizes to glutamatergic terminals. Consistent with

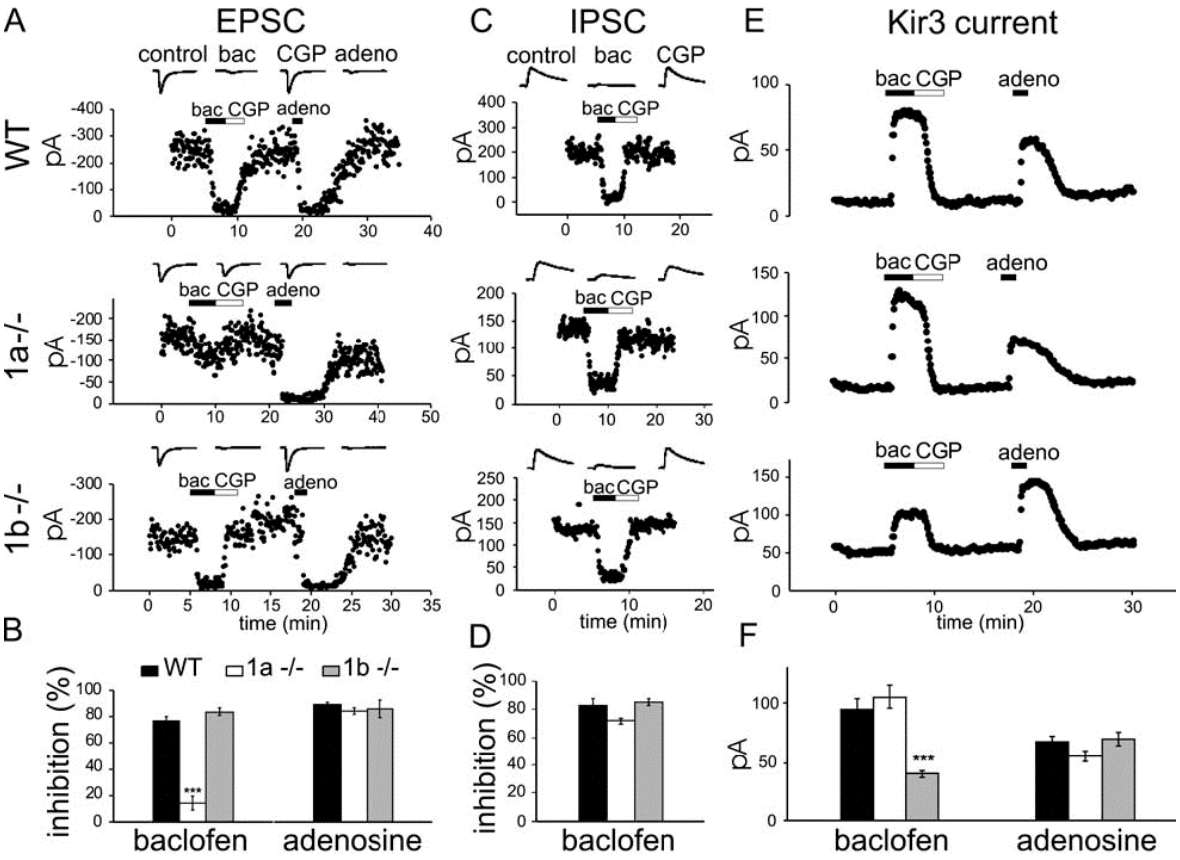

Figure 4. $GABA_B$ Responses in Wild-Type, $1a^{-/-}$, and $1b^{-/-}$ CA1 Pyramidal Neurons

(A and B) *Peak amplitudes and representative traces (A) and summary histogram (B) of monosynaptic EPSC inhibition by baclofen and adenosine. Baclofen (50 μM) depresses the amplitude of EPSCs in WT (76.5% ± 3.1% inhibition; n = 8) and $1b^{-/-}$ (83.4% ± 2.9% inhibition; n = 5) but not in $1a^{-/-}$ (15.9% ± 5.3% inhibition; n = 13; p < 0.001, ANOVA/Scheffe post hoc test) mice. Adenosine (100 μM) depresses EPSCs in all genotypes (WT: 89.1% ± 1.6% inhibition, n = 6; $1a^{-/-}$: 85.3% ± 1.8% inhibition, n = 13; $1b^{-/-}$: 85.6% ± 6.6% inhibition, n = 4).*

(C and D) *Peak amplitudes and representative traces (C) and summary histogram (D) of IPSC inhibition by baclofen. Baclofen significantly depresses the IPSC amplitude in all genotypes (WT: 82.7% ± 4.8% inhibition, n = 12; $1a^{-/-}$: 71.8% ± 2.3% inhibition, n = 9; $1b^{-/-}$ mice: 85.7% ± 2.4% inhibition, n = 7).*

(E and F) *Representative changes in the holding current of CA1 neurons following application of baclofen and adenosine (E) and summary histogram of the amplitude of baclofen- and adenosine-induced K^+ currents (F). The amplitude of the outward K^+ current induced by baclofen application is similar in $1a^{-/-}$ (99.3 ± 8.8 pA; n = 14) and WT (89.8 ± 7.7 pA; n = 16) neurons. In $1b^{-/-}$ cells, the amplitude of the baclofen-induced current is strongly reduced (37.4 ± 2.7 pA; n = 10; p < 0.001, ANOVA/Scheffe post hoc test). Control adenosine-induced K^+ currents are similar in all genotypes. (Vclamp: −50 mV, TTX 1 μM, $^{***}p < 0.001$, ANOVA/Scheffe post hoc test). All baclofen-induced responses (inhibition of PSCs and activation of K^+ currents) were fully blocked by the $GABA_B$ antagonist CGP54626 (1 μM). Values are expressed as mean ± SEM.*

residual heteroreceptor activity (Figures 4A and 4B), some presynaptic immunogold labeling persisted at glutamatergic *$1a^{-/-}$* synapses.

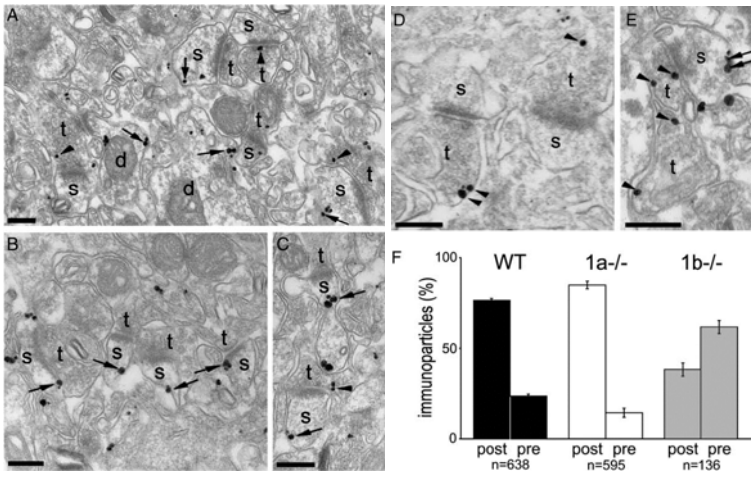

Figure 5. Preembedding Electron Micrographs Showing $GABA_{B1}$ Immunogold Labeling at Asymmetrical, i.e. Glutamatergic, Synapses in CA1 Stratum Radiatum

(A) *Pre- and postsynaptic immunogold labeling in WT mice.*

(B** and **C) *Predominant postsynaptic (B) and rare presynaptic (C) labeling (arrowhead) in $1a^{-/-}$ mice.*

(D** and **E) *Predominant presynaptic (D) and less frequent postsynaptic (E) labeling in $1b^{-/-}$ mice.*

(F) *Percentage of pre- and postsynaptic immunogold particles in WT, $1a^{-/-}$, and $1b^{-/-}$ mice (presynaptic: WT, 24% ± 1%; $1a^{-/-}$, 14% ± 3%; $1b^{-/-}$, 62% ± 4%; n = 3 for each genotype; mean ± SEM). Immunogold labeling was less frequent in $1b^{-/-}$ compared to $1a^{-/-}$ mice, which is reflected in the number of immunogold particles that were analyzed. Arrow: examples of immunogold particles in spines and dendritic shafts; arrowhead: examples of immunogold particles in presynaptic terminals. t, terminal; s, spine; d, dendrite; scale bars, 200 nm.*

Selective Localization of $GABA_{B1a}$ to Axons and $GABA_{B1b}$ to Dendritic Spines in Transfected Hippocampal Neurons

We analyzed whether GFP-tagged $GABA_{B1a}$ and $GABA_{B1b}$ proteins exhibit a distinct subcellular distribution when expressed in hippocampal neurons. For these experiments, we transfected organotypic hippocampal slice cultures, which preserve the basic CA3-CA1 connectivity, with expression vectors coding for $GABA_{B1a}$-GFP or $GABA_{B1b}$-GFP. We

coexpressed a freely diffusible red fluorescent protein (RFP), tdimer2, to normalize the green fluorescence to the red fluorescence. Both $GABA_{B1a}$-GFP and $GABA_{B1b}$-GFP proteins were robustly expressed in the dendrites of transfected CA1 pyramidal neurons (Figures 6A, 6B, and 6D). $GABA_{B1b}$-GFP was expressed in the majority of dendritic spines, while $GABA_{B1a}$-GFP was largely excluded from this location. This agrees with the electron microscopy data showing a preferential association of the $GABA_{B1b}$ protein with spines opposite to glutamate release sites (Figures 5B and 5C), a location where Kir3 channels are highly coclustered with $GABA_B$ receptors (Kulik et al., 2006). This may explain why predominantly $GABA_{B1b}$ mediates the activation of Kir3 currents (Figures 4E and 4F). The data further indicate an almost exclusive association of the $GABA_{B1a}$-GFP protein with distal axons (Figure 6), again in agreement with the electrophysiological (Figures 4A and 4B) and morphological data (Figures 5D and 5E).

Impaired Synaptic Plasticity in *1a*$^{-/-}$ Mice

Activation of postsynaptic $GABA_B$ receptors was shown to restrict long-term potentiation (LTP), whereas activation of autoreceptors promotes LTP (Davies and Collingridge, 1996 and Davies et al., 1991). A role for $GABA_B$ heteroreceptors in synaptic plasticity is not known. We therefore addressed whether the genetic loss of heteroreceptors in *1a*$^{-/-}$ mice affects LTP at CA3-to-CA1 synapses. In wild-type CA1 neurons, the pairing protocol induced a marked potentiation of the EPSC amplitude (268.9% ± 58.3%; n = 7) (Figures 7A and 7B). No LTP developed when NMDA receptors were antagonized (CPP + 7-Cl-kynurenic acid) or when the cell under recording was kept at −70 mV (Figure 7B). *1*$^{-/-}$ mice, which completely lack functional $GABA_B$ receptors (Schuler et al., 2001), did not exhibit notable LTP (9.4% ± 20.3%; n = 5), nor did *1a*$^{-/-}$ mice (−8.9% ± 9.3%; n = 9) (Figures 7A and 7B). In contrast, *1b*$^{-/-}$ mice exhibited normal LTP (228.7% ± 43.3%; n = 5). Wild-type neurons developed LTP even after acute pharmacological blockade of $GABA_B$ receptors with the antagonist CGP54626 (182.8% ± 54%; n = 6), showing that acute blockade of $GABA_B$ receptors does not prevent the induction of LTP. Adaptive changes (see below) due to the constitutive absence of heteroreceptors are therefore expected to underlie the lack of LTP in *1a*$^{-/-}$ neurons (Figure 7B).

Synaptic Modifications in $1a^{-/-}$ Mice

The amplitude ratio of evoked EPSCs in response to paired-pulse stimulation was similar in wild-type, $1a^{-/-}$, and $1b^{-/-}$ CA1 pyramidal neurons (Figure 7C). A change in the paired-pulse ratio is generally believed to reflect an underlying change in the presynaptic probability of release. The absence of differences in the paired-pulse ratio between the three genotypes therefore provides no evidence for a change in the release probability in $1a^{-/-}$ mice. Moreover, these results indicate that the paired-pulse protocol does not result in the activation of $GABA_B$ heteroreceptors in wild-type neurons, nor do heteroreceptors appear to be tonically activated by ambient GABA, in agreement with earlier studies (Morrisett et al., 1991 and Scanziani, 2000). CGP54626 had no effect on the miniature EPSC (mEPSC) frequency or amplitude in wild-type CA1 neurons, further supporting that ambient GABA does not tonically activate heteroreceptors under baseline conditions (Figure 7D). The frequency of spontaneous mEPSCs was significantly increased in $1a^{-/-}$ mice, while the mEPSC amplitude remained similar as in wild-type or $1b^{-/-}$ mice (Figure 7E). The observed increase in the baseline mEPSC frequency in $1a^{-/-}$ mice would normally argue for an increase in the probability of glutamate release. However, since CA3-to-CA1 synapses in $1a^{-/-}$ mice exhibit no change in the paired-pulse ratio and heteroreceptors remain inactive under baseline conditions, we favor that the increase in mEPSC frequency is indicative of an increased number of functional synapses. An increase in mEPSC frequency, with a concomitant modest increase in mEPSC amplitude, has been observed in cultured hippocampal neurons as a consequence of the unmasking of “silent” synapses (Liao et al., 1999). The insertion of AMPA receptors into synapses that only contain NMDA receptors is expected to result in a decrease in the coefficient of variation (CV) of the AMPA receptor-mediated component of the EPSC (CV_{AMPA}), with no change in the CV of the NMDA component (CV_{NMDA}) (Kullmann, 1994). We measured the variability of the AMPA and NMDA receptor-mediated EPSC amplitudes recorded in the same cells at −70 mV and +30 mV, respectively (Figure 7F). We found that the CV_{AMPA} was significantly higher for the wild-type (0.37 ± 0.04; $n = 12$) than for the $1a^{-/-}$ mice (0.24 ± 0.03; $n = 10$; $p < 0.02$), while the CV_{NMDA} for wild-type (0.23 ± 0.02; $n = 12$) and $1a^{-/-}$ mice (0.22 ± 0.03; $n = 10$) was similar. Comparison of the CV_{AMPA} and CV_{NMDA} between $1a^{-/-}$ and wild-type mice is therefore consistent with a decreased proportion of silent synapses in $1a^{-/-}$ mice (Figure 7G).

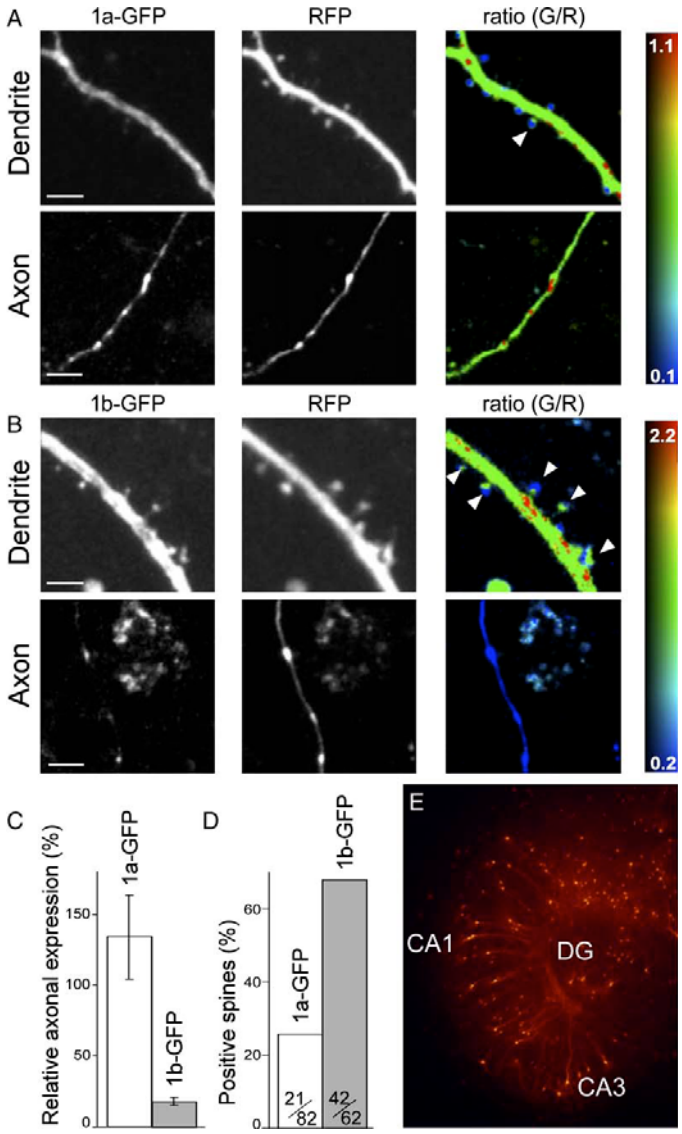

Figure 6. Expression of GFP-Tagged $GABA_{B1a}$ and $GABA_{B1b}$ Subunits in Organotypic Slice Culture

(A, B) *Maximum intensity projections of dendrites and axons in the CA1 region of the hippocampus expressing $GABA_{B1a}$-GFP (A) or $GABA_{B1b}$-GFP (B) in combination with the freely diffusible tdimer2 RFP are shown. The ratio of green-to-red fluorescence (G/R) is coded in rainbow colors. Scale bar, 5 µm.*

(C) *Predominantly $GABA_{B1a}$-GFP protein is expressed in axons. The axonal expression level of $GABA_{B1a}$ and $GABA_{B1b}$ was normalized to the dendritic expression level ($GABA_{B1a}$: 133.84% ± 29.53%, n = 9; $GABA_{B1b}$: 18.01% ± 2.80%, n = 5; mean ± SEM).*

(D) *$GABA_{B1b}$-GFP was expressed in the majority of dendritic spines, while $GABA_{B1a}$-GFP was excluded from most spines (spines positive for $GABA_{B1a}$-GFP: 21 of 82; spines positive for $GABA_{B1b}$-GFP: 42 of 62). Examples of positive spines are indicated by white arrowheads in the G/R ratio images in (A) and (B).*

(E) *Example of an organotypic hippocampal slice culture 7 days after cotransfection of $GABA_{B1b}$-GFP and tdimer2 expression vectors.*

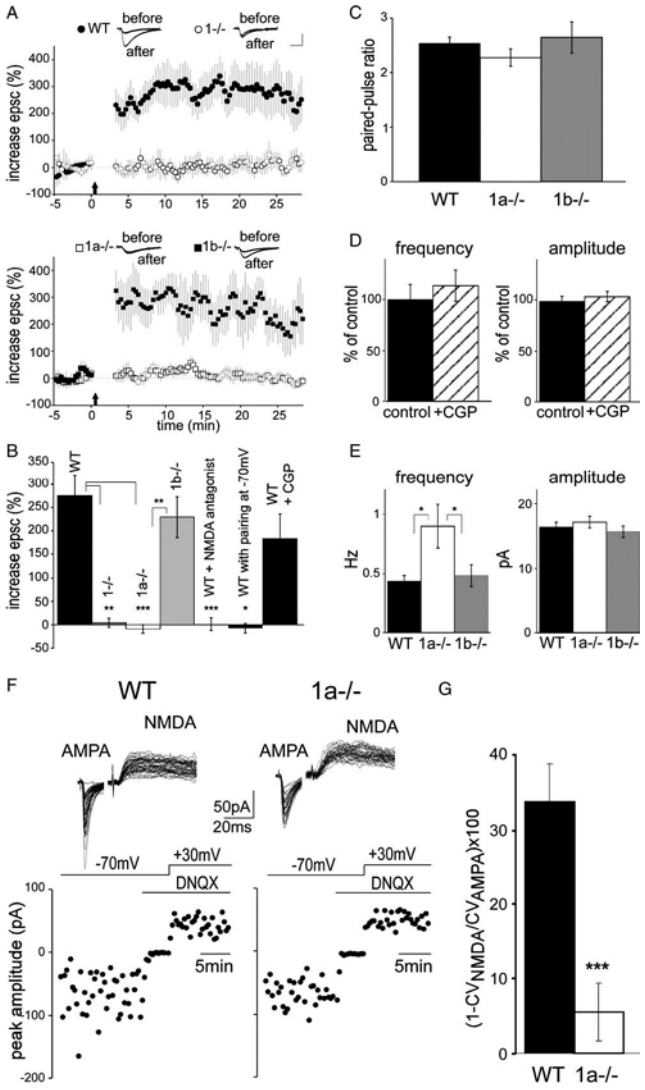

Figure 7. Lack of LTP and Reduction in the Proportion of Silent Synapses in $1a^{-/-}$ Mice

(A) *The pairing protocol fails to induce LTP in $1^{-/-}$ and $1a^{-/-}$ mice but induces a clear potentiation of the EPSC amplitude in WT and $1b^{-/-}$ mice. Averages of the maximal EPSC amplitudes (±SEM) are shown. Pairing induction is indicated with an arrow. (Insets) Mean of 10 to 15 successive EPSCs recorded before and after pairing. Scale, 20 ms, 50 pA.*

(B) *Summary histogram of LTP experiments. The percent increase in EPSC amplitude after pairing is shown. Values for EPSC potentiation were assessed 25 min after induction. No LTP is induced in WT mice in the presence of NMDA antagonists (5 μM R-CPP + 10 μM 7-Cl-kynurenate; WT + NMDA antagonist; $p < 0.001$ compared to WT, Student's t test) and in the absence of paradigm-associated depolarization (WT with pairing at −70 mV; $p < 0.05$ compared to WT, Student's t test). LTP is not significantly impaired in the presence of 1 μM CGP54626 (WT +CGP). The ANOVA/Scheffe post hoc test was used for the comparison of*

genotypes. For clarity, only the statistical significance between the genotypes linked by the brackets are shown ($^{*}p < 0.05$; $^{**}p < 0.01$; $^{***}p < 0.001$).

(C) *The paired-pulse ratio of EPSCs at CA3-to-CA1 synapses in WT (2.54 ± 0.11; n = 15), $1a^{-/-}$ (2.27 ± 0.16; n = 15) and $1b^{-/-}$ (2.64 ± 0.28; n = 8) mice was similar.*

(D) *The $GABA_B$ antagonist CGP54626 (1 μM) did not alter mEPSC frequency (increase of 13.6% ± 15.3% versus control; n = 11) or amplitude (increase of 4.3% ± 5.1%; n = 11) in WT mice.*

(E) *The frequency of mEPSCs was increased in $1a^{-/-}$ mice (WT: 0.44 ± 0.05 Hz, n = 11; $1a^{-/-}$: 0.90 ± 0.14 Hz, n = 15; $1b^{-/-}$: 0.49 ± 0.09 Hz, n = 8; $p < 0.05$, Student's t test). In contrast, the mEPSC amplitude did not differ between WT (16.39 ± 0.79 pA; n = 11), $1a^{-/-}$ (17.12 ± 0.78 pA; n = 18), and $1b^{-/-}$ (15.68 ± 0.88 pA; n = 8) mice.*

(F) *Raw traces of AMPA and NMDA receptor-mediated EPSCs components (top). The protocol used to determine the CV_{AMPA} and CV_{NMDA} is outlined. At −70 mV, NMDA receptors are blocked by Mg^{2+} ions, and the EPSCs are primarily mediated by AMPA receptors. NMDA receptor-mediated EPSCs were recorded in the same cell at +30 mV in the presence of 10 μM DNQX, a non-NMDA receptor antagonist.*

(G) *The variability of the AMPA compared to the NMDA EPSC component (calculated as $[1 - (CV_{NMDA}/CV_{AMPA})] \times 100$) is significantly smaller in $1a^{-/-}$ than in WT mice (WT: 34.0 ± 5.0, n = 12; $1a^{-/-}$: 5.6 ± 3.9, n = 10; $p < 0.01$, Student's t test), suggestive of a decreased proportion of silent synapses. WT mice were littermates of $1a^{-/-}$ mice. Data are represented as mean ± SEM.*

Impaired Object Recognition in $1a^{-/-}$ Mice

Changes in hippocampal LTP accompany certain alterations in cognitive function (Barnes et al., 1994). We used an object recognition task that depends on hippocampal function (Broadbent et al., 2004) to analyze whether impaired presynaptic heteroreceptor inhibition and lack of LTP in $1a^{-/-}$ mice is paralleled by memory deficits. The task relies upon the tendency of rodents to attend to a novel object more than to a familiar one. For each mouse, we scored the number of stretch attend postures (SAP, defined as head and shoulders extended toward the object) in response to a PVC disc presented at times 10 min and 24 hr following initial presentation at time 0, as well as to a novel PVC cone at 24 hr + 10 min. Wild-type and $1b^{-/-}$ mice, in contrast to $1a^{-/-}$ mice, showed a significantly reduced number of SAPs toward the familiar object (time 10 min) and subsequently an increased number of SAPs toward the novel versus familiar object (time 24 hr + 10 min) (Figure 8A). Calculation of discrimination indices (DIs) showed that $1a^{-/-}$ mice did not discriminate between familiar or novel objects (Figure 8B). Therefore, in $1a^{-/-}$ mice, the lack of LTP is correlated with an impairment of nonspatial hippocampal

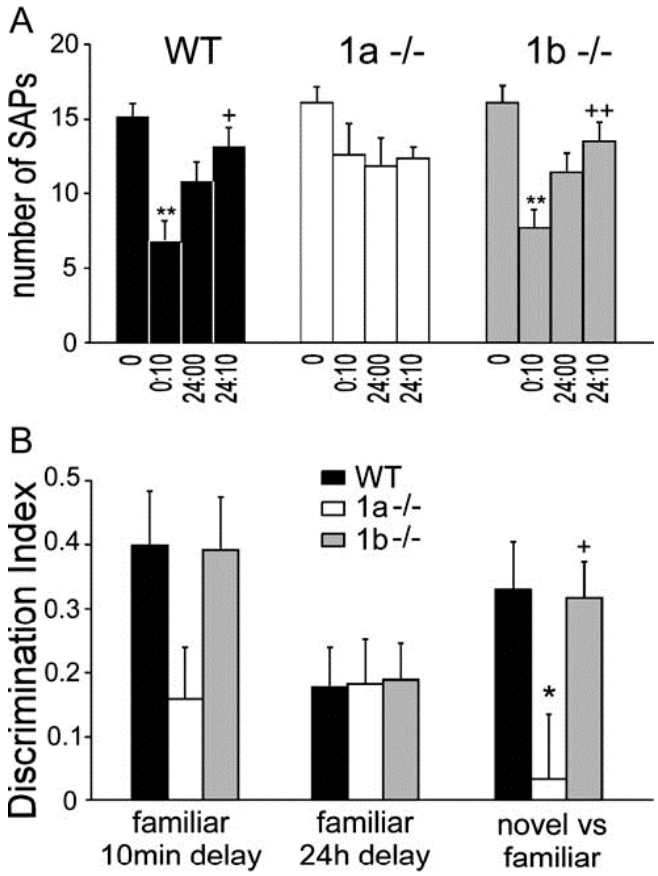

Figure.8. Impaired Object Recognition in $1a^{-/-}$ Mice

(A) *Data represent the number of SAPs (mean ± SEM) to a PVC disc presented at time 0 min (0), 10 min (0:10), and 24 hr (24:00), and to a novel PVC cone at 24 hr + 10 min (24:10).* $^{**}p < 0.01$ *versus 0 min; +p < 0.05 versus 10 min; ++p < 0.01 versus 10 min.* $1a^{-/-}$ *mice do not discriminate between familiar and novel objects (*$\chi^2 = 5.824$*, 3 df, p = 0.121), in contrast to WT (*$\chi^2 = 13.80$*, 3 df, p = 0.003) and* $1b^{-/-}$ *mice (*$\chi^2 = 23.016$*, 3 df, p < 0.001). This deficit of* $1a^{-/-}$ *mice was also evident in a separate cohort of mice (data not shown).*

(B) *Discrimination indices (DIs; mean ± SEM) in the object recognition test for WT,* $1a^{-/-}$*, and* $1b^{-/-}$ *mice. Time points for calculating DIs were chosen to reflect the following: short-term memory of a familiar object (familiar 10 min delay), long-term memory of a familiar object (familiar 24 hr delay), and short-term discriminative memory between a novel and familiar object (novel versus familiar). The mean DI for discrimination of a familiar object after 10 min delay appeared to be lower in* $1a^{-/-}$ *mice but failed to meet statistical significance [DI: F(2, 26) = 2.006; p = 0.149]. However, the decrease in the mean DI for discrimination of a novel versus a familiar object is significantly lower in* $1a^{-/-}$ *mice than in* $1b^{-/-}$ *or WT mice [F(2, 26) = 4.404; p = 0.023]. After a delay of 24 hr, the three genotypes similarly demonstrated a lack*

of familiarity with the previously presented disc [DI: F(2, 26) = 0.001; p = 0.999]. $^{*}p = 0.05$ versus WT; +p < 0.05 versus $1a^{-/-}$.

memoryformation. The effects on synaptic plasticity and memory formation in $1a^{-/-}$ mice emphasize that the $GABA_{B1b}$ protein cannot compensate for the loss of $GABA_{B1a}$ protein.

Discussion

The objective of this study was to determine if $GABA_{B1a}$ and $GABA_{B1b}$ exhibit functional or pharmacological differences in vivo. Our experiments with genetically modified mice indicate that, at CA3-to-CA1 synapses, $GABA_{B1a}$ assembles heteroreceptors inhibiting glutamate release, while predominantly $GABA_{B1b}$ mediates postsynaptic inhibition (Figure 4). This functional specialization relates, at least in part, to a distinct subcellular distribution of the $GABA_{B1}$ isoforms (Figure 5). Autoreceptor function is unaltered in the $1a^{-/-}$ and $1b^{-/-}$ mice (Figures 4C and 4D). Possibly, both $GABA_{B1a}$ and $GABA_{B1b}$ are present at GABAergic terminals impinging onto CA1 pyramidal neurons. However, since our recordings from the CA1 pyramidal soma cannot distinguish IPSCs from different types of GABAergic neurons, it is equally possible that some GABAergic terminals express $GABA_{B1a}$ and others express $GABA_{B1b}$. In general, the extent of subcellular segregation of $GABA_{B1a}$ and $GABA_{B1b}$ may vary according to brain regions and cell types. For example, GABAergic neurons impinging onto cortical layer 5 pyramidal neurons express $GABA_{B1a}$ but not $GABA_{B1b}$ at their terminals (Pérez-Garci et al., 2006). The distribution of $GABA_{B1a}$ and $GABA_{B1b}$ may also vary within the dendritic compartment. This is suggested by the organotypic slice culture experiments showing that $GABA_{B1a}$-GFP is mostly excluded from dendritic spines, while $GABA_{B1b}$-GFP is expressed in most spines (Figure 6).

No significant pharmacological differences were found in radioligand binding experiments with cortical membranes from $1b^{-/-}$ and $1a^{-/-}$ mice (Figure 3). This confirms that $GABA_B$ isoforms display a similar binding pharmacology in vivo, as already suggested by earlier experiments with the photoaffinity antagonist [^{125}I]CGP71872 (Malitschek et al., 1998). Of

note, receptors assembled from $GABA_{B1a}$ or $GABA_{B1b}$ may still display pharmacological differences in functional assays, depending on the local effector system and/or the receptor reserve. This may also be the reason why the data obtained in a functional assay (GTPγ[^{35}S] binding) and in ^{3}[H]baclofen binding show differences in the relative contribution to the total binding (Figures 3B and 3C). Depending on the subcellular localization, $GABA_{B1a}$ and $GABA_{B1b}$ may also be exposed to different concentrations of ambient GABA. Tonic activation of $GABA_B$ auto- but not heteroreceptors could, for example, account for different potencies of baclofen in inhibiting release at excitatory and inhibitory terminals (Lei and McBain, 2003 and Scanziani, 2000). Moreover, $GABA_{B1a}$ and $GABA_{B1b}$ may exhibit distinct desensitization properties depending on their localization and exposure to cyclic AMP-dependent protein kinase (Couve et al., 2002). These factors may have contributed to pharmacological differences between pre- and postsynaptic receptors reported in the past (Lei and McBain, 2003 and Pozza et al., 1999). However, they likely do not explain differences in the rank order of drug potencies at native $GABA_B$ receptors, which have been reported as well (Bonanno et al., 1997 and Cunningham and Enna, 1996).

An interesting question is how the functional segregation between the $GABA_{B1a}$ and $GABA_{B1b}$ isoforms is achieved. In principle, receptor compartmentalization could involve mechanisms such as mRNA trafficking, protein targeting, or protein retention (Horton and Ehlers, 2003 and Sampo et al., 2003). We addressed the mechanism underlying the differential compartmentalization by expressing GFP-tagged $GABA_{B1a}$ or $GABA_{B1b}$ proteins in hippocampal neurons in organotypic slice cultures. The data show an almost exclusive association of the $GABA_{B1a}$-GFP protein with the axons of transfected CA3 neurons (Figure 6). We therefore favor protein targeting or retention as the reason for $GABA_{B1a}$ compartmentalization, in which case the information for segregation is probably carried by the extracellular pair of sushi repeats, the only region of sequence divergence between $GABA_{B1a}$ and $GABA_{B1b}$. Interestingly, the two sushi repeats in $GABA_{B1a}$ have strikingly different structural properties (Blein et al., 2004). This led to the proposal that they participate in protein interactions with multiple partners, which could generate additional heterogeneity in the $GABA_B$ receptor system.

An open question remains why LTP at CA3-to-CA1 synapses is impaired in $1a^{-/-}$ mice. Since autoreceptor and postsynaptic $GABA_B$ functions are preserved in $1a^{-/-}$ mice (Figure

4), the impairment of LTP must relate to the constitutive absence of heteroreceptors. Heteroreceptors do not appear to be activated by ambient or released GABA under baseline conditions (Figures 7C and 7D), as already suggested in earlier experiments (Morrisett et al., 1991 and Scanziani, 2000). Presumably, heteroreceptors are only activated during periods of intense neuronal activity, when GABA released from interneurons spills over to the glutamatergic terminals. Uncontrolled release of glutamate during such periods is likely to trigger adaptive changes (Burrone and Murthy, 2003). For example, excess released glutamate may spill over to synapses at which glutamate release has not occurred (Scimemi et al., 2004), which could convert silent synapses to a functional state (Isaac et al., 1995 and Liao et al., 1995). The observed increase in the mEPSC frequency in $1a^{-/-}$ mice (Figure 7E) could reflect such an increase in the rate of activation of previously silent synapses (Liao et al., 1999). We addressed this possibility and compared the CVs of AMPA and NMDA receptor-mediated EPSCs in wild-type and $1a^{-/-}$ mice. The CV_{AMPA} was significantly reduced in $1a^{-/-}$ mice, while the CV_{NMDA} was unaffected by genotype, consistent with a decreased number of silent synapses in $1a^{-/-}$ mice (Kullmann, 1994). Since silent synapses provide an ideal substrate for LTP (Durand et al., 1996, Isaac et al., 1995, Kullmann, 1994, Liao et al., 1995 and Malinow and Malenka, 2002), the observed impairment of LTP in $1a^{-/-}$ mice could be explained by the decrease in the proportion of silent synapses. A plausible physiological role for heteroreceptors could therefore be to limit the loss of silent synapses and to ensure that plasticity processes are maintained in the dynamic range. However, the constitutive absence of heteroreceptors in $1a^{-/-}$ mice may have allowed time for other compensatory adaptations. For example, disinhibition of adenylate cyclase activity (Pineda et al., 2004), transcriptional (West et al., 2002) and/or morphological changes (Luthi et al., 2001) may contribute to the impairment of LTP and hippocampus-dependent memory. Importantly, however, the LTP and behavioral data reinforce that $GABA_{B1a}$ and $GABA_{B1b}$ convey separate functions in vivo.

In summary, our combined physiological, morphological, and behavioral analysis of $1a^{-/-}$ and $1b^{-/-}$ mice clearly establishes that $GABA_{B1a}$ and $GABA_{B1b}$ are differentially compartmentalized and fulfill distinct functions. We hypothesize that interactions with the sushi repeats are responsible for retaining $GABA_{B1a}$ at its specific location. From a

pharmaceutical perspective, the existence of functionally distinct receptor subtypes opens up new opportunities for therapeutic interference.

Experimental Procedures

Generation and Pharmacological and Biochemical Characterization of *1a*$^{-/-}$ and *1b*$^{-/-}$ Mice

Knockin mice were generated as outlined in Figure 1. All animal experiments were subjected to institutional review and conducted in accordance with Swiss guidelines and approved by the veterinary Office of Basel-Stadt. [^{125}I]CGP64213 was synthesized at Novartis and labeled to a specific radioactivity of >2000 Ci/mmol (ANAWA, Wangen, Switzerland). The probes used for Northern blot analysis, the [^{125}I]CGP64213 displacement experiments, immunoblot, and GTPγ[^{35}S] analysis were as described (Bischoff et al., 1999, Gassmann et al., 2004 and Kaupmann et al., 1997). Since we did not observe significant differences in any of our assays between wild-type littermates derived from *1a*$^{+/-}$ or *1b*$^{+/-}$ heterozygous breeding pairs, the data from wild-type mice were pooled.

Electrophysiology

Standard procedures were used to prepare 300 μm thick parasagittal hippocampal slices from P18–P28 mice. Slices were incubated for 45 min at 35°C in an interface chamber containing saline (124 mM NaCl, 2.7 mM KCl, 1.3 mM $MgCl_2$, 2 mM $CaCl_2$, 1.24 mM NaH_2PO_4, 26 mM $NaHCO_3$, 18 mM glucose, 2.25 mM ascorbate) equilibrated with 95% O_2/5% CO_2. Slices were then kept at room temperature for at least 45 min before starting recordings at 30°C–32°C. Whole-cell patch-clamp recordings were performed from the somata of CA1 pyramidal neurons to measure holding currents and synaptic responses; neurons were visualized using infrared and differential interference contrast optics. Drugs, applied by superfusion into the recording chamber, were kept as aliquots, and solutions were freshly prepared on the day of the experiment. K^+ currents induced by baclofen (50

μM) or adenosine (100 μM) were elicited at −50 mV in the presence of TTX (1 μM). Patch electrodes (~5 MΩ) were filled with a solution containing the following: 140 mM K-gluconate, 5 mM HEPES, 2 mM $MgCl_2$, 1.1 mM EGTA, 2 mM Na_2ATP, 5 mM phosphocreatine, 0.6 mM Tris-GTP, at pH 7.25 with KOH and 285 mOsm). EPSCs and IPSCs were elicited by voltage pulses (100 μs, 2–5 V stimuli) or by current pulses (100 μs, 0.1–0.3 mA stimuli) delivered through a bipolar Pt-Ir electrode (25 μm in diameter) placed in the stratum radiatum at a distance of 150–200 μm from the soma of the recorded cell. The recording electrode was filled with a solution containing the following: 140 mM Cs-gluconate, 10 mM HEPES, 10 mM phosphocreatine, 5 mM QX-314, 4 mM Mg-ATP, 0.3 mM Na-GTP, at pH 7.25 with CsOH and 285 mOsm. EPSCs were measured at −70 mV in the presence of 100 μM picrotoxin. In some cells, stimuli were delivered in pairs (interpulse interval 70 ms) (Palmer et al., 2004), and the paired-pulse ratio (PPR) was calculated as the ratio of the 2nd EPSC amplitude/1st EPSC amplitude. IPSCs were measured at 0 mV in the presence of 2 mM kynurenic acid. For the LTP experiments, the baseline stimulus frequency was set to 0.05 Hz to minimize "rundown" of the EPSC amplitudes (Gasparini et al., 2000 and Xiao et al., 2004). Cells were voltage clamped at −70 mV during baseline and recovery periods. LTP was induced by depolarizing the cell to 0 mV while delivering 40 stimuli at 0.5 Hz at baseline stimulus intensity (pairing paradigm) (Palmer et al., 2004). When the potentiation of EPSC amplitudes lasted for >30 min, we considered this as LTP. mEPSCs were recorded at −70 mV in the presence of 0.5 μM TTX and 10 μM bicuculline. Detection and analysis of mEPSCs were done using the MiniAnalysis software (Synaptosoft, Decatur, GA). For analysis of the CV_{AMPA} (Kullmann, 1994), AMPA receptor-mediated EPSCs were recorded in the presence of 100 μM picrotoxin and 5 μM bicuculline while neurons were clamped at −70 mV (0.05 Hz stimulation). Following 15–20 min recording, non-NMDA glutamate receptors were blocked with 10 μM DNQX, and the holding voltage was changed to +30 mV. For analysis of the CV_{NMDA}, NMDA receptor-mediated EPSCs were recorded for >10 min and, as a control, eventually blocked by adding CPP (5 μM) and 7-chlorokynurenate (10 μM) to the superfusion. CV_{AMPA} and CV_{NMDA} were calculated as SD/mean of AMPA and NMDA receptor-mediated EPSC peak amplitudes, respectively. Data were obtained with an Axopatch 200B (Axon Instruments, Union City, CA), filtered at 2 kHz and digitized at 10 kHz, and acquired and analyzed with pClamp9 (Axon Instruments, Union City, CA).

Values are expressed as mean ± SEM. The experimenter was blind to the genotype of the mice.

Immunohistochemistry and Preembedding Electron Microscopy

Hippocampal sections were treated for light and electron microscopy immunolabeling as described (Gassmann et al., 2004 and Kulik et al., 2002). For ultrastructural analysis, only immunogold particles inside the plasma membrane (closer than 30 nm) of morphologically identifiable terminals (with presynaptic active zone or clear vesicles) and dendrites/spines were counted. Unassigned particles represent background labeling and labeling in axonal fibers (Kulik et al., 2002). The immunogold particle density in $1^{-/-}$ mice, which completely lack $GABA_{B1}$ protein (Schuler et al., 2001), was 7% of that seen in wild-type mice. The presynaptic percentage of particles allocated to the plasma membrane in $1^{-/-}$ mice was 52%, thus showing that background labeling equally distributes over pre- and postsynaptic membranes. Only asymmetrical (glutamatergic) synapses were analyzed. An ultrastructural analysis of GABAergic (symmetrical) synapses in $1a^{-/-}$ and $1b^{-/-}$ mice was impossible due to infrequent $GABA_{B1}$ immunogold labeling (Kulik et al., 2002 and Kulik et al., 2003). The experimenter was aware of the genotype of the mice.

Transfection of Organotypic Slice Cultures and Two-Photon Laser Scanning Microscopy

Organotypic hippocampal slices were prepared from Wistar rats at postnatal day 5 as described (Stoppini et al., 1991). After 7 days in vitro, cultures were biolistically transfected with a Helios Gene Gun (Bio-Rad, CA) with $GABA_{B1a}$-GFP or $GABA_{B1b}$-GFP expression vectors in combination with a tdimer2 expression vector (gift from R. Tsien). Expression of $GABA_{B1a}$-GFP and $GABA_{B1b}$-GFP was under control of the neuron-specific *synapsin-1* promoter (gift from K. Svoboda) for 7–8 days. For imaging, we used a custom-built two-photon laser scanning microscope based on a BX51WI microscope (Olympus, Japan) and a pulsed Ti:Sapphire laser (Chameleon XR, Coherent, Scotland) tuned to λ = 870 nm, controlled by an open source software package (ScanImage) written in Matlab (Pologruto et al., 2003). Fluorescence was detected in epifluorescence (LUMPlan W-IR2

60 × 0.9 NA, Olympus) and transfluorescence mode (achromatic aplanatic condenser, 1.4 NA, Olympus) using four photomultiplier tubes (R2896, Hamamatsu, Japan). We used 725DCXR dichroic mirrors and E700SP blocking filters to reflect emitted photons into a secondary beamsplitter, containing a 560DCXR dichroic, 525/50 (green) and 610/75 (red) band-pass filters (AHF Analysentechnik AG, Tübingen, Germany). The slice was placed into a perfusion chamber and superfused continuously (2 ml/min) with ACSF (119 mM NaCl, 2.5 mM KCl, 4 mM $CaCl_2$, 4 mM $MgCl_2$, 26.2 mM $NaHCO_3$, 1 mM NaH_2PO_4, 11 mM glucose, gassed with 95% O_2 and 5% CO_2 at room temperature). Stacks of images (256 × 256 pixels) from secondary dendritic branches and thin axons were obtained from transfected CA3 and CA1 pyramidal neurons (Z step: 0.5 μm). Maximum intensity projections of green and red stacks were constructed. For the ratio images, we used a hue/saturation/brightness model, where hue was determined by the green/red ratio (using a rainbow color table), and the intensity in the red channel was used to set the brightness. For quantitative analysis, we calculated the green-to-red ratio in a region of interest (dendrite or axon) after subtracting the background fluorescence. To compensate for differences in laser power and expression level, we normalized the ratio in the axon by the average dendritic ratio. Spines were identified by anatomy from tdimer2 images. $GABA_{B1a}$-GFP- and $GABA_{B1b}$-GFP-positive spines were defined as having intensity in the green channel at least three standard deviations above background.

Object Recognition Test

The test was designed according to the principles of Ennaceur and Delacour (1988), which rely upon the natural tendency of rodents to attend to a novel object more than a familiar one. Male wild-type (n = 7), $1a^{-/-}$ (n = 8), and $1b^{-/-}$ (n = 13) single-housed mice, aged 21 (± 0.7) weeks, were used. Mice were habituated overnight (17–21 hr) to a novel enclosure [22 × 37 × 15 (h)cm], with ~2 cm sawdust and standard food and water provided ad libitum until testing began. All sessions were recorded on video while the experimenter was out of the testing room. The number of SAPs for each mouse in each 3 min period was scored by a trained observer blinded to the animals' genotypes. All videos were scored twice by the same observer, and duplicate SAP scores were averaged within animal and time point. The intrascorer correlation (Pearson Product Moment correlation) was 0.91. A

DI, the difference in SAP numbers at a pair of time points divided by the total number of SAPs at those time points, was calculated for each animal (Figure 8B). DIs reflect (1) short-term memory of a familiar object ([Number of SAPs at Time 0 min − Number of SAPs at Time 10 min]/[Total number of SAPs at both time points]); (2) long-term memory of a familiar object ([Number of SAPs at Time 0 min − Number of SAPs at Time 24 hr]/[Total number of SAPs at both time points]); and (3) short-term discriminative memory between a novel and a familiar object ([Number of SAPs at Time 24 hr + 10 min − Number of SAPs at Time 10 min]/[Total number of SAPs at both time points]). A DI of 1 reflects perfect discrimination, while a DI of 0 indicates complete loss of discrimination. SAP data were analyzed within a given genotype for the factor “Time” using the nonparametric Friedman repeated measures ANOVA on ranks test followed by Dunn's method for post hoc analysis. DIs were analyzed within a given time for the factor “Genotype” using one-way ANOVA followed by Fisher's LSD post hoc analysis.

Reagents

Tetrodotoxin (TTX) was from Latoxan (Valence, France). (R)-CPP [3-((R)-2-carboxypiperazin-4-yl)-1-phosphonic acid] and 7-chlorokynurenic acid (7-chloro-4-hydroxyquinoline-2-carboxylic acid) were from Tocris Cookson Ltd. (Bristol, UK). Baclofen and CGP54626 were from Novartis Pharma AG (Basel, Switzerland). All other reagents were from Fluka/Sigma (Buchs, Switzerland).

Acknowledgments

This study was supported by the Swiss Science Foundation (3100-067100.01; B. Bettler), the Désirée and Nils Yde Foundation (B. Bettler), the Danish Medical Research Council (H.B.-O.), the Human Frontier Science Program (R.T), the Grant Agency of the Czech Republic (309/03/1158; R.T.), the Wellcome Trust (International Senior Research Fellowship; R.T.), and the National Institutes of Mental Health/National Institute of Drug Abuse (U01 MH69062; J.F.C., K.K., L.H.J.). We thank A. Lüthi, M. Larkum, and M. Rüegg for critical reading of the manuscript. Some of the authors of this manuscript work

for Novartis Pharma AG, which has an interest in $GABA_B$ receptors as drug targets. The authors declare no competing financial interest.

Chapter III

THE SUSHI DOMAINS OF $GABA_B$ RECEPTORS FUNCTION AS A DOMINANT AXONAL TARGETING SIGNAL

Barbara Biermann, Amyaouch Bradaia, Klara Ivankova-Susankova, Valerie Besseyrias, Said Abdel Aziz, Josef P. Kapfhammer, Martin Gassmann, Bernhard Bettler

In preparation

Abstract

$GABA_B$ receptor subtypes are differentially localized and exhibit non-redundant synaptic functions in glutamatergic neurons. Here we demonstrate that the sushi domains (SDs), conserved protein interaction motifs present in the ectodomain of the $GABA_{B1a}$ subunit isoform direct axonal localization. In the absence of this isoform endogenous $GABA_B$ receptors are confined to the somatodendritic compartment and fail to form presynaptic receptors controlling glutamate release. When exogenously expressed in cultured hippocampal neurons, $GABA_{B1a}$ is targeted to axons, but not $GABA_{B1b}$, an isoform lacking the SDs. Moreover, mutations preventing disulfide bond formation within the SDs abolish axonal targeting of $GABA_{B1a}$, suggesting that appropriate folding of the SDs is essential. The SDs of $GABA_{B1a}$ are sufficient to redirect a somatodendritic metabotropic glutamate receptor to the axonal compartment, indicating dominance of the axonal determinant. Moreover, we provide evidence that somatodendritic targeting of $GABA_B$ receptors involves the cytoplasmic C-terminal domain of the $GABA_{B2}$ subunit. Thus a combination of extracellular/luminal and cytoplasmic targeting signals mediates axonal and dendritic localization of $GABA_B$ receptors.

Introduction

$GABA_B$ receptors are the G protein-coupled receptors for γ-aminobutyric acid (GABA), the main inhibitory neurotransmitter in the brain. Depending on their subcellular localization $GABA_B$ receptors exert distinct regulatory effects on synaptic transmission. Activation of presynaptic $GABA_B$ receptors suppresses neurotransmitter release at inhibitory as well as excitatory terminals, whereas postsynaptic $GABA_B$ receptors induce membrane hyperpolarization thereby inhibiting neuronal excitability. Molecular diversity in the $GABA_B$ system arises from the $GABA_{B1}$ subunit isoforms, $GABA_{B1a}$ and $GABA_{B1b}$ (Kaupmann et al., 1997). These isoforms differ in their N-terminal ectodomain by a pair of tandemly arranged sushi domains (SDs) that are unique to $GABA_{B1a}$ (Hawrot et al., 1998). Most if not all neurons in the central nervous system co-express both $GABA_{B1}$ isoforms, which combine with $GABA_{B2}$ subunits to form functional heteromeric receptors. Thus, it is generally accepted that two $GABA_B$ receptor subtypes, $GABA_{B(1a,2)}$ and $GABA_{B(1b,2)}$, are

assembled in individual neurons. We have recently shown that these two pharmacologically indistinguishable $GABA_B$ receptor subtypes exhibit non-redundant synaptic functions, most likely resulting from their differential compartmentalization. The most distinctive feature is the selective localization of the $GABA_{B1a}$ isoform at glutamatergic terminals at various synapses (Perez-Garci et al., 2006; Shaban et al., 2006; Ulrich et al., 2007; Vigot et al., 2006). It is likely that the SDs, the only region of sequence divergence between $GABA_{B1a}$ and $GABA_{B1b}$, play an important role in the axonal localization of $GABA_B$ receptors. SDs are conserved protein interaction motifs also known as complement control proteins (CCP) modules or short consensus repeats. They mediate protein interactions in proteins of the complement system as well as in a wide variety of adhesion molecules (Lehtinen et al., 2004; Morley and Campbell, 1984). Binding of the extracellular matrix (ECM) protein fibulin-2 to the SDs of $GABA_{B1a}$ has been reported (Blein et al., 2004), however, the physiological relevance of this interaction is unclear. SDs were recently identified as a structural module in the extracellular domains of other G protein-coupled receptors (GPCRs) (Grace et al., 2004), where they engage in ligand-binding or are thought to facilitate extracellular protein interactions (Perrin et al., 2006).

The accurate sorting and transport of proteins to distinct plasma membrane domains, such as axons and dendrites, is fundamental for neuronal signaling. Sorting generally occurs in the trans-Golgi network (TGN). There proteins are selectively packaged into axonal and/or somatodendritic carriers that are transported along microtubuli into the appropriate compartment where they fuse with the plasma membrane. Asymmetric distribution of neuronal membrane proteins can also be achieved following non-selective delivery into axons and dendrites via selective retention at the appropriate cell-surface domain and/or preferential endocytosis from the plasma membrane in inappropriate compartments (Craig and Banker, 1994; Horton and Ehlers, 2003; Winckler and Mellman, 1999). Usually sorting of membrane proteins in neurons relies on targeting signals, some of which are related to known determinants identified in polarized epithelial proteins. In particular, transport of membrane proteins to the somatodendritic compartment is often mediated by cytoplasmic signals involved in basolateral targeting in epithelial cells (Jareb and Banker, 1998; West et al., 1997). In contrast, axonal targeting usually involves diverse cytosolic or luminal sequence motifs, which are distinct from the known apical sorting determinants

(Winckler and Mellman, 1999). Thus, axonal targeting of NgCAM, a neural cell adhesion molecule, depends on sequences in its ectodomain, which mediate sorting into carriers that directly deliver their cargo to the axonal membrane (Sampo et al., 2003). However, an indirect axonal targeting pathway involving endocytosis of NgCAM from the somatodendritic domain was also proposed (Wisco et al., 2003). Similarly VAMP2, a synaptic vesicle v-SNARE protein is removed from the dendritic membrane and polarized to the axonal surface due to an endocytosis motif in its cytoplasmic domain (Sampo et al., 2003). A number of studies addressed the subcellular targeting of GPCRs and identified an important role of the cytosolic C-terminal domains (Das and Banker, 2006; Francesconi and Duvoisin, 2002; Jolimay et al., 2000; Stowell and Craig, 1999). A discrete tripeptide motif RRK was identified in the membrane proximal region of mGluR1, which directs axonal targeting of the shorter splice variant mGluR1b in retinal ganglion cells. In mGluR1a this motif is masked by its longer C-terminal tail also harboring somatodendritic targeting information (Francesconi and Duvoisin, 2002). For mGluR5 the interaction with different Homer1 proteins regulates axonal versus dendritic targeting in cerebellar granule cells (Ango et al., 2000). Moreover, a 60 amino acid sequence in the C-terminal tail of mGluR7 was shown to direct axonal targeting, whereas the homologous domain in mGluR2 mediates axonal exclusion (Stowell and Craig, 1999).

The present study aimed at identifying the sequence determinants and mechanisms underlying axonal localization of $GABA_B$ receptors. We designed epitope-tagged expression constructs of individual $GABA_B$ receptor subunits and investigated their axonal and dendritic targeting in cultured hippocampal neurons. Our data identify the SDs of $GABA_{B1a}$ as a novel axonal targeting signal that is able to function in the context of a heterologous protein. Additionally, we found that the cytosolic C-terminal domain of the $GABA_{B2}$ subunit harbours somatodendritic targeting information. Therefore, our data suggest a model in which differential targeting of heteromeric $GABA_B$ receptors is mediated by a co-operation of the SDs with dendritic targeting signals.

Results

Differential subcellular distribution of $GABA_{B1}$ isoforms in cultured hippocampal neurons.

Imaging studies in hippocampal slice cultures have shown that $GABA_{B1a}$, but not $GABA_{B1b}$ protein is present in the axons of transfected pyramidal neurons (Vigot et al., 2006). It is likely that the extracellular pair of SDs, the only region of sequence divergence between $GABA_{B1a}$ and $GABA_{B1b}$, dictates axonal localization. Because the SDs are evolutionary conserved protein interaction motifs we speculated that they mediate axonal localization through interaction with specific protein(s). However, the specific sequence determinant(s) for axonal localization of $GABA_{B1a}$ as well as the cellular mechanisms involved are unknown. We first investigated whether axonal localization of $GABA_{B1a}$ is retained when the characteristic cytoarchitecture of the hippocampus is disrupted. To this aim we assessed the distribution of specific $GABA_{B1}$ isoforms in dissociated hippocampal neurons, which provide a suitable experimental system to study axonal versus dendritic targeting of transmembrane proteins (Stowell and Craig, 1999).

Due to the lack of isoform-specific antibodies we determined the subcellular localization of endogenous $GABA_{B1}$ isoform in cultured hippocampal neurons established from mice lacking one or the other isoform (referred to as $1a^{-/-}$ and $1b^{-/-}$ mice, respectively) (Vigot et al., 2006). Pyramidal neurons, which typically make up 85-90% of neurons in cultured hippocampal neurons (Goslin K., 1998) were identified by their extensively branched spiny dendrites (Benson et al., 1994; Obermair et al., 2003). The discrimination between axons and dendrites was based on MAP2 staining, a somatodendritic marker protein (Caceres et al., 1984). In $1b^{-/-}$ pyramidal neurons, punctuate endogenous $GABA_{B1a}$ staining was observed in the somatodendritic domain as well as along the axon (Fig. 1 A). In contrast, in $1a^{-/-}$ pyramidal neurons $GABA_{B1b}$ labelling is restricted to the somatodendritic compartment (Fig. 1 A). This demonstrates that in dissociated hippocampal neurons $GABA_{B1a}$, but not $GABA_{B1b}$ localizes to axons, indicating that the axonal targeting of $GABA_{B1a}$ is achieved by a cell intrinsic mechanism.

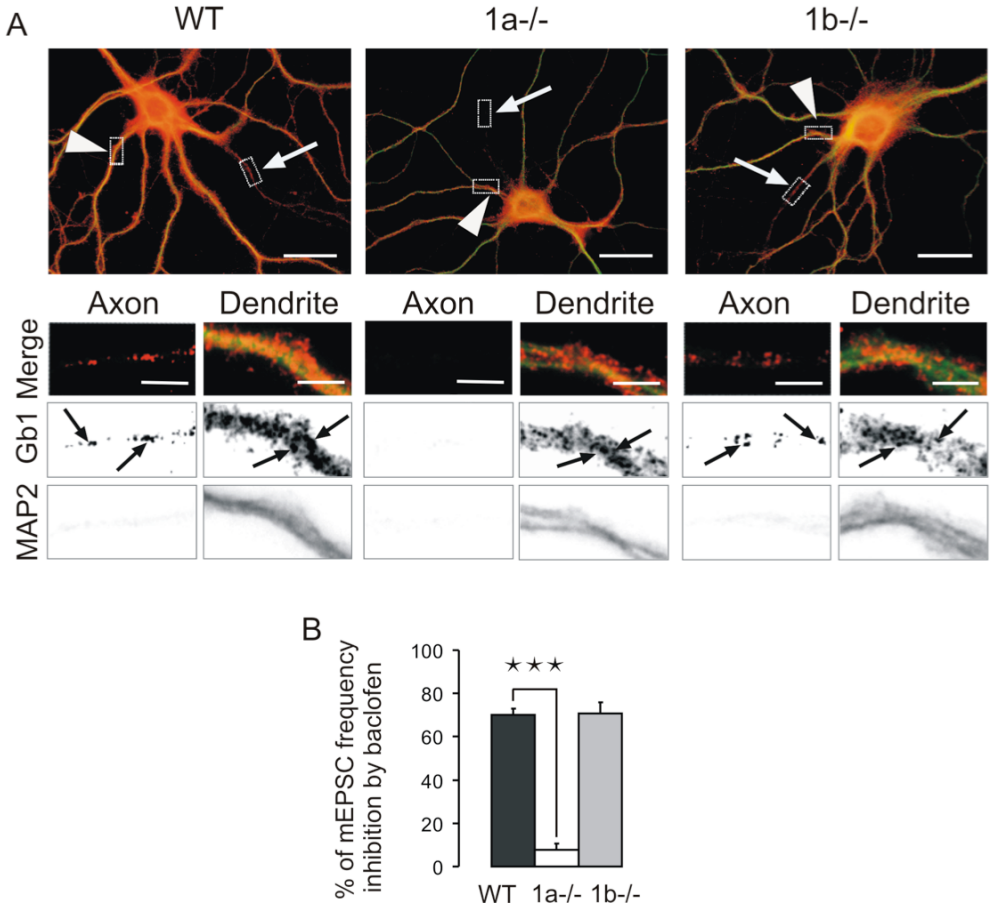

Figure 1. Differential subcellular distribution and functional segregation of $GABA_{B1}$ isoforms in cultured hippocampal neurons.

(A) *Cultured hippocampal neurons from wild-type (WT), $GABA_{B1a}^{-/-}$ (1a-/-) and $GABA_{B1b}^{-/-}$ (1b-/-) mouse embryos were fixed at DIV23, permeabilized and stained with a polyclonal antibody against the common C-terminal domain of $GABA_{B1}$ (Gb1) and an antibody against the dendritic marker MAP2. The upper panels show merged pictures of the antibody labelling against $GABA_{B1}$ (red) and MAP2 (green) on neurons from the genotypes indicated. The boxed areas marked by arrows (axons) and arrowheads (dendrites) are shown in the lower panels at higher magnification. Whereas in WT and 1b-/- neurons $GABA_{B1}$ staining is present in soma, axons and dendrites, in 1a-/- neurons it is only observed in soma and dendrites. This indicates that in cultured hippocampal neurons endogenous $GABA_{B1b}$ protein is excluded from axons. Scale bar upper panels 25 µm, lower panels 5 µm. Black arrows indicate distinct $GABA_{B1}$ labelled puncta along axons and dendrites.*

(B) *The percentage of mEPSC frequency inhibition by the selective $GABA_B$ receptor agonist baclofen was analyzed in 2-3 weeks old cultured hippocampal neurons obtained from WT, 1a-/- and 1b-/- mouse embryos (mean ± SEM, n = 10-16 per genotype). Baclofen (50 µM) inhibits the frequency of mEPSCs in WT (78.1 ± 3.1%), in 1b-/- (70.8 ± 5.1%) but not in 1a-/- (7.7 ± 2.8%) neurons. This demonstrates that 1a-/- neurons lack functional heteroreceptors controlling the release of glutamate from presynaptic terminals. Statistics: One-way ANOVA, Scheffe post-hoc test, p*** ≤ 0.001.*

$GABA_{B1a}$, but not $GABA_{B1b}$, assembles presynaptic receptors inhibiting glutamate release from cultured hippocampal neurons.

In hippocampal slices axonal localization of $GABA_{B1a}$ is associated with a functional specialization. Exclusively $GABA_{B1a}$ assembles heteroreceptors inhibiting glutamate release at CA3-to-CA1 synapse (Vigot et al., 2006). We therefore investigated whether this functional specialization is retained in cultured hippocampal neurons. Activation of heteroreceptors by baclofen, a specific $GABA_B$ agonist, inhibits the spontaneous release of glutamate resulting in a reduction of the frequency of miniature excitatory postsynaptic currents (mEPSCs) (Yamada et al., 1999). Accordingly, baclofen-induced inhibition of mEPSC frequency is a measure for functional $GABA_B$ heteroreceptors. As shown in Fig. 1 B, baclofen significantly reduced the frequency of mEPSCs recorded in WT neurons. While similar results were obtained in $1b^{-/-}$ neurons, the baclofen-induced effect on mEPSC frequency was not observed in $1a^{-/-}$ neurons. This demonstrates that functional heteroreceptors are lacking in $1a^{-/-}$ neurons. Thus, the electrophysiological data confirm that exclusively $GABA_{B1a}$ localizes to glutamatergic terminals. This shows that the distinct subcellular distribution and functional specialization of $GABA_{B1}$ isoforms observed in slice cultures is retained in cultured hippocampal neurons.

$GABA_{B1}$ isoforms expressed by the synapsin-1 promoter are differentially distributed in cultured hippocampal neurons.

We next assessed whether tagged $GABA_{B1}$ isoforms expressed in transfected cultured hippocampal neurons recapitulate the subcellular distribution of the endogenous isoforms. For these experiments, $GABA_{B1}$ isoforms with an N-terminal c-myc-epitope were transfected together with a freely diffusible red fluorescent protein (RFP/tdimer2) into cultured hippocampal neurons at 5 *days-in-vitro* (DIV5). Soluble RFP outlines the morphology of transfected neurons and was used as a reference to quantify the axonal versus dendritic distribution. The $GABA_{B1}$ isoforms were expressed under control of the synapsin-1 promoter, which mediates neuron-specific expression (Boulos et al., 2006; Kugler et al., 2001). Following transfection, neurons were fixed at DIV14, permeabilized and stained with antibodies against the *c*-myc-tag and the dendritic marker protein MAP2. As shown in Fig. 2 A, Myc-1a was present in axons, soma and dendrites, whereas Myc-1b

was restricted to the somatodendritic compartment. To quantify the axonal versus dendritic receptor distribution the c-myc-specific fluorescence intensity was normalized to the RFP signal and the axon-to-dendrite (A:D) ratio was determined (Gu et al., 2003; Sampo et al., 2003). In agreement with an increased association of Myc-1a with axonal processes, the A:D ratio for Myc-1b was significantly reduced compared to Myc-1a (Myc-1a: 0.38 ± 0.06, n = 8; Myc-1b: 0.14 ± 0.05, n = 10, **p < 0.01) (Fig. 2 B). However, for both constructs the (A:D) ratio was smaller than 1.0 indicating that Myc-1a as well as Myc-1b were robustly expressed in the somatodendritic compartment. From these results we can conclude that the SDs, the only region of sequence divergence between $GABA_{B1a}$ and $GABA_{B1b}$, contain axonal targeting information. In addition, we visualized $GABA_{B1}$ isoforms at the cell surface of transfected neurons by live-cell immunostaining against the N-terminal c-myc-epitope. We failed to detect robust cell surface expression for any of the $GABA_{B1}$ constructs analyzed (unpublished data). This suggests that when exogenously expressed in neurons, the majority of $GABA_{B1}$ protein is present in intracellular membranes (Couve et al., 1998; Filippov et al., 2000).

Mutation of the SDs in $GABA_{B1a}$ abolishes axonal targeting

SDs are protein interaction motifs originally discovered in proteins of the complement cascade and in cell-adhesion molecules. Whenever they occur towards the N-terminus of a cell-surface protein, as it is the case in $GABA_{B1a}$, they were shown to directly engage in protein interactions (Hawrot et al., 1998). For binding and function it is essential that SDs are correctly folded into a compact globular structure, which is maintained by disulfide bonds between highly conserved cysteine residues (Ichinose et al., 1990; Wei et al., 2001). To confirm the functional importance of the tertiary structure of the SDs for axonal localization of $GABA_{B1a}$, we replaced two cysteines in each SD with serines to generate Myc-1aCS (Fig. 3 A). The four single-residue mutations in Myc-1aCS prevent disulfide bond formation in both SDs. Following transfection into hippocampal neurons, Myc-1aCS was robustly expressed in distal dendrites, but absent from axons (Fig. 3 B). Accordingly, the A:D ratio in Myc-1aCS was significantly reduced compared to Myc-1a (Myc-1a: 0.37± 0.06, n = 7; Myc-1aCS: 0.14 ± 0.03, n = 10; **p < 0.01; Fig. 3 C). Of note, the Myc-1aCS distribution was similar to the one observed for Myc-1b (Fig. 2). Altogether, these results

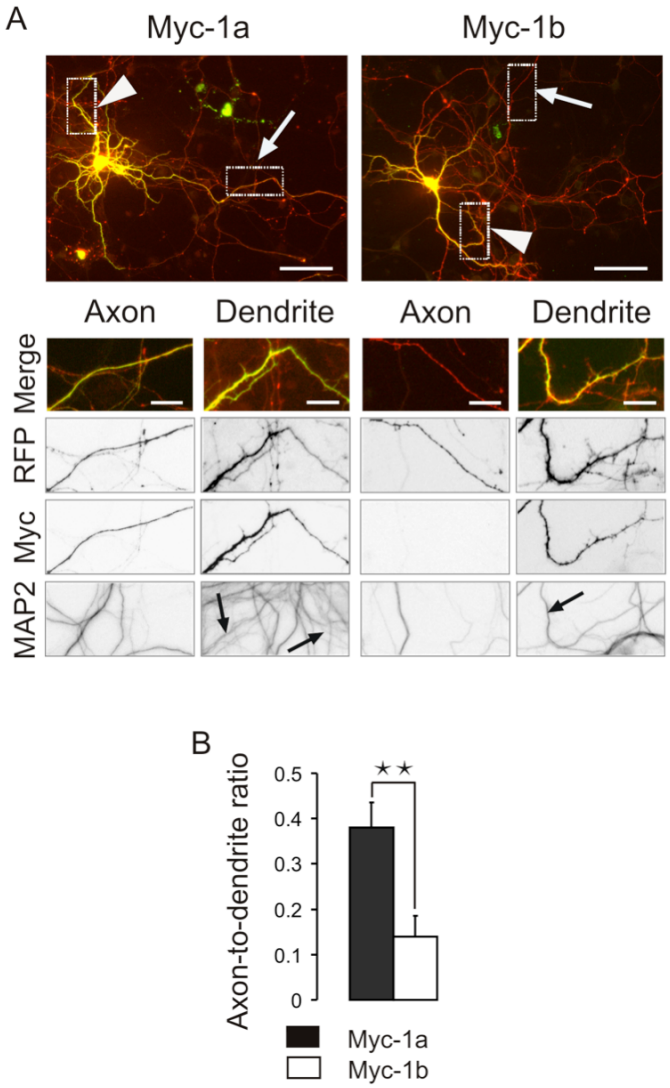

Figure 2. $GABA_{B1}$ isoforms expressed by the neuron-specific synapsin-1 promoter are differentially distributed in cultured hippocampal neurons.

(A) *Myc-tagged $GABA_{B1}$ isoforms were co-transfected with soluble RFP into cultured hippocampal neurons. At DIV14, neurons were fixed, permeabilized and stained with an antibody against the c-myc-epitope. Myc-$GABA_{B1a}$ (Myc-1a) is found in soma, axons and dendrites, whereas Myc-$GABA_{B1b}$ (Myc-1b) is restricted to the somatodendritic compartment. To distinguish between axons and dendrites the neurons were additionally stained with the dendritic marker MAP2. Pictures of the RFP signal (red) and the immunolabelling against the c-myc epitope (green) and MAP2 (blue) were merged. Scale bar upper panels 50 µm, lower panels 10 µm. Axons are marked with white arrows, dendrites with white arrowheads. MAP2-positive dendrites are indicated with black arrows.*

(B) *Axon-to-dendrite (A:D) ratio of Myc-1a and Myc-1b expression normalized to RFP (mean ± SEM, n = 8-10). The A:D ratio is significantly higher in Myc-1a than in Myc-1b transfected neurons. Statistics: Student's t-Test, p** ≤ 0.01.*

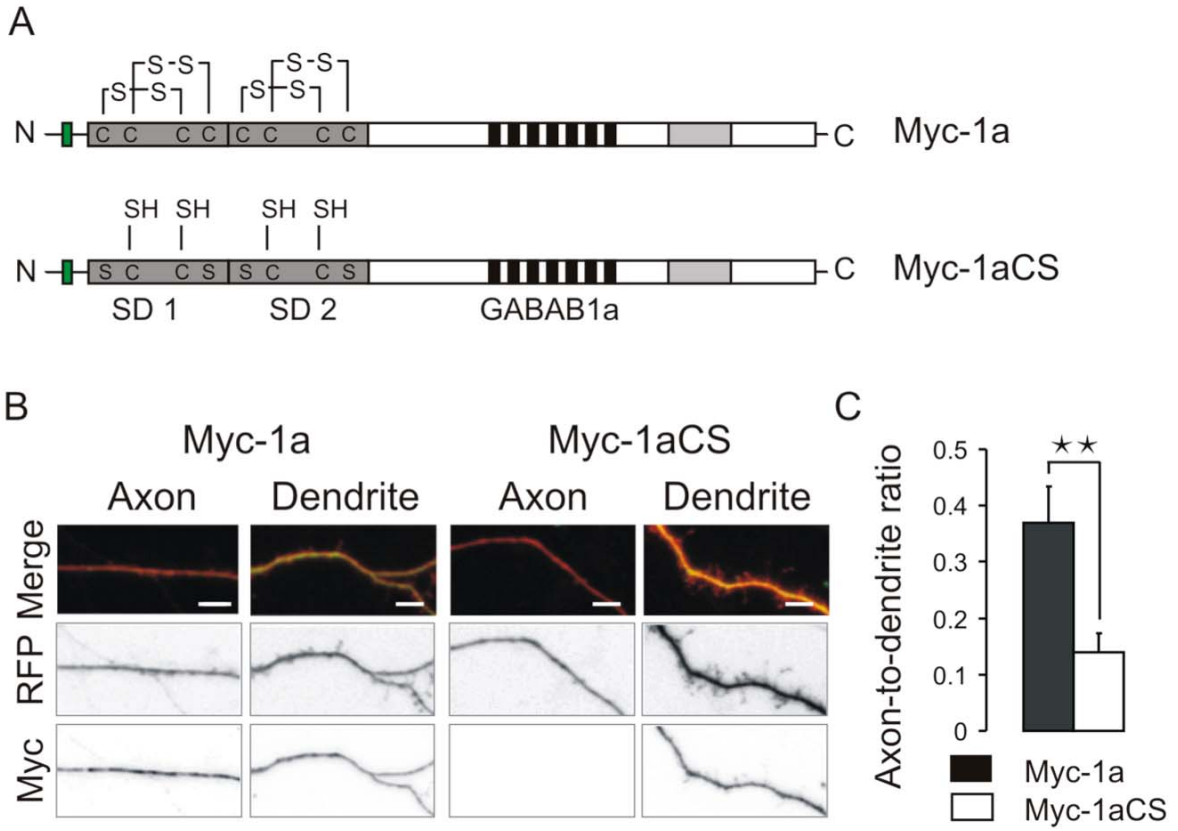

Figure 3. Mutation of the sushi domains (SDs) in $GABA_{B1a}$ abolishes axonal targeting.

(A) *Schematic representation of SD mutations on $GABA_{B1a}$. The tertiary structure of the SDs is maintained by disulfide bonds. Each SD (grey bar) possesses four cysteines (C) forming two disulfide bonds (-S-S-) in a 1-3 and 2-4 pattern (Kirkitadze & Barlow, 2001). To interfere with disulfide bond formation the first and fourth cysteine in each SD of Myc-1a were mutated to serine (S), thereby generating Myc-1aCS. The green bar represents the c-myc-epitope, black bars the transmembrane domains.*

(B) *Myc-1a and Myc-1aCS were co-transfected with soluble RFP into cultured hippocampal neurons. Neurons were fixed at DIV14, permeabilized and stained with an antibody against the c-myc-epitope. To distinguish between axons and dendrites the neurons were additionally stained with the dendritic marker MAP2 (not shown). Pictures of the RFP signal (red) and the immunolabelling against the c-myc epitope (green) were merged. In contrast to Myc-1a, Myc-1aCS is excluded from axons. Scale bar 10 µm.*

(C) *A:D ratio of Myc-1a and Myc-1aCS expression normalized to RFP (mean ± SEM, n = 7-10). The A:D ratio is significantly higher in Myc-1a than in Myc-1aCS transfected neurons. Statistics: Student's t-Test, p** ≤ 0.01.*

demonstrate that correct folding of the SDs is critical for axonal targeting of $GABA_{B1a}$. Therefore, it is likely that the SDs engage in specific protein interactions that are necessary for axonal localization of $GABA_{B1a}$.

The two $GABA_{B1a}$-specific SDs differ from each other. The first SD shows conformational heterogeneity under a wide range of conditions and interacts with the extracellular matrix protein fibulin-2, whereas the second SD is more compactly folded and shows stronger structural similarity to SDs in regulators of complement activation (Blein et al., 2004). It is therefore conceivable that the two SDs in $GABA_{B1a}$ exert different functions and interact with different proteins. Possibly, only one of the two SDs plays a role in axonal targeting. We therefore deleted either the first SD (Myc-1aΔSD1) or the second SD (Myc-1aΔSD2) from Myc-1a and analyzed their subcellular distribution in cultured hippocampal neurons. As shown in Fig. 4, both $GABA_{B1a}$ deletion mutants were observed in axons and exert no different A:D ratio compared to full-length Myc-1a (Myc-1aΔSD1: 0.49 ± 0.05, n = 8; Myc-1aΔSD2: 0.47 ± 0.04, n = 8; Myc-1a: 0.39 ± 0.06, n = 7). This suggests that each of the two SDs in $GABA_{B1a}$ is sufficient to mediate axonal localization.

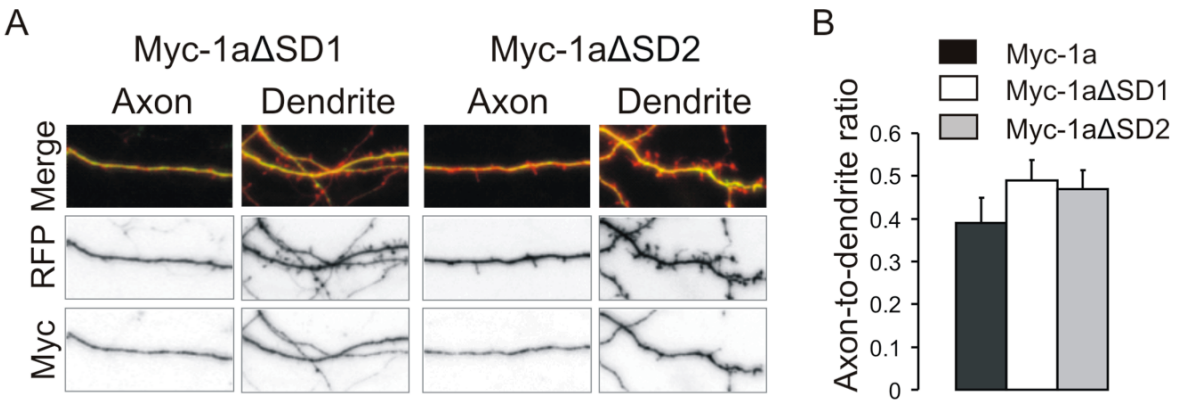

Figure 4. The individual SDs both mediate axonal targeting.

(A) *$GABA_{B1a}$ constructs missing either the first (Myc-1aΔSD1) or the second sushi domain (Myc-1aΔSD2) were co-transfected with soluble RFP into cultured hippocampal neurons. Myc-1aΔSD1 and Myc-1aΔSD2 are both found in axons and dendrites. In the upper panels, the pictures of the RFP signal (red) and the immunolabelling against the c-myc epitope (green) were merged. Scale bar 10 µm.*

(B) *A:D ratio of Myc-1a, Myc-1aΔSD1 and Myc-1aΔSD2 expression normalized to RFP (mean ± SEM, n = 7-8). No significant differences were observed between the A:D ratios of the three constructs. Statistics: One-way ANOVA, Scheffe post-hoc test, $p \geq 0.05$.*

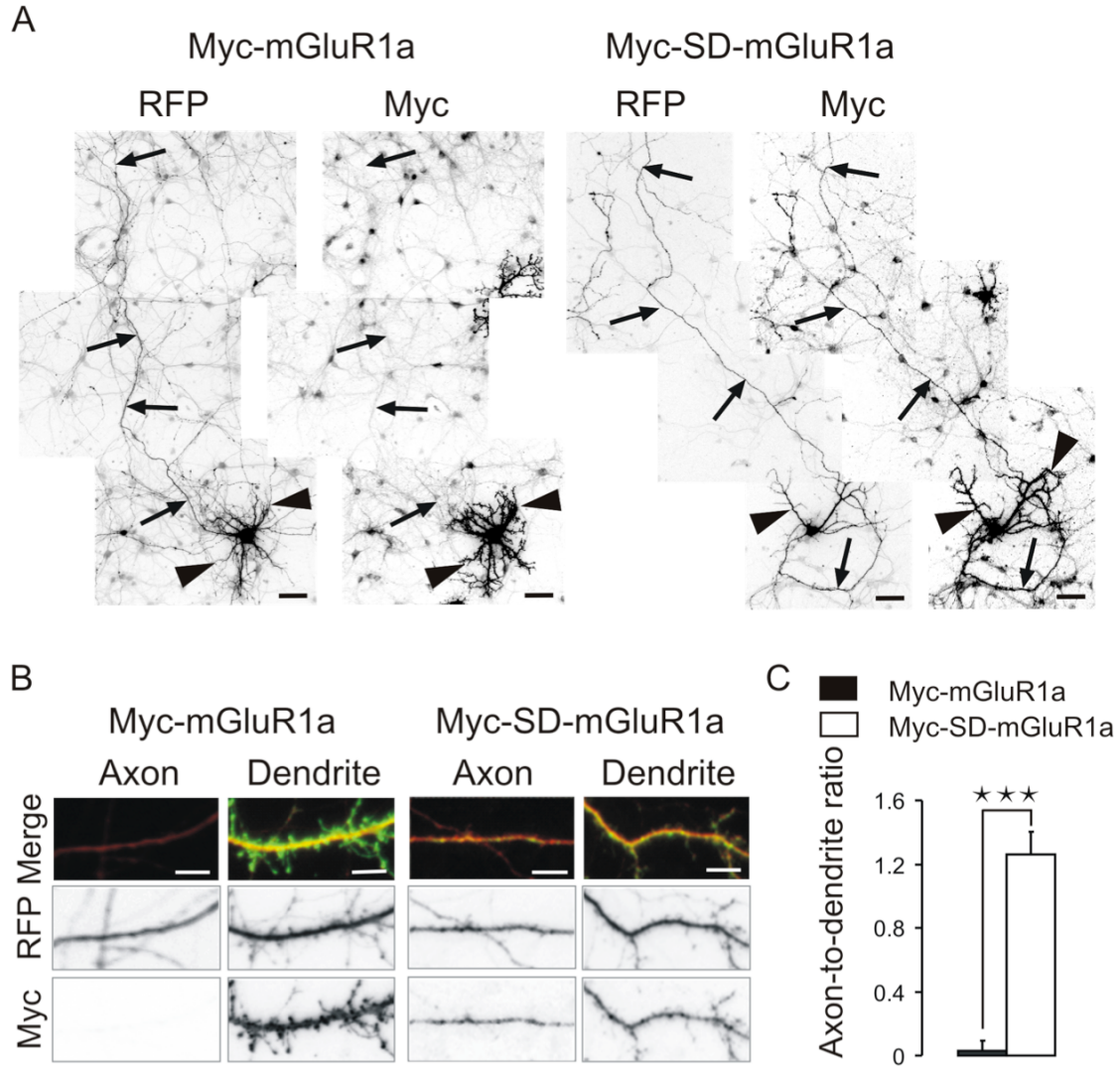

Figure 5. The SDs redirect a typical dendritic transmembrane receptor to the axon.

(A) *The SDs were fused to the extracellular N-terminal domain of metabotropic glutamate receptor 1a (mGluR1a), thereby generating Myc-SD-mGluR1a. Myc-mGluR1a and Myc-SD-mGluR1a were co-transfected with RFP into cultured hippocampal neurons. At DIV14, neurons were fixed, permeabilized and stained with an antibody against the c-myc-epitope. Myc-mGluR1a is restricted to the somatodendritic compartment, whereas Myc-SD-mGluR1a is found in the soma, axons and dendrites. Black arrows indicate the axon, black arrowheads the dendrites. Scale bar 25 µm.*

(B) *Axonal and dendritic sections of Myc-mGluR1a and Myc-SD-mGluR1a transfected neurons. In the upper panels the pictures of the RFP signal (red) and the immunolabelling against the c-myc epitope (green) were merged. Scale bar 10 µm.*

(C) *A:D ratio of Myc-mGluR1a and Myc-SD-mGluR1a expression normalized to RFP (mean ± SEM, n = 9-11). The A:D ratio is significantly higher in Myc-SD-mGluR1a compared to Myc-mGluR1a transfected neurons. Statistics: Student's t-Test, p*** ≤ 0.001.*

The SDs of $GABA_{B1a}$ redirects a typical dendritic transmembrane receptor to the axonal compartment.

We next investigated whether the SDs of $GABA_{B1a}$ are sufficient to redirect a transmembrane protein with a somatodendritic distribution to the axonal compartment. For these experiments we chose the metabotropic glutamate receptor 1a (mGluR1a), which is polarized to dendrites and clusters at postsynaptic sites (Das and Banker, 2006; Francesconi and Duvoisin, 2002). We constructed a myc-tagged SD-mGluR1a chimera, in which both SDs of $GABA_{B1a}$ were fused N-terminally to the ectodomain of mGluR1a. As expected, when expressed in cultured hippocampal neurons, "wild-type" Myc-mGluR1a was polarized to the somatodendritic compartment (Fig. 5, A and B). In contrast, Myc-SD-mGluR1a was additionally observed in axonal processes and its A:D ratio was significantly increased (Myc-mGluR1a: 0.03 ± 0.06, n = 9; Myc-SD-mGluR1a: 1.26 ± 0.15, n = 11; p*** < 0.001; Fig. 5 C). This demonstrates that the SDs of $GABA_{B1a}$ are sufficient to redirect a somatodendritic receptor to the axonal compartment. Moreover it shows that they are able to function in the context of a heterologous protein, which identifies them as a general axonal targeting signal.

The C-terminal domain of $GABA_{B1b}$ is dispensable for somatodendritic targeting.

$GABA_{B1b}$ is highly polarized to the somatodendritic compartment (Figs. 1 A and 2 A). It is therefore likely that $GABA_{B1b}$ is specifically targeted to dendrites, a process generally mediated through signals within cytoplasmic domains. Interestingly, the C-terminal tail of $GABA_{B1b}$ contains two dileucine- as well as one tyrosine-based motif reminiscent of dendritic targeting motifs identified in other membrane proteins (Jareb and Banker, 1998; Poyatos et al., 2000; Rivera et al., 2003; West et al., 1997). To evaluate the role of the C-terminal domain of $GABA_{B1b}$ in dendritic localization we generated constructs with C-terminal truncations (Fig. 6 A). Myc-1bP812 has a C-terminal truncation of 32 residues but retains the coiled-coil domain, which is important for C-terminal interaction with $GABA_{B2}$ (Pagano et al., 2001). In contrast, Myc-1bI744 lacks the entire C-terminus. When expressed in cultured hippocampal neurons both truncated $GABA_{B1b}$ subunits were observed in dendrites but not in axons, similar to full-length Myc-1b (Fig. 6 B). Accordingly, there were no significant differences between the A:D ratios of the three

constructs (Myc-1b: 0.15 ± 0.03, n = 10; Myc-1bI744: 0.17 ± 0.05, n = 10; Myc-1bP812: 0.16 ± 0.03, n = 11; Fig. 6 C). This indicates that none of the potential C-terminal dendritic targeting motifs is essential for dendritic localization and polarization of $GABA_{B1b}$.

The distal C-terminal domain of $GABA_{B2}$ is required for dendritic polarization.

A structural feature of $GABA_B$ receptors is that they assemble into heteromeric complexes composed of $GABA_{B1}$ and $GABA_{B2}$, which are both required for normal receptor functioning (Marshall et al., 1999a; Marshall et al., 1999b). Therefore, somatodendritic targeting information for $GABA_B$ receptors could also be associated with the $GABA_{B2}$ subunit. To test this hypothesis we generated a truncated $GABA_{B2}$ subunit, Myc-R2P820, which lacks the C-terminal 120 amino acid sequence downstream of the coiled-coil domain (Fig. 7 A). Wild-type $GABA_{B2}$ as well as Myc-R2P820 were both shown to dimerize with $GABA_{B1}$ in heterologous cells (Pagano et al., 2001) and it is expected that exogenously expressed $GABA_{B2}$ subunits dimerize to some extend with endogenous $GABA_{B1}$ subunits in neurons. Endogenous $GABA_{B1a}$ could therefore target exogenously expressed $GABA_{B2}$ subunits to the axon, which would compromise the identification of sequence determinants critical for dendritic polarization. To circumvent this problem we used for the following experiments cultured hippocampal neurons established from $1a^{-/-}$ mice. As shown in Fig. 7 B, full-length $GABA_{B2}$ (Myc-R2) was polarized to the somatodendritic compartment, while the C-terminally truncated $GABA_{B2}$ protein (Myc-R2P820) was relocated to the axon to some extent. Accordingly, the A:D ratio of Myc-R2P820 is significantly increased compared to Myc-R2 (Myc-R2: 0.3 ± 0.03, n = 9; Myc-R2P820: 0.45 ± 0.06, n = 5; Fig. 7 C). These results demonstrate that the C-terminal 120 amino acids of $GABA_{B2}$ are involved in dendritic targeting.

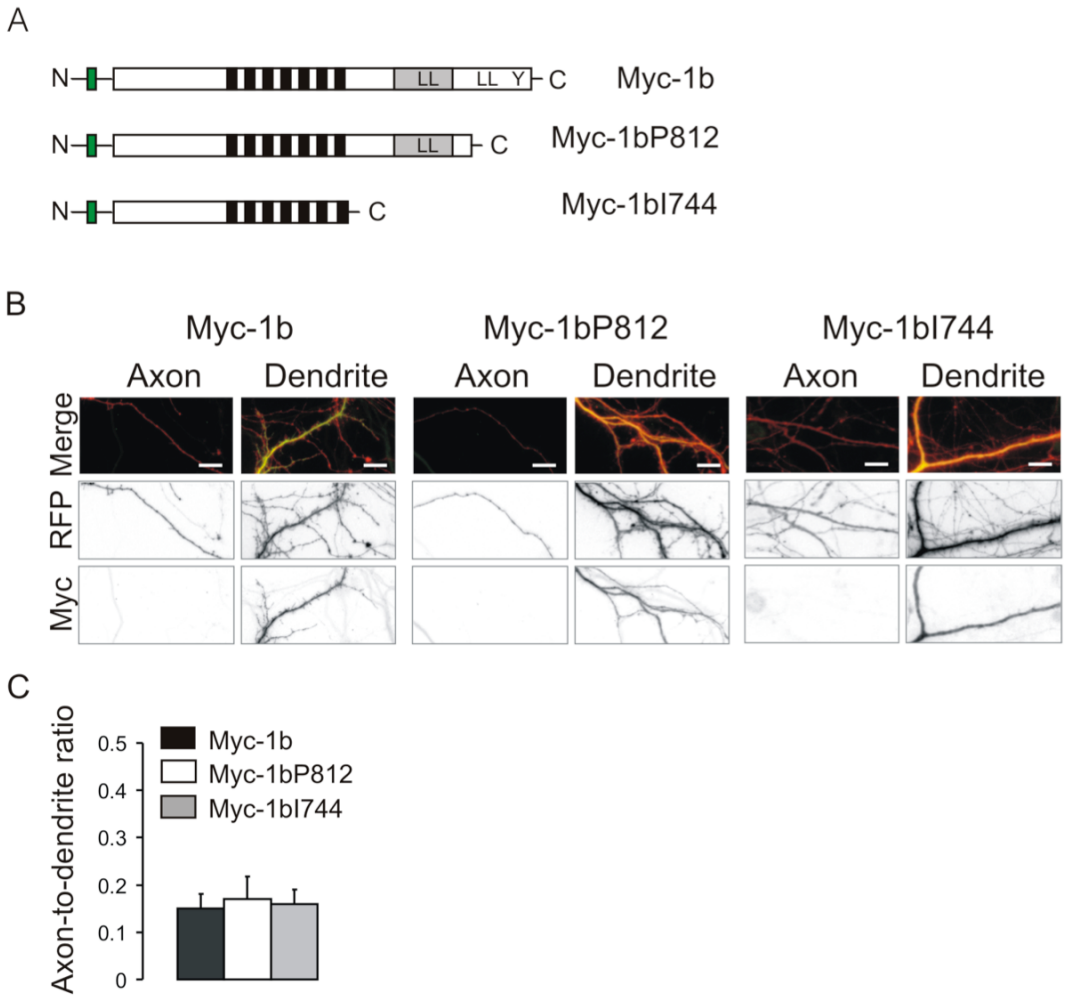

Figure 6. The C-term of $GABA_{B1}$ is not involved in somatodendritic targeting.

(A) *Schematic representation of $GABA_{B1b}$ expression constructs used in this experiment. The $GABA_{B1b}$ C-terminal domain possesses a number of putative somatodendritic targeting signals: two dileucine-based motifs (LL) and one tyrosine-based motif (Y). Myc-1b was used to generate two deletion constructs, missing either the last 32 C-terminal amino acids (Myc-1bP812) or the entire C-terminal domain (Myc-1bI744). The green bar represents the c-myc epitope, black bars the transmembrane domains, grey bars the coiled-coil domain.*

(B) *Myc-1b, Myc-1bP812 and Myc-1bI744 were co-transfected with soluble RFP into dissociated hippocampal neurons. In the upper panel, pictures of the RFP signal (red) and the immunolabelling against the c-myc epitope (green) were merged. Both truncated proteins are restricted to the somatodendritic compartment, similar to Myc-1b. Scale bar 10 µm.*

(C) *A:D ratio of Myc-1b, Myc-1bP812 and Myc-1bI744 expression constructs normalized to RFP (mean ± SEM, n = 10-11). The A:D ratio is not significantly different between the three constructs. Statistics: One-way ANOVA, Scheffe post-hoc test, $p \geq 0.05$.*

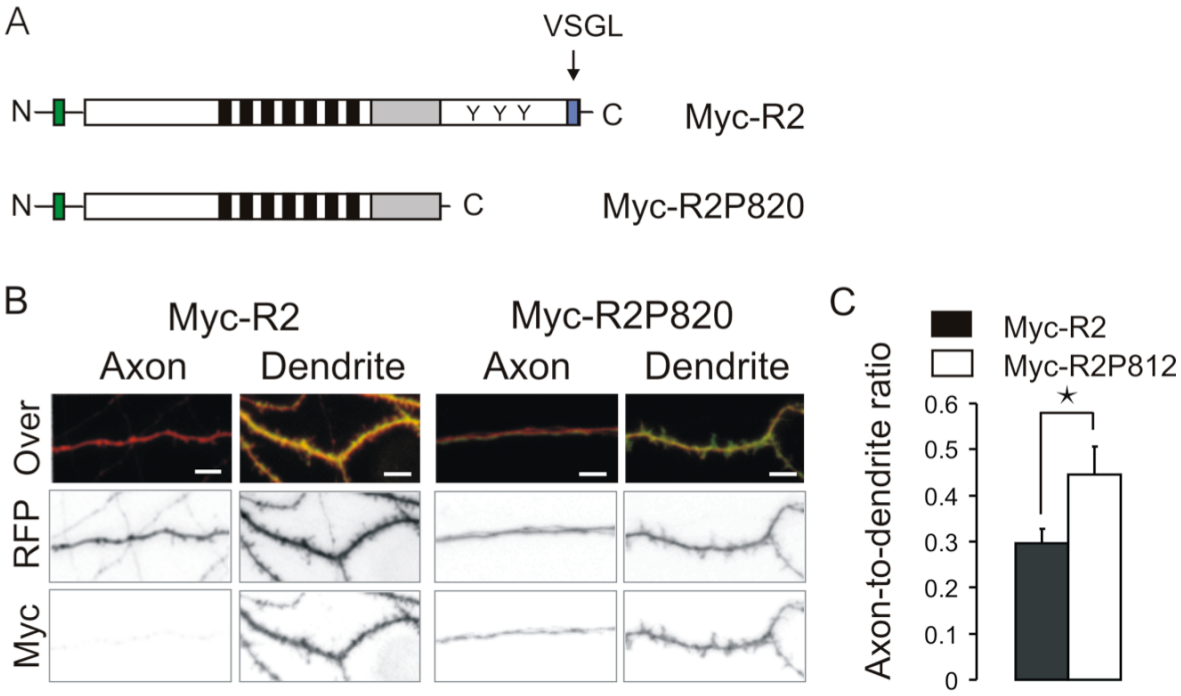

Figure 7. The C-terminal domain of $GABA_{B2}$ is important for somatodendritic polarization.

(A) *Schematic representation of $GABA_{B2}$ expression constructs used in this experiment. The distal C-terminal domain of Myc-R2 harbours three putative tyrosine-based somatodendritic targeting motifs (Y) and a PDZ-binding motif (VSGL) (blue bar). A deletion construct was generated missing the entire C-terminal domain downstream of the coiled-coil domain (Myc-R2P820). The green bars represent the c-myc epitope, black bars the transmembrane domains, grey bars the coiled-coil domain.*

(B) *Full-length $GABA_{B2}$ (Myc-R2) and Myc-R2P820 were co-transfected with soluble RFP into $GABA_{B1a}^{-/-}$ cultured hippocampal neurons. In the upper panels, the pictures of the RFP signal (red) and the immunolabelling against the c-myc epitope (green) were merged. Both proteins are found in dendrites, but in contrast to Myc-R2, Myc-R2P820 is additionally present in axons. Scale bar 10 µm.*

(C) *A:D ratio of Myc-R2 and Myc-R2P820 expression normalized to RFP (mean ± SEM, n = 5-9). The A:D ratio is significantly higher for Myc-R2P820 compared to Myc-R2. Statistics: Student's t-Test, $p^* \leq 0.05$.*

Discussion

Recently published data provided compelling evidence that $GABA_{B1a}$ conveys non-redundant synaptic functions, most likely due to its specific localization within neurons (Perez-Garci et al., 2006; Shaban et al., 2006; Ulrich et al., 2007; Vigot et al., 2006). Imaging analysis demonstrated that $GABA_{B1a}$ but not $GABA_{B1b}$ protein is present in the axons of transfected CA3 pyramidal neurons (Vigot et al., 2006). It was speculated that the SDs, the only region of sequence divergence between $GABA_{B1a}$ and $GABA_{B1b}$, dictate axonal localization. However, an understanding of the underlying mechanism, as well as which SD is involved, remained elusive. Here, we demonstrate that the SDs of $GABA_{B1a}$ are the critical determinant for axonal localization. They are sufficient to override dendritic signals in the C-terminal region of mGluR1a (Das and Banker, 2006; Francesconi and Duvoisin, 2002), and are therefore able to function in the context of a heterologous protein. Accordingly, the SDs of $GABA_{B1a}$ can be considered a general axonal targeting motif. Moreover, we provide evidence that each SD on its own is capable of mediating axonal localization of $GABA_{B1}$ subunits.

Mechanisms of SD-mediated axonal targeting

An important question is how the SDs mediate axonal localization. Our finding that disulfide bond formation is critical for axonal localization of $GABA_{B1a}$ demonstrates that proper folding of the SDs into their unique tertiary structure is essential. This suggests that the SDs engage in a specific protein interaction that is required for targeting $GABA_{B1a}$ to axons. In principle, the SDs may function at any stage in protein targeting. They could mediate sorting of $GABA_{B1a}$ into axonal transport vesicles by interaction with proteins in the lumen of the TGN. Such a mechanism has been suggested for NgCAM, a member of the L1 family of adhesion molecules harboring five fibronectin typeIII-like repeats in its ectodomain responsible for axonal localization (Sampo et al., 2003). Not all proteins in a transport vesicle have sorting signals that allow them to be selectively targeted. Proteins that lack such motifs are transported “piggyback style” through association with proteins that have sorting signals (Roos and Kelly, 2000). Thus, the SDs might interact with another axonal protein within the lumen of the transport vesicle. This is in line with experiments

showing that elements of a mature presynaptic terminal, e.g. calcium channel subunits, endocytic proteins and synaptic vesicle proteins are transported along axons as discrete "transport packets" (Ahmari et al., 2000). Therefore, the sorting sequences of many axonal destined proteins may be actually regions that allow interactions between components of the presynaptic terminal within the lumen of the carrier. Interestingly, presynaptic $GABA_B$ receptors appear to be mostly localized near the active zone (Kulik et al., 2003), which is in agreement with their close link with the release machinery (Vigot et al., 2006). However, it remains to be elucidated whether there is a direct interaction of $GABA_B$ receptors with other elements of presynaptic terminals.

Another mechanism proposed to establish polarity in neurons is selective retention (Sampo et al., 2003). There, post-Golgi carriers are non-selectively transported to axons and dendrites and sorting is achieved directly at the plasma membrane by selective fusion, selective interaction with scaffold proteins or selective internalization. In this regard, the SDs could convey selective retention through interaction with a membrane bound or extracellular matrix protein that anchors $GABA_{B1a}$ at specific sites. As a prerequisite for selective retention of $GABA_{B1a}$ versus $GABA_{B1b}$, both isoforms must be delivered to the axonal domain. In line with previous results obtained from organotypic slice cultures (Vigot et al., 2006), the experiments presented herein provide evidence that this is not the case because endogenous as well as exogenously expressed $GABA_{B1b}$ is excluded from the distal axons in dissociated pyramidal hippocampal neurons (Figs. 1 and 2). Furthermore the SDs were capable of directing axonal localization of mGluR1a (Fig. 5), which is known to be directly targeted to dendrites (Das and Banker, 2006; Stowell and Craig, 1999). Thus, the available data argue against a role of the SDs in selective retention of $GABA_{B1a}$ in the axonal domain.

The two SDs of $GABA_{B1a}$ exhibit strikingly different structural properties (Blein et al., 2004). This led to the proposal that they participate in protein interactions with multiple partners. Our observation that the two SDs are independently capable of directing axonal localization suggests that they interact with proteins of similar function or with different domains on the same protein(s). Although we did not observe a quantitative difference in axonal localization between $GABA_{B1}$ subunits with one or two SDs it cannot be excluded

that the two SDs cooperate in directing axonal localization. A potential binding partner of the first SD is the ECM protein fibulin-2, which was identified in a yeast-two-hybrid screen (Blein et al., 2004). The fact, however, that cultured hippocampal neurons recapitulate the differential localization of $GABA_{B1a}$ and $GABA_{B1b}$, suggests that receptor compartmentalization is cell autonomous and independent of a structured ECM. Thus, the putative SD-binding protein mediating axonal localization of $GABA_{B1a}$ in glutamatergic neurons remains unknown.

Dendritic targeting of $GABA_B$ receptors

Endogenous as well as exogenously expressed $GABA_B$ receptors are observed in the soma and throughout dendrites of cultured hippocampal neurons (Figs. 1 and 2; (Correa et al., 2004)). This indicates that they are actively targeted into dendrites. Our experiments using deletion constructs reveals that the 120 amino acid C-terminal sequence of $GABA_{B2}$ contains essential dendritic targeting information. While full-length $GABA_{B2}$ was restricted to the somatodendritic compartment, a significant amount of the C-terminally truncated $GABA_{B2}$ protein was localized to the axon. The 120 amino acids C-terminal sequence of $GABA_{B2}$ contains two putative tyrosine-based motifs that were shown to directly target proteins to dendritic endosomes or plasma membranes in neurons (de Hoop et al., 1995; Jareb and Banker, 1998; West et al., 1997), as well as a C-terminal PDZ-binding motif (VSGL) that was shown to direct interaction with Mupp-1, a PDZ-scaffold protein (Balasubramanian et al., 2007). It remains to be elucidated whether any of these motifs contribute to the dendritic localization of $GABA_B$ receptors. Although the C-terminally truncated $GABA_{B2}$ protein was present throughout axons and dendrites, it was still polarized to the somatodendritc domain, indicated by an average A:D ratio of 0.42. For a completely unpolarized receptor protein one would expect an A:D ratio of approximately 1.0 (Das and Banker, 2006; Jareb and Banker, 1998). Therefore, our experiments indicate that in addition to the 120 amino acid C-terminal sequence other $GABA_{B2}$ domains mediate dendritic localization. In this regard, our results are in agreement with other studies addressing the targeting of GPCRs in cultured hippocampal neurons. For example, it was shown that although the C-terminal domain of mGluR1a

contains a signal sufficient for dendritic localization, its deletion caused only a modest reduction in dendritic polarity (Das and Banker, 2006).

Similarly we investigated the role of the C-terminal domain of $GABA_{B1}$ in dendritic targeting. Deleting the entire C-terminus of $GABA_{B1b}$ resulted neither in axonal localization nor did it prevent targeting into distal dendrites. This demonstrates that the C-terminal domain of $GABA_{B1}$, which contains a number of "putative" dendritic targeting signals (Winckler and Mellman, 1999), is not essential for dendritic targeting. Therefore it is likely that $GABA_{B1}$ subunits are targeted into dendrite in a complex with $GABA_{B2}$ and do not harbour any dendritic targeting information themselves. However, recent evidence suggests that $GABA_{B1}$ subunits may be transported into dendrites prior to assembly into heteromeric complexes (Vidal et al., 2007). In this respect, our finding that deletion of the entire C-terminus of $GABA_{B1b}$ did not affect dendritic localization could indicate that other regions of the protein are capable of mediating dendritic targeting.

A combination of distinct targeting signals regulates differential axonal localization of $GABA_B$ receptors subtypes

Our findings are compatible with two possible scenarios for subcellular targeting of heteromeric $GABA_{B(1a,2)}$ and $GABA_{B(1b,2)}$ receptors in neurons. In the first model, both $GABA_{B(1a,2)}$ and $GABA_{B(1b,2)}$ receptors are transported into dendrites, either in somatodendritic post-Golgi carriers or while still residing in the ER (Vidal et al., 2007). Additionally, $GABA_{B(1a,2)}$ receptors are selectively packed into axonal transport carriers. The C-terminal domain of $GABA_{B2}$ would thereby mediate dendritic polarization unless the SDs in the ectodomain of $GABA_{B1a}$ interact with a protein in the lumen of the TGN mediating axonal sorting. The availability of this putative SD-binding protein would thereby provide the limiting factor for axonal targeting of $GABA_{B(1a,2)}$. Alternatively, both $GABA_{B(1a,2)}$ and $GABA_{B(1b,2)}$ are initially exclusively transported to the somatodendritic compartment, where they are inserted into the plasma membrane. Subsequently, some $GABA_{B(1a,2)}$ receptors are internalized and redistributed to the axonal compartment, a mechanism referred to as transcytosis (Wisco et al., 2003). In this model, the SDs in the ectodomain of $GABA_{B1a}$ would mediate internalization through interaction with its

putative binding protein, possibly another transcytosed transmembrane protein. Elucidating the precise cellular mechanism underlying $GABA_B$ receptor compartmentalization needs to be further addressed using live cell imaging. The cooperation between extracellular/luminal and cytoplasmic targeting signals revealed in this study will be useful for studying subcellular targeting of other heteromeric receptors in neurons.

Materials and Methods

Mice

Primary neuronal cultures were prepared from wild-type Balb/c mice or $GABA_{B1}^{-/-}$-, $GABA_{B1a}^{-/-}$- and $GABA_{B1b}^{-/-}$ mice generated in the Balb/c inbred background (Schuler et al., 2001; Vigot et al., 2006). All animal experiments were subjected to institutional review and conducted in accordance with Swiss guidelines and approved by the veterinary Office of Basel-Town.

Generation of mutant expression plasmids

Cloning of myc-tagged expression constructs was based on a strategy described earlier (Pagano et al., 2001). Briefly, to allow detection of transiently expressed receptors, the endogenous signal peptides were replaced by 36 residues encoding the mGluR5 signal peptide MVLLLILSVLLLKEDVRGSAQS, followed by the c-myc epitope, TREQKLISEEDLTR (replaced residues: Myc-1a, 1-16 (Kaupmann et al., 1997); Myc-1b, 1-29 (Kaupmann et al., 1997); Myc-R2, 1-41 (Kaupmann et al., 1998); Myc-mGluR1a, 1-20 (Masu et al., 1991)). The mGluR5 signal peptide was used because it is known to accurately release N-terminal epitope-tags (Ango et al., 1999). To generate Myc-1aCS the four cysteine residues at position 29, 95, 99 and 156 (Kaupmann et al., 1997) were mutated to serines in Myc-1a by site directed mutagenesis of thymine to adenine. To generate Myc-1aΔSD1 and Myc-1aΔSD2 residues G^{28} to C^{95} or V^{96} to Q^{157} (Kaupmann et al., 1997) were deleted in Myc-1a, respectively. To generate Myc-SD-mGluR1a, residues G^{17} to S^{134} of $GABA_{B1a}$ (Kaupmann et al., 1997) were introduced behind the myc epitope in Myc-

mGluR1a. To generate the C-terminal deletion constructs Myc-1bI744, Myc-1bP812 and Myc-R2P820 a stop codon was introduced by site directed mutagenesis after the residues indicated. Initially all constructs were subcloned into the cytomegalovirus-based eukaryotic expression vector pCI (Promega, Madison, WI) to confirm protein expression in HEK293 cells. Subsequently all constructs were shuttled into plasmid pMH4-SYN-1 for expression in cultured hippocampal neurons under control of the neuron-specific synapsin-1 promoter (gift from T.G. Oertner and K. Svoboda). All constructs were verified by sequencing.

Neuronal culture and transfection

Cultured hippocampal neurons were prepared as described previously (Brewer, 1993; Goslin K., 1998). Briefly, embryonic day 16.5 mouse hippocampi were dissected, digested with 0.25 % trypsin in Hank`s solution (GIBCO) for 15 min at 37°C, dissociated by trituration and plated on glass coverslips coated with 1 mg/ml poly-L-lysine hydrobromide (Sigma) in 0.1 M borate buffer (boric acid/sodium tetraborate). Neurons were thereby either seeded at low-density (~100-150 cells/mm^2) for endogenous $GABA_{B1}$ labeling or at high-density (~750 cells/mm^2) if needed for transfection or electrophysiological recordings and incubated at 37°C /0.5% CO_2. For low-density cultures, neurons were cultivated in HC-MEM medium (1x MEM with Glutamax, 0.3% glucose (w/v), 10% horse serum and 1% Pen/Strep) for the first 4 hours to allow attachment. Subsequently, the coverslips were transferred to a feeder-layer of primary astrocytes in serum-free medium (1x MEM with Glutamax, 0.3% glucose (w/v) and 1 % Pen/Strep) supplemented with 1% N2 (Invitrogen). Primary astrocytes were obtained from newborn P0-P1 Balb/c mice. To prevent extensive proliferation of astrocytes 5 µM arabinoside (AraC, Sigma) was further added to the culture medium after 2 days. In contrast, high-density cultures were grown in Neurobasalmedium supplemented with B27 (Invitrogen), 0.5 mM L-glutamine and 50-100 µg/ml Pen/Strep. In addition, 25 µM glutamic acid was added to the medium for the first 3 days. At DIV4, neurons were co-transfected with the appropriate expression constructs and soluble RFP (pMH4-SYN-tdimer2-RFP; gift from R. Tsien) using Lipofectamine 2000 transfection reagent (Invitrogen).

Electrophysiology

Hippocampal neurons were cultured for 2-3 weeks. On the day of the experiment, coverslips were placed in an interface chamber containing saline (140 mM NaCl, 3 mM KCl, 2.5 mM $CaCl_2$, 1.2 mM $MgCl_2$, 11.1 mM glucose, 10 mM Hepes, ph 7.2) equilibrated with 95% O_2/5% CO_2 and recordings were performed at 30-32 °C. Whole-cell patch-clamp recordings were performed from the somata of neurons to measure holding currents and synaptic responses. Neurons were visualized using infrared and differential interference contrast optics. Drugs were applied by superfusion into the recording chamber. Na^+ currents induced by baclofen (100 μM) were elicited at –50 mV in the presence of TTX. Patch and recording electrode (~5 MΩ) was filled with a solution containing: 140 mM Cs-gluconate, 10 mM Hepes, 10 mM Phosphocreatine, 5 mM QX-314, 4 mM Mg-ATP, 0.3 mM Na-GTP, pH 7.25, 294 mOsm. Miniature EPSCs (mEPSCs) were recorded at -70 mV in the presence of 0.5 μM TTX and 10 μM bicuculline. Detection and analysis of mEPSCs were done using the MiniAnalysis software (Synaptosoft, Decatur, GA, USA). During the experiment $GABA_B$ receptors were activated using the agonist baclofen and inactivated by the selective antagonist CGP54626 (2 μM).

Immunocytochemistry

Neurons were fixed at 14 *days-in-vitro* (DIV14) in 4% PFA/120 mM sucrose/phosphate buffered saline (137mM NaCl, 8.5mM Na_2HPO_4, 1.5mM KH_2PO_4, 3.0mM KCl) for 20 min at RT, permeabilized with 0.25% Triton-X-100 for 10 min and blocked for 1 h with 10% normal goat serum (NGS) in phosphate buffered saline (PBS). Primary antibodies were diluted in 10% NGS/PBS and incubated overnight at 4°C. After washing with 1xPBS, neurons were incubated with secondary antibodies diluted in 1% NGS/PBS for 1 h at RT. Primary antibodies: chicken anti-MAP2 (1:10000; Abcam), rabbit anti-$GABA_{B1}$-C-term (1:500; Clone B17; (Kulik et al., 2002); generously provided by Ryuichi Shigemoto), mouse anti-myc (1:500; Roche). Secondary antibodies: Alexa goat anti-chicken 647, Alexa goat anti-rabbit 568 and Alexa goat anti-mouse 488 (1:500; Molecular probes).

Microscopy

Immunolabeled neurons were viewed on a Leica DM5000B fluorescence microscope. Glutamatergic neurons were discriminated from GABAergic neurons by their extensively branched spiny dendrites visualized by the RFP filling (Benson et al., 1994; Obermair et al., 2003). Pictures were captured with a digital camera (F-View; Soft Imaging System, Lakewood, CO, USA) using AnalySIS® software (Soft Imaging System) and processed identically in Adope Photoshop®. Three different filters were used to detect secondary antibodies: L5-filter to visualize Alexa goat anti-mouse 488 bound to the monoclonal antibody against the myc-epitope, Y5-filter to detect Alexa goat anti-chicken 647 binding to antibody against MAP2 and a Y3-filter visualizing RFP or Alexa goat anti-rabbit 568 binding to the polyclonal $GABA_{B1}$ antibody. Pictures were taken with each filter individually and overlaid thereafter. Pictures from the endogenous $GABA_{B1}$ staining were captured using a 63x oil objective with 1.32 numerical aperture (NA) wetted with immersion oil without autofluorescence (Leica Microsystems Cat N^o 11513859, Germany). Images to evaluate the axonal versus dendritic distribution of transfected $GABA_B$ expression constructs were photographed using a 20x 0.7 NA lens.

Quantification of polarized distribution

The axon-to-dendrite (A:D) ratio of epitope-tagged receptor constructs was determined essentially as described elsewhere (Gu et al., 2003; Sampo et al., 2003). Briefly, using *Metamorph Imaging* software one-pixel-wide lines were traced along the axons and dendrites on the RFP image. Next to each line, a quadrangle was drawn for background subtraction. Subsequently, the lines and quadrangles were transferred to the corresponding picture of the antibody labeling against the c-myc epitope detecting the different receptor constructs. Average pixel intensities were determined along the traced lines and in the background quadrangles. After background subtraction, the signal of the antibody labeling was normalized to the RFP signal in axons and dendrites and subsequently the A:D ratio was determined. The analysis was done for approx. 10 neurons from at least two culture preparations for each construct. Neurons that expressed the receptor constructs at very high levels or exhibited an irregular RFP filling were excluded from the analysis. SPSS software was used to determine the significance of the data (T-Test or one-way ANOVA together

with Scheffe post-hoc test. *$p \leq 0.05$; **$p \leq 0.01$; ***$p \leq 0.001$. Error bars: standard error of the mean).

Reagents

Tetrodotoxin (TTX) was from Latoxan (Valence, France). Baclofen and CGP54626 were from Novartis Pharma AG (Basel, Switzerland). Hepes was from AppliChem (Cat. No. A1069.0100). All other reagents were from Fluka/Sigma (Buchs, Switzerland).

Acknowledgements

The rat mGluR1a cDNA clone was obtained from Robert M. Duvoisin. This study was supported by the Swiss Science Foundation (3100-067100.01; B. Bettler.) and the Désirée and Nils Yde Foundation (B. Bettler).

Chapter VI

THE SUSHI DOMAINS OF SECRETED $GABA_{B1A}$ ISOFORMS SELECTIVELY IMPAIR $GABA_B$ HETERORECEPTORS

Tiao JY**,** Bradaia A*, Biermann B*, Kaupmann K, Pless E, Barlow PN, Gassmann M, Bettler B

*These authors contributed equally to this work

In preparation

My contribution to this paper

Data presented in chapter II provided evidence that selectively $GABA_{B1a}$, but not the $GABA_{B1b}$ assembles functional receptors at glutamatergic terminals. The SDs provide the only region of sequence divergence between the two $GABA_{B1}$ subunit isoforms. I thus aimed at deciphering the role of the SDs in specifying heteroreceptors by two different approaches. First, I studied whether the SDs play a role in the axonal targeting of $GABA_{B(1a,2)}$ receptors in glutamatergic neurons (chapter III). Second, I wanted to clarify whether interference with the SDs impairs the function of heteroreceptors.

For this purpose I undertook several experiments:

1) To investigate whether disruption of disulfide bond formation abolishes heteroreceptor function I produced two lentiviruses expressing either $GABA_{B1a}$ wildtype protein or $GABA_{B1a}$ protein with disrupted SDs. By measuring the frequency of mEPSCs after baclofen-application I aimed at investigating to which extent the two viral proteins assemble functional heteroreceptors in infected $GABA_{B1a}^{-/-}$ cultured hippocampal neurons. For this experiment a nearby 100% transfection efficiency is needed since many glutamatergic terminals make synapses with the analyzed neuron. The viral particles I produced transfected HEK293 cells up to about 80 %, but unfortunately were not sufficiently transfecting cultured hippocampal neurons.
2) In a second experiment I took advantage of a monoclonal SD antibody, which was made by a technician in our lab. I applied this antibody directly to the culture medium to scaven a putative SD-binding protein at the neuronal surface. However, the antibody had no effect on mEPSCs frequencies after baclofen application (ACSF was used as control).
3) In a third experiment I used a soluble recombinant SD protein made by a postdoctoral fellow in our laboratory to scavenge the putative SD interacting protein. The results are illustrated in figure 4 of this chapter.

Abstract

$GABA_B$ receptors are the G-protein-coupled receptors for γ-aminobutyric acid (GABA), the main inhibitory neurotransmitter in the brain. Receptor subtypes are based on the subunit isoforms $GABA_{B1a}$ and $GABA_{B1b}$. $GABA_{B1a}$ differs from $GABA_{B1b}$ in its ectodomain by a pair of conserved protein-binding motifs, the sushi domains (SDs). Here we describe $GABA_{B1j}$, an abundant secreted $GABA_{B1}$ isoform essentially comprising the two SDs. We show that the SDs, when expressed as soluble proteins, impair the activity of $GABA_B$ heteroreceptors at glutamatergic terminals. In contrast, soluble SD proteins have no effect on the activity of $GABA_B$ autoreceptors at GABAergic terminals or postsynaptic $GABA_B$ receptors. Likely, therefore, soluble SD proteins interfere with the binding of heteroreceptors to an auxiliary protein at the cell surface. These results show that naturally occurring $GABA_{B1j}$ isoforms can regulate the level of presynaptic inhibition at excitatory synapses. Of importance for drug discovery, these findings also show that a selective therapeutic targeting of $GABA_B$ heteroreceptors is possible.

Introduction

$GABA_B$ receptors mediate pre- and postsynaptic inhibition in the central nervous system and are considered promising drug targets for a wide spectrum of psychiatric and neurological disorders including anxiety, depression and epilepsy (Bettler et al., 2004). $GABA_B$ receptors generate slow inhibitory postsynaptic currents (IPSCs) via activation of K^+ channels (Lüscher et al., 1997). Moreover, they prevent neurotransmitter release via inhibition of presynaptic Ca^{2+} channels (Dunlap and Fischbach, 1981) and second-messenger-mediated effects on vesicle priming (Sakaba and Neher, 2003). Presynaptic $GABA_B$ receptors are commonly divided into auto- and heteroreceptors depending on whether they control the release of GABA or other neurotransmitters, respectively. Recombinant and native studies showed that functional $GABA_B$ receptors are obligate heterodimers composed of $GABA_{B1}$ and $GABA_{B2}$ subunits (Gassmann et al., 2004; Marshall et al., 1999; Prosser et al., 2001; Schuler et al., 2001). At a molecular level, diversity in the $GABA_B$ receptor system arises from the expression of multiple $GABA_{B1}$

subunit isoforms from a single gene. To date, the best characterized isoforms are $GABA_{B1a}$ and $GABA_{B1b}$, which are generated by alternative promoter usage (Steiger et al., 2004). Structurally, the $GABA_{B1a}$ and $GABA_{B1b}$ isoforms differ in their N-terminal ectodomain by a tandem pair of SDs that are present in $GABA_{B1a}$ but not $GABA_{B1b}$ (Blein et al., 2004). SDs, also known as complement control modules or short consensus repeats, mediate protein-interactions in a variety of adhesion molecules (Lehtinen et al., 2004) and participate in hormone binding in Family B GPCRs (Perrin et al., 2006). We recently generated genetically modified $GABA_{B1a}^{-/-}$($1a^{-/-}$) and $GABA_{B1b}^{-/-}$($1b^{-/-}$) mice that selectively express either one or the other isoform (Vigot et al., 2006). This facilitated the dissociation of individual isoform functions and showed that heteroreceptors almost exclusively use the $GABA_{B1a}$ subunit (Shaban et al., 2006; Ulrich and Bettler, 2007; Vigot et al., 2006). In contrast, autoreceptors and postsynaptic $GABA_B$ receptors can be assembled with $GABA_{B1a}$ or $GABA_{B1b}$ subunits. It is therefore expected that the SDs of $GABA_{B1a}$ bind to protein(s) that are necessary for the recruitment of heteroreceptors to glutamatergic terminals (Ulrich and Bettler, 2007). A known binding partner of the SDs is the extracellular matrix (ECM) protein fibulin-2 (Blein et al., 2004), however, it has yet to exhibit a function in the context of $GABA_B$ receptors.

$GABA_{B1}$ subunits, but also several other membrane-linked receptors, produce secreted isoforms comprising SDs (Bulanova et al., 2007; Holter et al., 2005; Mosley et al., 1989; Schwarz et al., 2000; Wei et al., 2001a). These isoforms were shown to produce dominant-negative effects in some instances (Bulanova et al., 2007; Mosley et al., 1989), but the physiological relevance of secreted $GABA_{B1}$ isoforms remains unclear. Here we report the identification of an additional secreted $GABA_{B1}$ isoform, $GABA_{B1j}$, which is abundantly expressed in the central nervous system. Conspicuously, all known secreted $GABA_{B1}$ isoforms feature SDs. We therefore analyzed whether soluble SDs have the potential to regulate $GABA_B$ receptor functions in a dominant-negative manner.

Results

$GABA_{B1j}$ encodes a secreted glycoprotein.

We screened a non-amplified rat cortex/cerebellum cDNA library with a SD-specific hybridization probe and isolated several $GABA_{B1j}$ clones with an identical insert of ~1.6 kb. $GABA_{B1j}$ diverges from $GABA_{B1a}$ downstream of exon 4 and encodes a protein of 229 amino acids (Fig. 1*A*; supporting information (SI) Fig. 5*A*). The N-terminal 157 amino acids of $GABA_{B1j}$ are identical to $GABA_{B1a}$ and encode the signal peptide and the two SDs; the C-terminal 72 residues exhibit no significant homology to known proteins. Northern blot analysis revealed a $GABA_{B1j}$ transcript of ~1.6 kb in brain tissue and cultured cortical neurons (Fig. 1*B*). The SD-specific hybridization probe demonstrated that $GABA_{B1j}$ transcripts and full-length $GABA_{B1a}$ transcripts are of similar abundance. Hydropathicity analysis of the protein sequence revealed that $GABA_{B1j}$ lacks transmembrane domains and probably encodes a secreted protein (SI Fig. 5*B*). Immunoblot analysis of transiently transfected HEK293 cells showed that the myc-tagged $GABA_{B1j}$ protein has a molecular weight of ~29kD (Fig. 1*C*). Deglycosylation of $GABA_{B1j}$ with peptide N-glycosidase F (PNGase F) decreased the molecular weight to 25kD (data not shown), which corresponds to the calculated molecular weight of the mature protein. Immunoprecipitation experiments recovered $GABA_{B1j}$ but not $GABA_{B1a}$ from cell-conditioned culture medium, confirming that $GABA_{B1j}$ is a secreted protein (Fig. 1*C*).

Soluble SD protein selectively impairs the activity of $GABA_B$ heteroreceptors. For dominant-negative experiments, we produced a recombinant glycosylated SD protein (RSDP) in a yeast expression system (SI Fig. 6). It is known that the binding ability of the SDs is dependent on the integrity of their conserved disulfide bridges (Hashiguchi et al., 1993; Perrin et al., 2006; Wei et al., 2001b). For control experiments, therefore, we produced mutRSDP, a protein with disrupted disulfide bridges (see supplementary information). We first analyzed whether RSDP interferes with presynaptic inhibition mediated by $GABA_B$ heteroreceptors. Under control conditions in artificial cerebro-spinal fluid (ACSF), activation of $GABA_B$ heteroreceptors by baclofen (100 μM) resulted in the

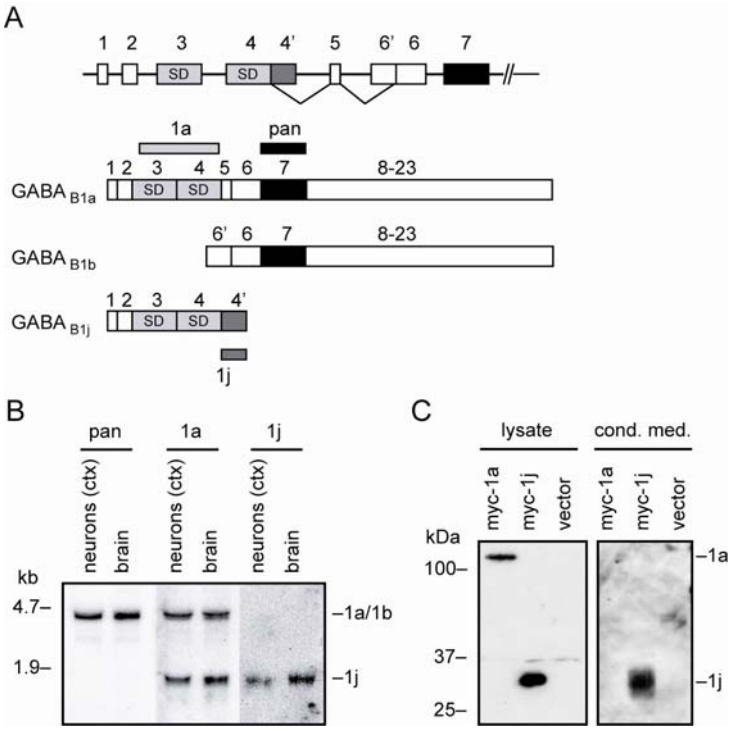

Figure 1. Characterization of the $GABA_{B1j}$ subunit isoform.

(A) *Schematic representation of the 5' end of the $GABA_{B1}$ gene indicating the exons specifying the $GABA_{B1a}$, $GABA_{B1b}$ and $GABA_{B1j}$ isoforms. $GABA_{B1j}$ results from an 870 bp extension of exon 4 at its 3' end (exon 4'), generating an open reading frame of 687 nucleotides. The SDs are indicated.*

(B) *Northern blot analysis of $GABA_{B1a}$ and $GABA_{B1j}$ mRNA expression. Total RNA extracted from primary cortical neurons in culture (ctx) or mouse brain was hybridized to the ^{32}P-labeled probes indicated in A. The pan probe encodes part of the extracellular GABA binding domain and detects ~4.5 kb $GABA_{B1a}$ and ~4.1 kb $GABA_{B1b}$ transcripts. The 1a probe encodes the two SDs and detects $GABA_{B1a}$ and ~1.6 kb $GABA_{B1j}$ transcripts. The 1j specific probe encodes 510 nucleotides of exon 4'.* ***(C)*** *Analysis of transfected HEK293 cells expressing myc-tagged $GABA_{B1a}$ (myc-1a) and $GABA_{B1j}$ (myc-1j). Conditioned medium (cond. med.) was subjected to immunoprecipitation with a rabbit anti-myc antibody and analyzed together with 10 μg of total cell lysate (lysate) on Western blots with a mouse anti-myc antibody. $GABA_{B1a}$ protein was only detected in the cell lysate while secreted $GABA_{B1j}$ protein was additionally detected in the cell-conditioned medium.*

expected marked reduction of excitatory postsynaptic currents (EPSCs), which were evoked by extracellular stimulation of the Schaffer collaterals and recorded in CA1 pyramidal neurons (Fig. 2*A*). Incubation of hippocampal slices with RSDP (1.0 μg/ml) for 6 hours essentially abolished $GABA_B$ heteroreceptor function, as indicated by the failure of

baclofen to reduce EPSC amplitudes (Fig. 2*A*). Incubation of slices with mutRSDP or RSDP that was kept in a reduced state (incubation with 20 mM DTT) had no effect on heteroreceptor function (Fig. 2*A*). This shows that the effect of RSDP on heteroreceptor function depends on the correct folding of the SDs. Activation of adenosine A1 receptors reduced EPSC amplitudes to the same extent in the presence or absence of RSDP, demonstrating that presynaptic inhibition by another GPCR remained intact (Fig. 2*A*). We next analyzed whether RSDP interferes with presynaptic inhibition by $GABA_B$ autoreceptors. Baclofen depressed the amplitude of IPSCs, which were evoked by extracellular stimulation of the Schaffer collaterals and recorded from CA1 pyramidal neurons, to the same extent in the presence or absence of RSDP (Fig. 2*B*). This demonstrates that RSDP has no measurable effect on $GABA_B$ autoreceptors. Likewise, baclofen elicited similar K^+ currents in CA1 neurons in the presence or absence of RSDP, demonstrating that RSDP has no effect on postsynaptic $GABA_B$ receptors either (Fig. 2*C*). In addition, we tested whether the extracellular matrix protein fibulin-2, which binds to the SDs of $GABA_{B1a}$ *in vitro* (Blein et al., 2004), can interfere with heteroreceptor function. Recombinant fibulin-2 (THS-fibulin2) (SI Fig. 7), when applied alone or in equimolar combination with RSDP to hippocampal slices, was without effect on heteroreceptors. This suggests that fibulin-2 is not an auxiliary signaling component of $GABA_B$ heteroreceptors. $GABA_B$ heteroreceptors not only inhibit evoked but also spontaneous neurotransmitter release (Yamada et al., 1999). We therefore investigated whether RSDP can interfere with the baclofen-induced reduction of the miniature EPSCs (mEPSCs) frequency. As expected, under control conditions (ACSF), baclofen significantly reduced the frequency but not the amplitude of mEPSCs recorded in CA1 pyramidal neurons (Fig. 3*A*). In the presence of RSDP, baclofen no longer reduced the mEPSC frequency (Fig. 3*A*). When applied alone, RSDP had no effect on the baseline mEPSC frequency. RSDP had no effect on autoreceptor-mediated inhibition of the mIPSC frequency (Fig. 3*A*), confirming that RSDP selectively acts on heteroreceptors.

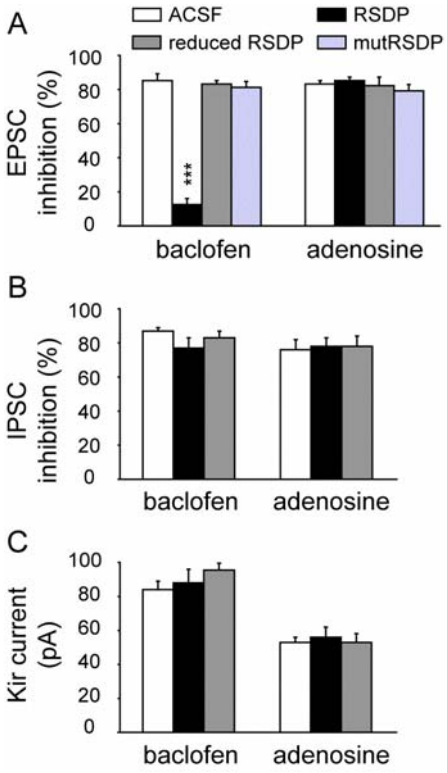

Figure 2. RSDP selectively interferes with $GABA_B$ heteroreceptor function.

(A) *Summary histogram of the inhibition of evoked EPSC by baclofen (100 μM) and adenosine (100 μM) after incubation of hippocampal slices with RSDP (1.0 μg/ml) or ACSF alone (control) for 6 h. Baclofen reduced the EPSC amplitudes recorded from CA1 pyramidal neurons in the presence of ACSF but not of RSDP (ACSF: 85 ± 4 % inhibition, n = 6; RSDP: 12.5 ± 3.5 % inhibition, n = 6; ***p < 0.001, Student's t test). Adenosine reduced the EPSC amplitude in the presence of RSDP or ACSF alone to the same extent (ACSF: 83 ± 2 % inhibition, n = 6; RSDP: 85 ± 3 % inhibition, n = 6). RSDP treated with reducing agents (DTT) or mutated RSDP without disulfide bridges was without effect on heteroreceptor activity.*

(B) *Summary histogram of evoked IPSC inhibition by baclofen (100 μM) and adenosine (100 μM). Baclofen and adenosine depressed the amplitude of evoked IPSCs recorded from CA1 pyramidal neurons under control conditions and after incubation with RSDP to the same extent.*

(C) *Summary histogram of the amplitude of baclofen- and adenosine-induced K^+ currents. The amplitude of the outward K^+ current induced by baclofen is similar in the presence of RSDP (n=6) or ACSF alone (n=6). Similarly, adenosine-induced currents were unaffected by the presence of RSDP (Vclamp: -50 mV, TTX 1 μM). Abbreviations: ACSF, artificial cerebrospinal fluid. Values are expressed as mean ± SEM.*

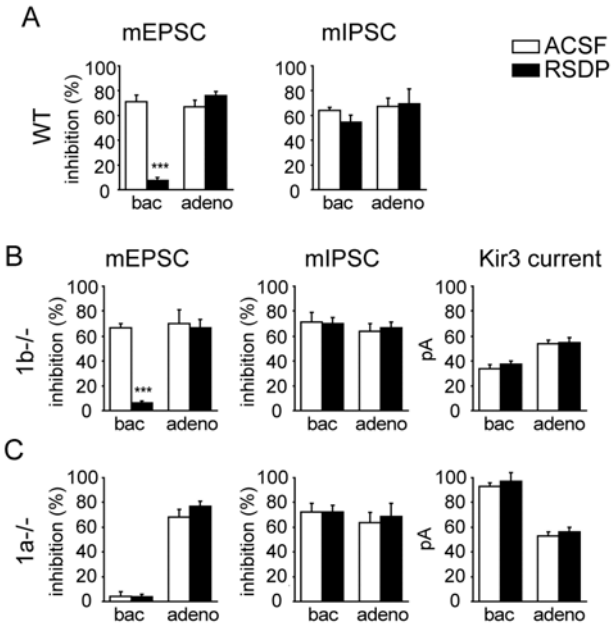

Figure 3. RSDP interferes with $GABA_B$ receptor-mediated inhibition of spontaneous glutamate release

(A) *Summary histogram of mEPSC inhibition by baclofen (100 μM) and adenosine (100 μM) under control condition (ACSF) and after incubation with RSDP (1.0 μg/ml) for 6 h. Baclofen depressed the frequency of mEPSCs recorded from CA1 pyramidal neurons in control slices but not in slices incubated with RSDP (ACSF: 71.0 ± 5.4 % inhibition, n = 5; RSDP: 7.6 ± 2.2 % inhibition, n = 9; ***p < 0.001, Student's t test). As a control, adenosine depressed the frequency of mEPSCs under control conditions and after incubation with RSDP (ACSF: 67.0 ± 5.3 % inhibition, n = 5; RSDP: 76.0 ± 3.0 % inhibition, n = 9). Summary histogram of IPSC inhibition by baclofen (100 μM) and adenosine (100 μM). Baclofen and adenosine depressed the frequency of mIPSCs recorded from CA1 pyramidal neurons under control conditions and after incubation with RSDP. Effects of RSDP in $1b^{-/-}$ and $1a^{-/-}$ hippocampal slices.*

(B) *Summary histograms of mEPSC frequency inhibition by baclofen and adenosine. Incubation with RSDP (1.0 μg/ml) for 6 h impedes the baclofen-mediated frequency inhibition observed under control condition in $1b^{-/-}$ mice (ACSF: 67.0 ± 3.0 % inhibition; SD protein: 6.0 ± 2.0 % inhibition; n = 4; ***p < 0.001, Student's t test).*

(C) *In $1a^{-/-}$ mice, even under control condition, baclofen failed to depress the frequency of mEPSCs indicating the lack of functional $GABA_B$ heteroreceptors. (B and C) Summary histograms of mIPSC frequency inhibition by baclofen and adenosine. Baclofen and adenosine depressed the frequency of mIPSCs recorded from $1b^{-/-}$ as well as $1a^{-/-}$ CA1 pyramidal neurons under control conditions and after incubation with RSDP. (B and C) Summary histograms of the amplitude of baclofen- and adenosine-induced K^+ currents. The amplitude of the outward K^+ current induced by baclofen is not affected by incubation with RSDP in slices established from $1b^{-/-}$ as well as $1a^{-/-}$ mice. Control adenosine-induced currents are similarly unaffected by incubation with RSDP in both genotypes (Vclamp: -50 mV, TTX 1 μM). Abbreviations: ACSF, artificial cerebrospinal fluid; bac, baclofen; adeno, adenosine. Values are expressed as mean ± SEM.*

RSDP interferes with a subset of $GABA_{B1a}$-containing receptors.

The above data show that RSDP selectively interferes with the function of $GABA_B$ heteroreceptors, which are known to be predominantly assembled with the $GABA_{B1a}$ subunit (Vigot et al., 2006). However, the $GABA_{B1a}$ subunit also significantly contributes to autoreceptors and postsynaptic $GABA_B$ receptors (Vigot et al., 2006). In fact, the complete lack of $GABA_{B1b}$ subunits in $1b^{-/-}$ mice does measurably impair the functions of $GABA_B$ autoreceptors or postsynaptic $GABA_B$ receptors. We therefore studied, in hippocampal slices of $1b^{-/-}$ mice, whether RSDP can interfere with autoreceptors and postsynaptic $GABA_B$ receptors that are assembled with the $GABA_{B1a}$ subunit. Incubation of $1b^{-/-}$ slices with RSDP neither interfered with autoreceptor responses (Fig. 3*B*) nor with $GABA_B$-mediated K^+ channel responses (Fig. 3*B*). However, RSDP strongly impaired heteroreceptor responses in $1b^{-/-}$ slices (Fig. 3B), thus corroborating data obtained with WT hippocampal slices (Fig. 3A). RSDP had no effect on pre- and postsynaptic $GABA_B$ receptors in hippocampal slices of $1a^{-/-}$ mice, where all receptors are assembled with the $GABA_{B1b}$ subunit (Fig. 3C). In all experiments with $1b^{-/-}$ or $1a^{-/-}$ mice, RSDP failed to interfere with pre- and postsynaptic adenosine A1 receptor responses (Fig. 3*B,C*). Altogether, these results demonstrate that RSDP selectively impairs the activity of $GABA_{B1a}$-containing receptors at glutamatergic terminals.

We next wanted to determine the time course of heteroreceptor impairment by RSDP. For these experiments we used hippocampal neuronal cultures, which enabled rapid access of RSDP to its site of action. We measured the inhibitory effect of RSDP on the baclofen-induced reduction of the mEPSC frequency. At high concentrations, 1.0 μg/ml of RSDP, a partial impairment of $GABA_B$ heteroreceptor function was observed as early as 10 min after RSDP application, while a total impairment was observed after 1 hour (Fig. 4*A,B*). At 0.1 μg/ml of RSDP, a maximal impairment of heteroreceptor function was observed 12 hours after RSDP application. As observed in hippocampal slices (Fig 2, 3), RSDP did not interfere with presynaptic inhibition mediated by adenosine A1 receptors (Fig. 4*C,D*).

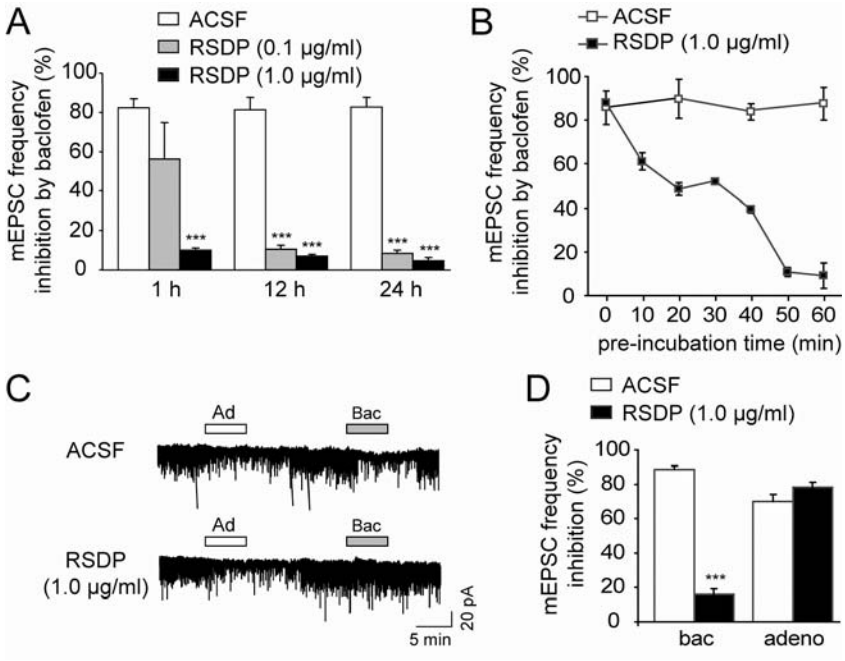

Figure 4. RSDP acts within minutes and in a dose-dependent manner.

(A) *The inhibition of mEPSC frequency by baclofen was assessed in 2-3 week-old mouse primary hippocampal neurons incubated with RSDP for 1 hour, 12 hours or 24 hours. Two different doses of RSDP were applied: 0.1 µg/ml and 1.0 µg/ml. ACSF was used as a control. mEPSCs were recorded from individual neurons and the baclofen-induced percentage inhibition of mEPSC frequency was determined. After 1 h incubation with 1.0 µg/ml RSDP the baclofen-induced mEPSC frequency inhibition is completely abolished.*

(B) *Time course of the RSDP-mediated reduction of baclofen-induced mEPSC frequency inhibition illustrating that the RSDP exerts its effect within minutes.*

(C** and **D) *Representative trace (C) and summary histogram (D) illustrating that the RSDP selectively abolishes baclofen-induced mEPSC frequency inhibition. Primary hippocampal neurons were incubated with 1.0 µg/ml RSDP for 1 h and the inhibition of mEPSC frequency by adenosine and baclofen was assessed in the same cell. ACSF was used as a control. Pre-incubation with RSDP specifically impedes baclofen-mediated mEPSC frequency inhibition (ACSF: 88.6 ± 2.4 %; SD protein: 15.7 ± 3.2 %, n = 5, ***p < 0.001, Student's t test). Values are expressed in percentage inhibition of mEPSC frequency (mean ± SEM).*

Discussion

Recent data suggest that excitatory axons can express factors that are necessary for the recruitment and functioning of $GABA_B$ heteroreceptors (Ulrich and Bettler, 2007). In this study we characterized a new $GABA_{B1}$ isoform, $GABA_{B1j}$, which joins a growing number

of secreted $GABA_{B1}$ isoforms that all feature SDs (Holter et al., 2005; Schwarz et al., 2000; Wei et al., 2001a). We hypothesized that secreted $GABA_{B1}$ isoforms could act by scavenging an auxiliary extracellular binding partner. Indeed we found that RSDP, a soluble protein that solely consists of the SDs, can selectively interfere with the activity of $GABA_B$ heteroreceptors. These results clearly demonstrate that naturally occurring secreted $GABA_B$ isoforms have the potential to exert dominant-negative effects. It therefore appears that the level of presynaptic inhibition at glutamatergic synapses is not only dynamically regulated through the control of $GABA_{B1a}$ transcription (Steiger et al., 2004) and recruitment (Vigot et al., 2006), but also through dominant-negative effects via secreted $GABA_{B1}$ isoforms. Both the recruitment and the dominant-negative effects depend on the SDs and may therefore be mechanistically linked.

It remains unclear how $GABA_B$ heteroreceptors are inactivated following RSDP exposure. We can exclude that RSDP acts as competitive antagonists of $GABA_B$ receptors, because RSDP did not prevent the activation of $GABA_{B(1a,2)}$ receptors expressed in HEK293 cells (data not shown), nor did it impair the functioning of autoreceptors or postsynaptic $GABA_B$ receptors assembled with $GABA_{B1a}$ subunits. Likewise, it does not appear that receptors rapidly internalize as a consequence of disrupting an extracellular interaction, since $GABA_B$ autoreceptors or postsynaptic $GABA_B$ receptors in $1b^{-/-}$ animals assembled with $GABA_{B1a}$ subunits are stably expressed at the cell surface in the absence of such an interaction. As heteroreceptor impairment is seen within minutes of RSDP application in cultured neurons, we consider it more likely that RSDP interferes with the signaling rather than the axonal delivery of heteroreceptors. Possibly, SD-interacting protein(s) act as diffusion traps that keep heteroreceptors and effector Ca^{2+} channels in close proximity; RSDP treatment may cause the disassembly of this signaling complex. Alternatively, the putative SD-interacting protein could be directly involved in the regulation of synaptic vesicle release.

The extracellular auxiliary factor binding to the SDs of $GABA_{B1a}$ remains enigmatic. The ECM protein fibulin-2, which binds to the first SD of $GABA_{B1a}$ (Blein et al., 2004), had no measurable effect on $GABA_B$-mediated control of glutamate release. The fact that cultured hippocampal neurons reproduce the differential compartmentalization of $GABA_B$ receptor isoforms also supports that heteroreceptor specification is cell autonomous and independent of ubiquitously expressed ECM proteins. We additionally addressed whether

the SDs can recruit heteroreceptors through homophilic interactions. We found that RSDP does not co-immunoprecipitate with $GABA_{B1a}$ when applied to HEK cells transiently expressing surface targeted $GABA_{B1}$ receptors, rendering this possibility unlikely (data not shown). Deciphering the mechanistic aspects of $GABA_B$ receptor regulation will largely depend on the identification of their extracellular binding partner(s). Extracellular binding partners were recently identified for several neurotransmitter receptors and shown to regulate their synaptic localization and function (Gally et al., 2004; Saglietti et al., 2007; Sia et al., 2007).

Drug development in the $GABA_B$ field has been hampered by the fact that receptor subtypes have indistinguishable pharmacological properties. From a drug discovery point of view it would be desirable to selectively interfere with pre- and postsynaptic $GABA_B$ receptors. Our study now provides the first evidence that it is possible to selectively manipulate the activity of $GABA_B$ heteroreceptors. It is now safe to conclude that small molecular weight compounds interfering with SD interactions would have a different spectrum of activity than currently available $GABA_B$ antagonists, which are in a Phase II clinical trial for the treatment of mild cognitive impairment (Froestl et al., 2004).

Materials and Methods

Characterization of $GABA_{B1j}$ cDNA and mRNA

Oligo (dT) primed double-stranded cDNA was synthesized from 5 μg poly(A)$^+$ RNA isolated from the cortex/cerebellum of postnatal 7-day-old rats and cloned into pCDNAI using *Bst*XI adaptors (Invitrogen, Carlsbad, CA). The cDNA library was screened with a ^{32}P-labelled SD-specific cDNA hybridization probe (Kaupmann et al., 1997). For Northern blot analysis, total RNA was isolated from mouse brain and primary mouse cortical neurons using TRIZOL reagent (Invitrogen, Carlsbad, CA). RNA was blotted to a nylon membrane (Gene Screen Hybridization Transfer Membrane, NEN Life Sciences) after electrophoretic separation on agarose/formaldehyde gels. The membrane was hybridized with random primed ^{32}P-labeled cDNA probes using Perfect Hyb hybridization buffer (Sigma) at 68°C. After washing in 0.2 x SSC, 0.1% SDS at 65°C the membrane was

exposed to Kodak Bio-Max maximum resolution X-ray films (Sigma-Aldrich, St. Louis, MO) for 72 hours.

$GABA_{B1j}$ expression in HEK293 cells

A $GABA_{B1j}$-specific antibody is lacking. We therefore tagged $GABA_{B1a}$ and $GABA_{B1j}$ with the c-myc epitope (Pagano et al., 2001) and inserted the resulting cDNAs in the expression vector pCI (Promega, Madison, WI). The conditioned medium of transfected HEK293 cells (Lipofectamine 2000, Invitrogen) was collected after 48 hours and used to immunoprecipitate secreted $GABA_{B1}$ protein. Briefly, the medium was incubated with Protein G-agarose (Roche, Mannheim Germany) for 2 hours, pre-cleared by centrifugation at 10000g for 10 minutes and then incubated overnight with a monoclonal anti-myc antibody (9E10, Sigma, diluted 1:1000) coupled to Protein G-agarose. After 5 washes in RIPA buffer (150 mM NaCl, 1% Nonidet P-40, 0.5% sodium deoxycholate containing Complete protease inhibitor cocktail (Roche, Mannheim Germany) immunoprecipitated proteins were eluted from the Protein G-agarose using 2 x SDS loading buffer, separated on SDS-PAGE and analyzed by Western blotting. To control for $GABA_{B1a}$ and $GABA_{B1j}$ expression levels, we lysed transfected HEK cells in RIPA buffer, pre-cleared the lysate at 10000xg for 10 min before mixing it with 2 x SDS loading buffer. Western blot analysis was with a rabbit polyclonal anti-myc (PRB-150C; Covance, Berkley, CA, diluted 1:1000) and a peroxidase-coupled secondary antibody (donkey anti-rabbit or anti-mouse HRP-conjugates, Amersham Biosciences UK Ltd., Little Chalfont, Buckinghamshire, UK; diluted 1:2500). Blots were developed using the enhanced chemiluminescence detection system (Amersham Biosciences UK, Ltd., Little Chalfont, Buckinghamshire, UK) and exposed to Kodak Bio-Max maximum resolution X-ray films (Sigma-Aldrich, St. Louis, MO).

Production and purification of RSDP

RSDP containing a polyhistidine tag was expressed in *P.pastorsis* and purified using Ni^{+}-charged resin (GraviTrap, Amersham, Supplementary information). To prepare RSDP for use in electrophysiological recordings, the eluted protein sample was concentrated and

dialysed against artificial cerebral spinal fluid (ACSF). The concentration of recombinant protein was achieved by ultrafiltering the sample solution though an anisotropic membrane YM-10 Centricon (Millipore, Billerica, MA). Following protein concentration, samples were immediately dialysed against freshly prepared ACSF according to manufacturer's instructions (Pierce, Rockford, IL) (SI Fig. 8).

Electrophysiology in hippocampal slices

Standard procedures were used to prepare 300 μM thick horizontal hippocampal slice from P22-P28 mice in cooled ACSF (119 mM NaCl, 2.5 mM KCl, 1.3 mM $MgCl_2$, 2.5 mM $CaCl_2$, 1.0 mM NaH_2PO_4, 26.2 mM $NaHCO_3$ and 11 mM glucose, continuously bubbled with 95 % O_2 and 5 % CO_2). After 1 h, slices were incubated for a minimum of 6 h with 1.0 μg/ml of SD protein. After 6 h, slice were transferred to the recording chamber and superfused (2 ml/min) with ACSF at 30-32°C. Whole-cell patch-clamp recordings were performed from the somata of CA1 pyramidal neurons to measure miniature excitatory postsynaptic currents (mEPSCs). Neurons were visualized using infrared and differential interference contrast optic. Drugs, applied by superfusion into the recording chamber, were kept as aliquots and solutions were freshly prepared on the day of the experiment. The effect of adenosine (100 μM) and baclofen (100 μM) on mEPSCs and mIPSCs were elicited at – 60 mV and recorded in the presence of tetrodotoxin (1 μM) and picrotoxin (100 μM). Patch electrodes (~3 MΩ) were filled with a solution containing the following: 140 mM Cs-gluconate, 10 mM HEPES, 10 mM phosphocreatine, 5 mM-314, 4 mM Mg-ATP, 0.3 mM Na-GTP, at pH 7.2 with Cs-OH and 285 mOsm. During the experiment $GABA_B$ receptors were activated using the agonist baclofen and inactivated by the selective antagonist CGP54626 (1 μM). MiniAnalysis software (version 6.0.4, Synaptosoft, Decatur, GA) was used for detection and analysis of mEPSCs and mIPSCs. Significant differences between two distributions of mEPSC and mIPSC amplitudes and interevent intervals were determined by using the Kolmogorov-Smirnov test, with *P* value < 0.01 indicating significance. The electrophysiologist was blinded to the treatment of the slice.

EPSCs and IPSCs were elicited by voltage pulses (100 μs, 2-5 V stimuli) delivered through a bipolar Pt-Ir electrode (25 μm in diameter) placed in the stratum radiatum at a distance of

150-200 μm from the soma of the recorded cell. The recording electrode was filled with a solution containing (in mM): 140 Cs-gluconate, 10 HEPES, 10 phosphocreatine, 5 QX-314, 4 Mg-ATP, 0.3 Na-GTP, at pH 7.25 with CsOH and 285 mOsm. EPSCs were measured at –70 mV in the presence of 100 μM picrotoxin.

Electrophysiology with cultured neurons

Primary hippocampal neurons were prepared from 16.5-day mouse embryos as described (Goslin K., 1998). Neurons were cultured in Neurobasal medium (Invitrogen, Carlsbad, CA) with B27 supplement (Invitrogen, Carlsbad, CA), 0.5 mM L-glutamine and 50-100 μg/ml Pen/Strep for 2-3 weeks at a density of ~ 750 cells/mm^2 on poly-L-lysine-coated glass cover slips. For the first three days, the culture medium was supplemented with 25 μM glutamic acid. On the day of the experiment, cover slips were placed in an interface chamber containing saline (140 mM NaCl, 3 mM KCl, 2.5 mM $CaCl_2$, 1.2 mM $MgCl_2$, 11.1 mM glucose, 10 mM Hepes, pH 7.2) equilibrated with 95% O_2 / 5% CO_2. Whole-cell patch clamp recordings were performed at 30-32 °C.

Acknowledgments

We would like to thank R. Turecek and K. Vogt for critical reading of the manuscript and V. Besseyrias for the genotyping of mice. This study was supported by the Swiss Science Foundation (3100-067100.01).

The $GABA_{B1j}$ cDNA sequence was deposited under the EMBL accession number AM418837.

Supporting Information

Recombinant protein expression in *P. pastoris*.

To express the $GABA_{B1a}$ RSDP, two oligonucleotides (forward: 5'-TTTGCGGCCGCGAGAACCTGTACGTACAGGGCGGGGCTCAGACCCCC-3'; reverse: 5'- AAATCTAGAGTCTGTACGTACAGGTTCTCGTGTGGCGTTCGATT-3') with unique restriction sites inserted were designed against published sequence of the mouse $GABA_{B1a}$ gene (accession no. AF114168). In addition, TEV cleavage sites were incorporated into the oligonucleotides (SI Fig. 7*A*). Using PCR, the two oligonucleotides will amplify sequence corresponding to residues 17–163 of the mouse $GABA_{B1a}$ gene (where residue 17 is Gly and residue 163 is His). The amplification was performed using the Expand High Fidelity PCR System (Roche, Mannheim, Germany) according to the manufacturer's instructions and the fidelity of the PCR product confirmed by sequencing. For subcloning into the yeast expression plasmid pPICZα (Invitrogen, Carlsbad, CA), plasmid DNA was digested with the restriction enzymes NotI and XbaI and ligation reactions performed according to manufacture's instructions. Ligation reactions were tranformed into chemically competent TOP10F' cells and positive clones were selected on low-salt LB/Zeocin plates. For expression of mutRSDP, the same primer sets for PCR were used in combination with a rat $GABA_{B1a}$ template with mutated cysteine residue (Gift from S. Abdel Aziz). Mutations were designed based on the $GABA_{B1a}$ sequence entry, accession no. Y10369; the cysteine residues C29, C95, C99 and C156, were mutated to serine residues to prevent the formation of disulfide bridges ritical for correct SD folding.

For transformation into *P. pastoris*, strain KM71H (Mut^s), 20 μg of linearised $GABA_{B1a}$ sushi-domain yeast expression vector was transformed into electrocompetent KM71H yeast prepared according to manufacturer's instructions (Invitrogen). To isolate yeast with multiple genomic integration of the expression vector, recombinants were selected on YPD media containing 500 μg/ml of Zeocin. For large-scale protein production, the manufacturer's instructions were followed. Briefly, 10 ml of buffered minimal medium with glycerol as the sole carbon source (BMGY) was inoculated with one colony of yeast. After overnight growth at 30 ^{o}C, with vigorous shaking, cells were diluted in 1000 ml of BMGY and grown for a further 18 h. To induce protein production, cells were harvested

by centrifugation and resuspended in 200 ml of induction medium containing methanol (0.5 % (v/v) final concentration) in place of glycerol (BMMY). Protein induction was maintained for 4 days with fresh methanol added every 24 h. At the end of the protein induction period, the recombinant protein containing supernatant was clarified by centrifugation and the recombinant $GABA_{B1a}$ sushi-domain protein purified with Ni^{+}-charged resin (GraviTrap, Amersham Biosciences UK Ltd., Little Chalfont, Buckinghamshire, UK). Following protein immobilisation, columns were washed with phosphate buffer containing 20 mM imidazole and the purified protein was eluted with phosphate buffer containing 500 mM imidazole. The identity of the purified recombinant $GABA_{B1a}$ sushi-domain protein was analysed by SDS-PAGE and verified by Coomassie blue staining or Western blotting with monoclonal anti-c-myc (Roche, Mannheim, Germany)/anti-polyhistidine (Amersham Biosciences UK Ltd., Little Chalfont, Buckinghamshire, UK) antibody (SI Fig. 6*B*)

Recombinant protein expression in *E. coli*.

To express recombinant fibulin-2 protein, the pET32a(+) expression vector containing the fibulin-2 C-terminal residues 1069-1184 (gift from P.N. Barlow) was transformed into *Escherichia coli* strain BL21(DE3) Gold. Cells containing the plasmid were grown in LB selective media at 30^{o}C. For protein induction, cells grown to an OD_{600nm} = 0.5 were induced by the addition of 0.1 mM isopropyl-β-D-thiogalactopyranoside for 2 h at 30^{o}C. Protein purification was performed using Ni^{+}-charged resin (GraviTrap, Amersham Biosciences UK Ltd., Little Chalfont, Buckinghamshire, UK) following cell lysis with B-PERII (Pierce, Rockford, IL) supplemented with Complete protease inhibitor cocktail (Roche, Mannheim Germany). Following protein immobilisation, columns were washed with phosphate buffer containing 50 mM imidazole and the purified protein was eluted with phosphate buffer containing 500 mM imidazole. The identity of the purified recombinant fibulin2 protein was analysed by SDS-PAGE and verified by Western blotting with monoclonal anti-polyhistidine (Amersham Biosciences UK Ltd., Little Chalfont, Buckinghamshire, UK) antibody (SI Fig. 7A). For electrophysiological recordings samples were dialysed against freshly prepared ACSF according to manufacturer's instructions (Pierce, Rockford, IL).

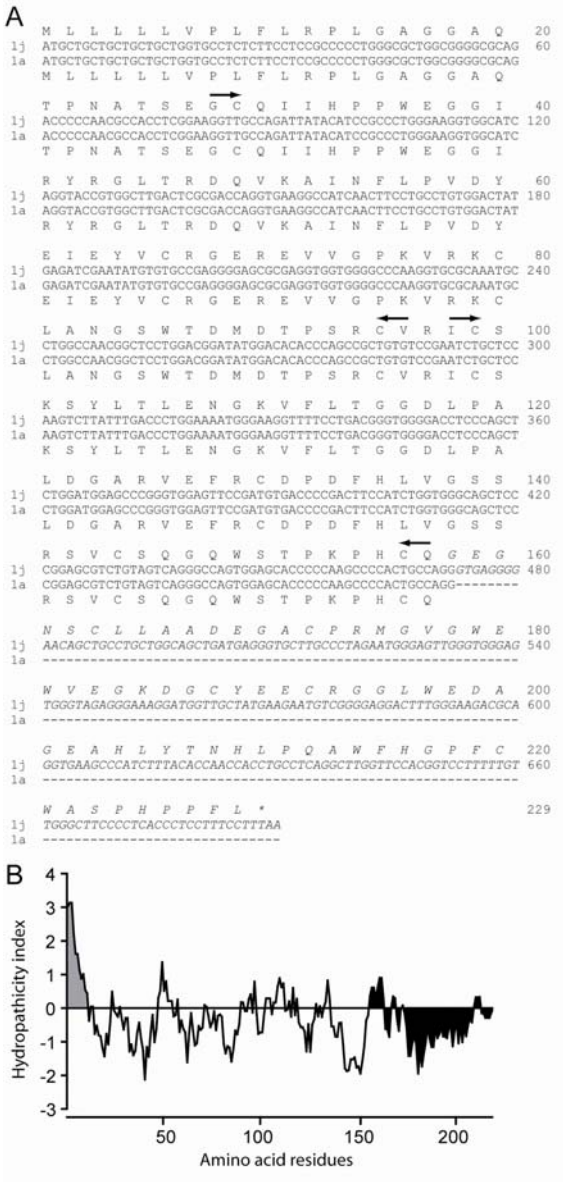

Figure 5.

(A) *Aligned nucleotide and predicted amino acid sequence of $GABA_{B1j}$ isoform compared to the N-terminal region of $GABA_{B1a}$. $GABA_{B1j}$ results from an extension of exon 4 at its 3' end for 870 bp. This generates an open reading frame (ORF) of 687 nucleotides encoding the first 157 amino acids of $GABA_{B1a}$ and 72 unrelated residues (in italics) without significant homology to known proteins. Note that only the region containing the predicted ORF is shown. Arrows delimit the two SDs, the stop codon in $GABA_{B1j}$ is indicated by an asterisk.*

(B) *Hydropathicity plot of $GABA_{B1j}$ according to Kyte and Doolittle indicating the lack of putative membrane-spanning segments besides the hydrophobic N-terminal signal peptide (grey coloring). Black coloring indicates the $GABA_{B1j}$-specific C-terminal region.*

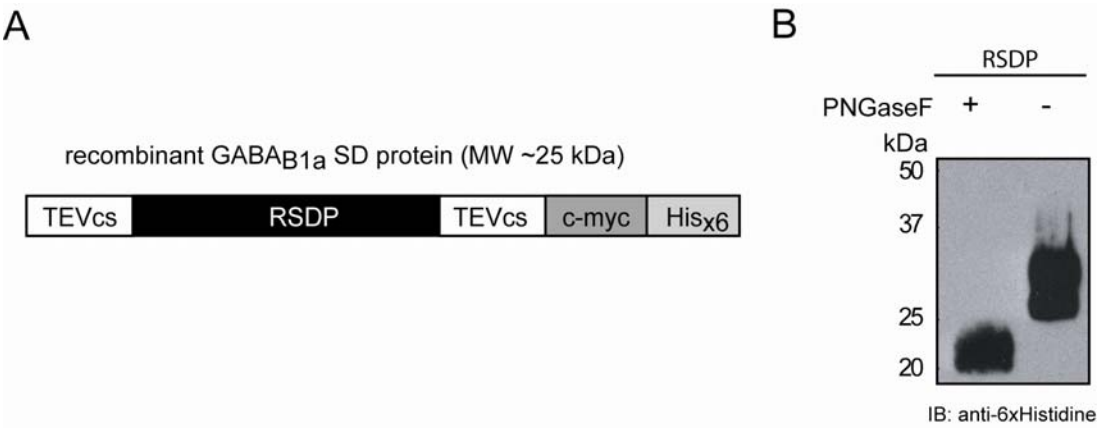

Figure 6.

(A) *Schematic representation of the RSDP expressed in P .pastoris. The recombinant protein contains the entire GABA$_{B1a}$ sushi-domain that is flanked by two Tobacco Etch Virus cleavage sites (TEVcs) followed by a c-myc and polyhistidine (His$_{x6}$) tag at the carboxyl-terminus. The predicted molecular weight of the recombinant protein is ~25 kDa.*

(B) *Protein analysis of the RSDP. The N-glycosylation of the RSDP (5 µg) was analysed by treatment with or without N-Glycosidase F overnight at 37^{o}C according to manufacturer's instructions (Roche). In addition, the RSDP thermalstability was examined by incubating the protein at 37^{o}C for 7 days. Individually treated protein samples were resolved in 15 % SDS-PAGE and protein visualised by Coomassie blue staining, or Western blotting with a mouse anti-myc antibody. The RSDP is N-glycosylated as indicated by the presence of a predicted molecular weight protein band in glycosidase treated samples, whilst untreated samples resolved at a higher molecular weight (~30 kDa). Degradation of the RSDP was not detected following prolonged incubation at 37^{o}C (Data not shown).*

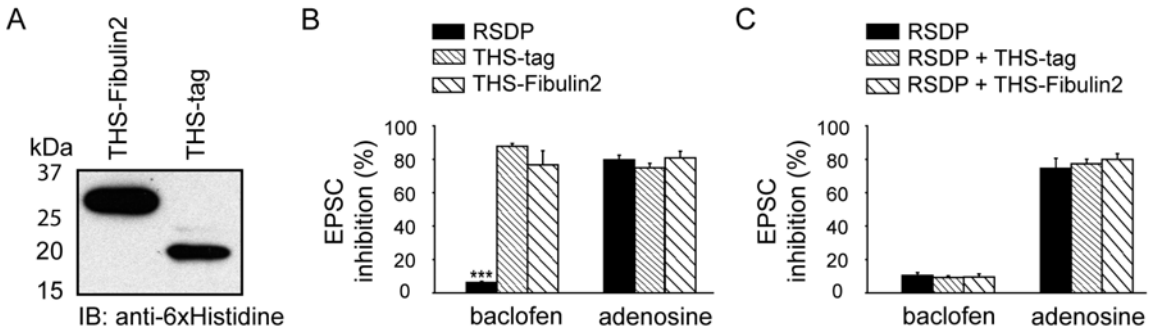

Figure 7. Recombinant fibulin-2 C-terminal (THS-fibulin2) protein does not interfere with $GABA_B$ heteroreceptor function or RSDP effects.

(A) *Summary histogram of the inhibition of evoked EPSC by baclofen (100 μM) and adenosine (100 μM) after incubation of hippocampal slices with RSDP, THS-tag (control) or THS-fibulin2 protein alone (1.0 μg/ml) for 6 h. Baclofen reduced the EPSC amplitudes recorded from CA1 pyramidal neurons in the presence of THS-fibulin2 and control but not of RSDP (THS-tag: 88.8 ± 1.7 % inhibition, n = 4; THS-fibulin2: 77.6 ± 8.5 % inhibition, n = 5; RSDP: 6.3 ± 0.7 % inhibition, n = 3; ***p < 0.001, Student's t test). Adenosine reduced the EPSC amplitude in the presence of RSDP, THS-fibulin2 or THS-tag to the same extent (RSDP: 80.7 ± 2.7 % inhibition, n = 3; THS-tag: 75.8 ± 2.7 % inhibition, n = 4; THS-fibulin2: 81.8 ± 4.1 % inhibition, n = 5).*

(B) *Summary histogram of the inhibition of evoked EPSC by baclofen (100 μM) and adenosine (100 μM) after incubation of hippocampal slices with RSDP protein alone or pre-incubated overnight with THS-fibulin2 / THS-tag (RSDP alone: 10.5 ± 1.7 % inhibition, n = 5; RSDP + THS-tag: 9.2 ± 1.0 % inhibition, n = 5; RSDP + THS-fibulin2: 9.5 ± 1.9 % inhibition, n = 6). Adenosine reduced the EPSC amplitude in the presence of RSDP alone or RSDP + THS-tag / THS-fibulin2 to the same extent (RSDP alone: 74.4 ± 6.1 % inhibition, n = 5; RSDP + THS-tag: 77.2 ± 2.7 % inhibition, n = 5; RSDP + THS-fibulin2: 79.8 ± 3.4 % inhibition, n = 6) (Abbreviations: RSDP, recombinant SD-protein; THS-tag, $TrxHis_{x6}S$-tag; THS-fibulin-2, $TrxHis_{x6}S$-tag fibulin2 C-terminal.) Values are expressed as mean ± SEM.*

Chapter V

DISCUSSION AND PERSPECTIVES

Discussion and Perspectives

The aim of this doctoral thesis was to unravel the role of the $GABA_{B1a}$-specific SDs in the pre- versus postsynaptic distribution and functional segregation of $GABA_B$ receptor subtypes. The central findings of this work have been described in chapter 2, 3 and 4 and will be discussed in the following section with respect to the current understanding of $GABA_B$ receptor signaling.

Short summary of the presented data

Using genetically modified mice with point-mutations in the translation start codons of either $GABA_{B1a}$ or $GABA_{B1b}$ we initially demonstrated that the two $GABA_{B1}$ isoforms localize to distinct synaptic sites and convey non-redundant functions (chapter 2). Most strikingly it was observed that at CA3-to-CA1 synapses in the hippocampus, $GABA_{B1a}$ assembles heteroreceptors controlling glutamate release, while predominantly $GABA_{B1b}$ mediates postsynaptic inhibition. This functional segregation of $GABA_B$ receptor subtypes was confirmed in the thalamus, cortex and lateral amygdala (Perez-Garci et al., 2006; Shaban et al., 2006, Ulrich et al., 2007). These results indicated for the first time that $GABA_{B1}$ isoforms differentially compartmentalize in glutamatergic neurons. To further unravel the underlying molecular mechanism we aimed at identifying sequence determinants accounting for the selective occurrence of $GABA_{B1a}$ at glutamatergic terminals. We studied the axonal versus dendritic distribution of transfected $GABA_B$ expression constructs in cultured hippocampal neurons and demonstrate a role for the $GABA_{B1a}$-specific SDs in axonal targeting of $GABA_{B(1a,2)}$ receptors (chapter 3). In addition, we show that the cytoplasmic C-terminal domain of the $GABA_{B2}$ subunit harbors dendritic targeting information. Thus, a combination of distinct signals compartmentalizes $GABA_B$ receptors to pre- and postsynaptic sites. Last, we show that a recombinant soluble protein encoding the SDs (RSDP) is able to selectively abolish heteroreceptor function, whilst leaving auto- and postsynaptic receptors unaffected (chapter 4). Likely, RSDPs interfere with the binding of the SDs to auxiliary proteins at the cell surface. It thus appears that the SDs in $GABA_{B1a}$ exert at least two functions: besides determining axonal targeting of $GABA_{B(1a,2)}$ receptors, the SDs are further subject to modulation thereby controlling

heteroreceptor function. Of note, this data provides a first potential tool for a selective therapeutic interference within the $GABA_B$ receptor system.

How do the SDs mediate axonal targeting?

In principle, $GABA_B$ receptor compartmentalization could involve mechanisms such as differential mRNA trafficking, protein targeting or protein retention (Horton & Ehlers, 2003; Sampo et al., 2003). However, transfected CA3 neurons show an almost elusive association of $GABA_{B1a}$ protein with axons (chapter 2, figure 6), which suggest protein targeting underlying axonal localization of $GABA_{B(1a,2)}$ receptors. Furthermore, the data presented in chapter 3 clearly identified the SDs as the critical axonal determinant. Nevertheless, an unsolved question is by which mechanism the SDs determine axonal localization.

Our finding that disulfide bond formation is important for the axonal localization of $GABA_{B1a}$ (chapter 3, figure 3) demonstrates that proper folding of the SDs into their unique tertiary structure is essential. This suggests that the SDs engage in a specific protein interaction required for targeting $GABA_{B(1a,2)}$ receptors to axons. The SDs are localized in the extracellular domain of $GABA_{B1a}$. Thus, along the biosynthetic route, the SDs face the luminal part of the endoplasmatic reticulum (ER), trans-Golgi network (TGN) and transport vesicle and are turned towards the extracellular matrix after insertion into the plasma membrane. Three different mechanisms are thus conceivable for explaining the mediating of axonal localization of $GABA_{B(1a,2)}$ receptors by the SDs.

First, the SDs could interact with membrane bound or ECM proteins in the axonal compartment, thereby anchoring $GABA_{B(1a,2)}$ receptors at glutamatergic terminals (“selective retention”). Second, the SDs could specifically sort $GABA_{B(1a,2)}$ receptors into axonally destined carriers through interaction with luminal proteins in the TGN (“selective delivery” or “direct targeting”). Third, binding of an unknown protein to the SDs could induce internalization of $GABA_{B(1a,2)}$ receptors from the somatodendritic membrane, followed by subsequent redistribution to axons, a process referred to as “transcytosis”.

Selective retention

In the case of selective retention, protein-laden post-Golgi carriers are non-selectively transported to axons and dendrites, leading to insertion of the delivered cargo into the plasma membrane of both compartments. Subsequently, those membrane proteins reaching the appropriate compartment bind to specific proteins and are thereby retained at particular sites. Without this anchoring, the membrane proteins are internalized and degraded or resorted (Sampo et al., 2003; Winckler, 2004). Our finding that exogenous application of soluble recombinant SD protein (RSDP) interferes with heteroreceptor function in a dominant-negative manner (chapter 4) indicates that the SDs in $GABA_{B1a}$ bind to proteins at the cell surface. This result is thus compatible with the SDs acting as retention signal at glutamatergic terminals. However, a prerequisite for selective retention is a uniform distribution of carriers and an equal insertion of $GABA_{B1a}$ and $GABA_{B1b}$ isoforms into the presynaptic membrane. $GABA_{B1b}$ protein was found neither in distal axons of cultured pyramidal neurons (chapter 2, figure 1 and 2) nor in axons of pyramidal neurons in organotypic slice cultures (chapter 2, figure 6). It is thus unlikely that selective retention accounts for the axonal localization of $GABA_{B(1a,2)}$ receptors.

Selective delivery

The second possible mechanism, selective delivery, implies that transported membrane proteins are sorted into specific axonal or somatodendritic destined carrier vesicles in the TGN. Such a mechanism for axonal targeting has been suggested for NgCAM, which uses five fibronectin type-III like repeats in its ectodomain as targting signals (Sampo et al., 2003). Extracellular protein sequences like the SDs cannot directly interact with cytosolic molecular motor or adaptor proteins. It was thus suggested that $GABA_{B(1a,2)}$ receptors are transported “piggyback style” by interacting with presynaptic proteins in the lumen of the transport vesicles, similar to other axonally destined proteins (Roos and Kelly, 2000). The elements of a mature presynaptic terminal, e.g. calcium channel subunits, endocytic proteins and synaptic vesicle proteins are transported along axons as discrete “transport packets” (Ahmari et al., 2000). Since $GABA_B$ receptors are localized near the active zone (Kulik et al., 2003) and are closely linked to the release machinery (Vigot et al., 2006) it is conceivable that $GABA_{B(1a,2)}$ receptors are transported towards glutamatergic terminals in such preassembled carriers.

Nevertheless, if the SDs mediate axonal targeting how is this compatible with $GABA_{B1a}$ isoforms assembling functional postsynaptic receptors (chapter 2)? Possibly, both $GABA_B$ receptor subtypes are sorted into somatodendritic post-Golgi carriers unless the SDs bind to a protein in the lumen of the TGN mediating axonal sorting. The availability of such a

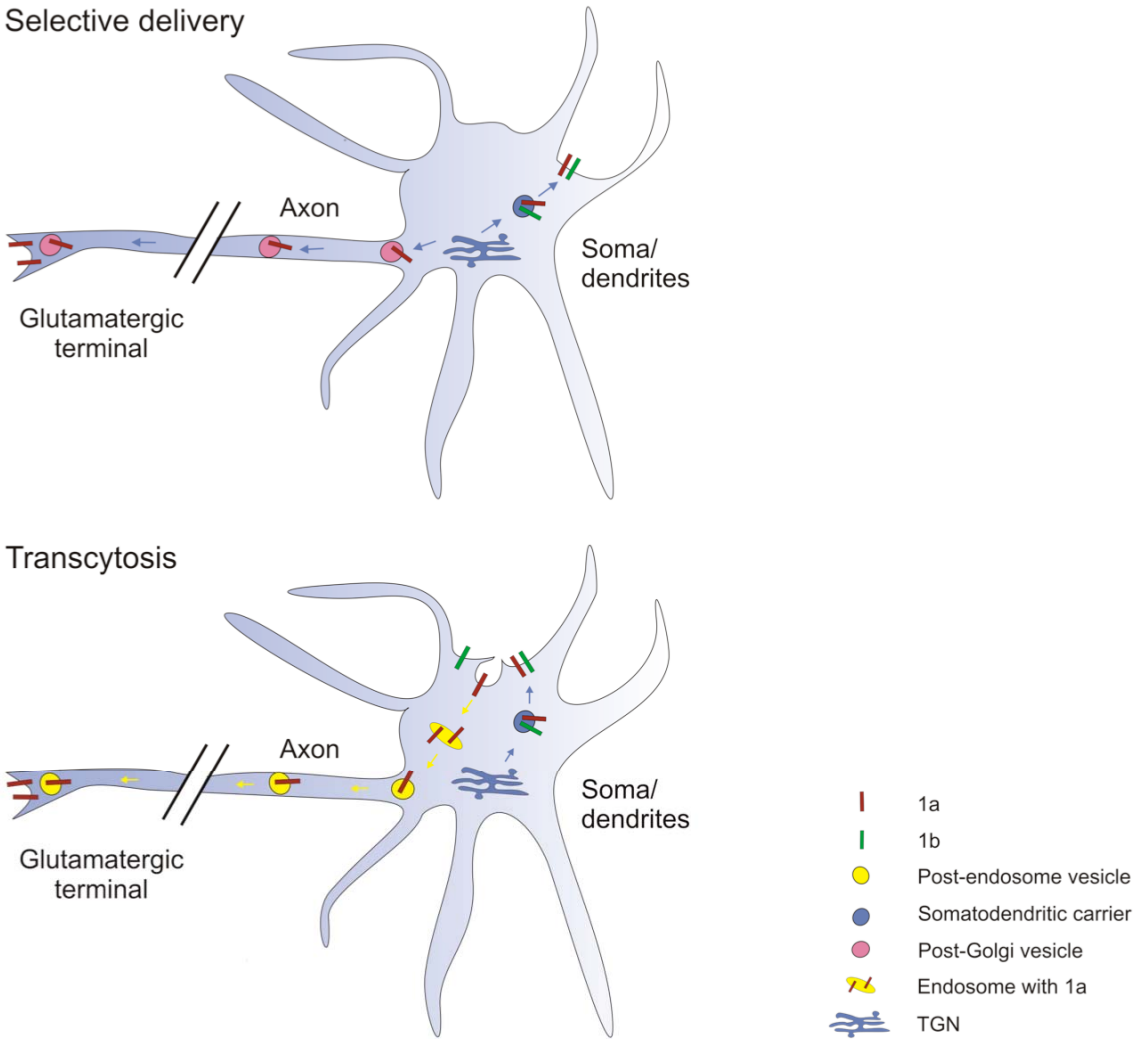

Figure 1. Schematic representation of the two possible mechanisms underlying $GABA_{B1a}$ axonal targeting, selective delivery and transcytosis.

<u>Selective delivery:</u> Both $GABA_{B(1a,2)}$ (1a) and $GABA_{B(1b,2)}$ receptors (1b) are transported towards dendrites in somatodendritic post-Golgi carriers. Additionally, $GABA_{B(1a,2)}$ receptors are selectively packaged into axonal transport carriers probably through a specific interaction of the SDs in the lumen of the TGN.

<u>Transcytosis:</u> Both $GABA_{B(1a,2)}$ and $GABA_{B(1b,2)}$ receptors are first eclusively transported to the somatodendritic compartment, where they are inserted into the plasma membrane. Subsequently, some

$GABA_{B(1a,2)}$ receptors are internalized and redistributed to axons, a scenario which could be induced through interaction of the SDs with surface proteins or other transcytosed membrane proteins.
Direct vesicle targeting to axons or dendrites is indicated by blue arrows, the indirect route by yellow arrows.

putative SD-binding protein could be limited so that a subset of $GABA_{B(1a,2)}$ receptors is sorted into somatodendritic carriers by default.

Transcytosis

The third possible mechanism for the mediation of axonal localization of $GABA_{B(1a,2)}$ receptors by the SDs is transcytosis. There, post-Golgi vesicles transport and insert their cargo initially into the somatodendritic membrane. Subsequently, membrane proteins destined for the axonal compartment are internalized and redirected to axons. In this regard, binding of a ligand or a secreted protein to the SDs in the ectodomain of $GABA_{B(1a,2)}$ receptors could modify receptor stability and potentially induce transcytosis. Alternatively, the SDs could associate with other transcytosed proteins thereby triggering internalization of $GABA_{B(1a,2)}$ receptors.

In the context of transcytosis, the presence of functional $GABA_{B(1a,2)}$ receptors at postsynaptic sites is relatively easy to explain. Individual dendritic segments have distinct molecular compositions and functional properties (Horton & Ehlers, 2003). Thus, a SD interacting surface or transmembrane protein presumably inducing transcytosis could be restricted to some dendritic subdomains. Furthermore, the endocytosis machinery could differ between dendritic segments. It is thus interesting to study whether the $GABA_{B1a}$ isoform assembles functional receptors all along the dendritic surface or whether the expression of $GABA_{B(1a,2)}$ receptors is restricted to some dendritic subdomains.

Outlook

Proposed experiments to further decipher the mechanism underlying $GABA_{B(1a,2)}$ receptor axonal targeting

Our data is compatible with two of the above discussed models, selective delivery and transcytosis. Nevertheless, deciphering which of these two scenarios eventually determines the localization of $GABA_{B(1a,2)}$ receptors at glutamatergic terminals requires further experiments. The identification of proteins binding to the SDs would probably constitute a decisive step in this context. Moreover, evidence for a selective internalization of $GABA_{B1a}$, but not $GABA_{B1b}$ protein from the somatodendritic membrane or its co-localization with endosomal markers would support the transcytosis scenario. Alternatively, the movement of eGFP-tagged $GABA_{B1a}$ protein could be analyzed in living cultured hippocampal neurons. This would help to distinguish between a direct vesicle movement from the TGN to glutamatergic terminals or an indirect, transcytotic pathway via the somatodendritic membrane. Of note, both selective delivery and transcytosis were shown to underlie the axonal targeting of NgCAM, a neuronal cell adhesion molecule (Sampo et al., 2003; Wisco et al., 2003). This suggests that the two scenarios are not mutually exclusive. Possibly, the two mechanisms occur in parallel, take place at variant time points and/or happen in different subsets of neurons.

Deciphering sequence motifs involved in somatodendritic targeting of $GABA_B$ receptors

Our data clearly identify the SDs as the axonal targeting determinant. We further provide evidence that the cytoplasmic 120 amino acid C-terminal sequence of the $GABA_{B2}$ subunit is involved in somatodendritic targeting (chapter 2, figure 7). Nevertheless, C-terminal truncated $GABA_{B2}$ protein was still present in dendrites. This indicates that additional sequence information must determine dendritic targeting. The identified 120 amino acid motif on the $GABA_{B2}$ subunit harbors a PDZ binding motif (VSGL) that has been shown to interact with Mupp-1, a PDZ-scaffold protein (Balasubramanian et al., 2007). It is thus possible that a so far unidentified targeting signal mediates dendritic transport of $GABA_B$ receptors, which are subsequently anchored at postsynaptic sites via the cytoplasmic C-terminal domain of the $GABA_{B2}$ subunit. It is thus important to narrow the amino acids in the cytoplasmic C-terminal domain of $GABA_{B2}$ essential for somatodendritic targeting as well as to clarify which additional sequences on the heteromer might further underlie dendritic targeting.

A putative role for the SDs at postsynaptic sites

Both $GABA_{B1}$ isoforms are localized and functional at postsynaptic sites (chapter 2 and 3), but it remains to be determined whether they exert different functions in dendrites. A first indication for a differential distribution of $GABA_{B1}$ isoforms in dendrites was given in chapter 2: tansfected CA3 pyramidal neurons show a selective occurrence of $GABA_{B1b}$ in dendritic spines, whereas both $GABA_{B1a}$ and $GABA_{B1b}$ are present in dendritic shafts. One possible explanation is that the SDs bind to a surface protein that anchor $GABA_{B(1a,2)}$ receptors in the extrasynaptic membrane, whereas $GABA_{B(1b,2)}$ receptors can freely move towards dendritic spines. The diffusion properties of eGFP-tagged $GABA_{B1a}$ and $GABA_{B1b}$ protein in the surface membrane between dendritic shafts and spine necks could be monitored in living neurons of e.g. organotypic slices cultures using two-photon laser scanning microscopy. Our data presented in chapter 3 further indicate that the majority of $GABA_B$ receptors is localized in intracellular pools. Possibly, $GABA_{B1a}$ and $GABA_{B1b}$ isoforms are differentially recruited from intracellular membranes. Thus, to further decipher the ratio of surface versus intracellular $GABA_{B1a}$ and $GABA_{B1b}$ protein in a quantitative manner the use of pH-sensitive GFP would be beneficial.

The SDs exert multiple functions

The data presented in this dissertation indicate multiple functions for the SDs. The SDs act as an axonal targeting signal, are subject to modulation of heteroreceptor function and likely play a role at postsynaptic sites. Of note, the two SDs in $GABA_{B1a}$ exhibit strikingly different structural properties (Blein et al., 2004). It is thus conceivable that individual SDs bind to different proteins and thereby convey different functions. Further deciphering the (distinct) function(s) of the SDs deeply depends on the identification of their extracellular and/or intracellular binding partners. The first N-terminal SD in $GABA_{B1a}$ was recently shown to interact with the ECM protein fibulin-2. However, a functional correlation with $GABA_B$ receptors remains elusive. In chapter 3 we have demonstrated that both SDs are able to mediate axonal targeting of $GABA_{B(1a,2)}$ receptors in glutamatergic neurons (chapter 3, figure 4). Nevertheless, it remains to be determined whether individual SDs exert distinct functions at postsynaptic sites or differentially modulate heteroreceptor function. Of note, different binding properties and diverse functions of the two SDs could account

for some of the heterogeneity in the $GABA_B$ receptor system that was previously observed in native studies.

Conclusion

The data presented in this dissertation provide the first evidence for a functional compartmentalization of $GABA_B$ receptor subtypes in glutamatergic neurons. This pre- versus postssynaptic segregation is mediated by the SDs in the ectodomain of $GABA_{B1a}$. Furthermore, our finding that RSDP selectively abolishes heteroreceptor function via the SDs provides a first potential tool for a selective therapeutic interference with individual $GABA_B$ receptor subtypes. This work thus indicates multiple functions for the SDs and provides a first potential tool for a selective therapeutic interference within the $GABA_B$ field.

References

Ahmari, S.E., J. Buchanan, and S.J. Smith. 2000. Assembly of presynaptic active zones from cytoplasmic transport packets. *Nat Neurosci*. 3:445-51.

Alvarez, J., A. Giuditta, and E. Koenig. 2000. Protein synthesis in axons and terminals: significance for maintenance, plasticity and regulation of phenotype. With a critique of slow transport theory. *Prog Neurobiol*. 62:1-62.

Ango, F., S. Albani-Torregrossa, C. Joly, D. Robbe, J.M. Michel, J.P. Pin, J. Bockaert, and L. Fagni. 1999. A simple method to transfer plasmid DNA into neuronal primary cultures: functional expression of the mGlu5 receptor in cerebellar granule cells. *Neuropharmacology*. 38:793-803.

Ango, F., J.P. Pin, J.C. Tu, B. Xiao, P.F. Worley, J. Bockaert, and L. Fagni. 2000. Dendritic and axonal targeting of type 5 metabotropic glutamate receptor is regulated by homer1 proteins and neuronal excitation. *The Journal of neuroscience*. 20:8710-6.

Baas, P.W. 1998. The role of motor proteins in establishing the microtubule arrays of axons and dendrites. *J Chem Neuroanat*. 14:175-80.

Baas, P.W., J.S. Deitch, M.M. Black, and G.A. Banker. 1988. Polarity orientation of microtubules in hippocampal neurons: uniformity in the axon and nonuniformity in the dendrite. *Proc Natl Acad Sci U S A*. 85:8335-9.

Balasubramanian, S., S.R. Fam, and R.A. Hall. 2007. GABAB Receptor Association with the PDZ Scaffold Mupp1 Alters Receptor Stability and Function. *J Biol Chem*. 282:4162-71.

Balasubramanian, S., J.A. Teissere, D.V. Raju, and R.A. Hall. 2004. Hetero-oligomerization between GABAA and GABAB receptors regulates GABAB receptor trafficking. *J Biol Chem*. 279:18840-50.

Barnes, C.A., M.W. Jung, B.L. McNaughton, D.L. Korol, K. Andreasson, and P.F. Worley. 1994. LTP saturation and spatial learning disruption: effects of task variables and saturation levels. *J Neurosci*. 14:5793-806.

Benke, D., M. Honer, C. Michel, B. Bettler, and H. Mohler. 1999. gamma-aminobutyric acid type B receptor splice variant proteins GBR1a and GBR1b are both associated with GBR2 in situ and display differential regional and subcellular distribution. *J Biol Chem*. 274:27323-30.

Benson, D.L., F.H. Watkins, O. Steward, and G. Banker. 1994. Characterization of GABAergic neurons in hippocampal cell cultures. *J Neurocytol*. 23:279-95.

Bettler, B., K. Kaupmann, J. Mosbacher, and M. Gassmann. 2004. Molecular structure and physiological functions of GABA(B) receptors. *Physiol Rev*. 84:835-67.

Bettler, B., and J.Y. Tiao. 2006. Molecular diversity, trafficking and subcellular localization of GABA(B) receptors. *Pharmacol Ther*. 110:533-43.

Billinton, A., N. Upton, and N.G. Bowery. 1999. GABA(B) receptor isoforms GBR1a and GBR1b, appear to be associated with pre- and post-synaptic elements respectively in rat and human cerebellum. *Br J Pharmacol*. 126:1387-92.

Bischoff, S., S. Leonhard, N. Reymann, V. Schuler, R. Shigemoto, K. Kaupmann, and B. Bettler. 1999. Spatial distribution of GABA(B)R1 receptor mRNA and binding sites in the rat brain. *J Comp Neurol*. 412:1-16.

Blein, S., R. Ginham, D. Uhrin, B.O. Smith, D.C. Soares, S. Veltel, R.A. McIlhinney, J.H. White, and P.N. Barlow. 2004. Structural analysis of the complement control protein (CCP) modules of GABA(B) receptor 1a: only one of the two CCP modules is compactly folded. *J Biol Chem*. 279:48292-306.

Bonanno, G., F. Carita, P. Cavazzani, C. Munari, and M. Raiteri. 1999. Selective block of rat and human neocortex GABA(B) receptors regulating somatostatin release by a GABA(B) antagonist endowed with cognition enhancing activity. *Neuropharmacology*. 38:1789-95.

Bonanno, G., A. Fassio, G. Schmid, P. Severi, R. Sala, and M. Raiteri. 1997. Pharmacologically distinct GABAB receptors that mediate inhibition of GABA and glutamate release in human neocortex. *Br J Pharmacol*. 120:60-4.

Bonanno, G., and M. Raiteri. 1993. Multiple GABAB receptors. *Trends Pharmacol Sci*. 14:259-61.

Bonifacino, J.S., and L.M. Traub. 2003. Signals for sorting of transmembrane proteins to endosomes and lysosomes. *Annu Rev Biochem*. 72:395-447.

Boulos, S., B.P. Meloni, P.G. Arthur, C. Bojarski, and N.W. Knuckey. 2006. Assessment of CMV, RSV and SYN1 promoters and the woodchuck post-transcriptional regulatory element in adenovirus vectors for transgene expression in cortical neuronal cultures. *Brain Res*. 1102:27-38.

Bowery, N.G. 2006. GABAB receptor: a site of therapeutic benefit. *Curr Opin Pharmacol*. 6:37-43.

Bowery, N.G., B. Bettler, W. Froestl, J.P. Gallagher, F. Marshall, M. Raiteri, T.I. Bonner, and S.J. Enna. 2002. International Union of Pharmacology. XXXIII. Mammalian gamma-aminobutyric acid(B) receptors: structure and function. *Pharmacol Rev*. 54:247-64.

Brauner-Osborne, H., and P. Krogsgaard-Larsen. 1999. Functional pharmacology of cloned heterodimeric GABAB receptors expressed in mammalian cells. *Br J Pharmacol*. 128:1370-4.

Brewer, G.J. 1993. Optimized survival of hippocampal neurons in B-27 supplemented Neurobasal, a new serum-free medium combination. *J. Neurosci. Res.* 35:567-576.

Broadbent, N.J., L.R. Squire, and R.E. Clark. 2004. Spatial memory, recognition memory, and the hippocampus. *Proc Natl Acad Sci U S A.* 101:14515-20.

Brock, C., L. Boudier, D. Maurel, J. Blahos, and J.P. Pin. 2005. Assembly-dependent surface targeting of the heterodimeric GABAB Receptor is controlled by COPI but not 14-3-3. *Mol Biol Cell*. 16:5572-8.

Bulanova, E., V. Budagian, E. Duitman, Z. Orinska, H. Krause, R. Ruckert, N. Reiling, and S. Bulfone-Paus. 2007. Soluble Interleukin IL-15Ralpha is generated by alternative splicing or proteolytic cleavage and forms functional complexes with IL-15. *J Biol Chem*. 282:13167-79.

Burack, M.A., M.A. Silverman, and G. Banker. 2000. The role of selective transport in neuronal protein sorting. *Neuron*. 26:465-72.

Burrone, J., and V.N. Murthy. 2003. Synaptic gain control and homeostasis. *Curr Opin Neurobiol*. 13:560-7.

Burton, P.R., and J.L. Paige. 1981. Polarity of axoplasmic microtubules in the olfactory nerve of the frog. *Proc Natl Acad Sci U S A.* 78:3269-73.

Caceres, A., L.I. Binder, M.R. Payne, P. Bender, L. Rebhun, and O. Steward. 1984. Differential subcellular localization of tubulin and the microtubule-associated protein MAP2 in brain tissue as revealed by immunocytochemistry with monoclonal hybridoma antibodies. *J Neurosci*. 4:394-410.

Calver, A.R., C.H. Davies, and M. Pangalos. 2002. GABA(B) receptors: from monogamy to promiscuity. *Neurosignals*. 11:299-314.

Conn, P.J., and J.P. Pin. 1997. Pharmacology and functions of metabotropic glutamate receptors. *Annu Rev Pharmacol Toxicol*. 37:205-37.

Correa, S.A., R. Munton, A. Nishimune, S. Fitzjohn, and J.M. Henley. 2004. Development of GABAB subunits and functional GABAB receptors in rat cultured hippocampal neurons. *Neuropharmacology*. 47:475-84.

Couve, A., A.K. Filippov, C.N. Connolly, B. Bettler, D.A. Brown, and S.J. Moss. 1998. Intracellular retention of recombinant GABAB receptors. *J Biol Chem*. 273:26361-7.

Couve, A., J.T. Kittler, J.M. Uren, A.R. Calver, M.N. Pangalos, F.S. Walsh, and S.J. Moss. 2001. Association of GABA(B) receptors and members of the 14-3-3 family of signaling proteins. *Mol Cell Neurosci*. 17:317-28

.

Couve, A., S. Restituito, J.M. Brandon, K.J. Charles, H. Bawagan, K.B. Freeman, M.N. Pangalos, A.R. Calver, and S.J. Moss. 2004. Marlin-1 a novel RNA binding protein associates with GABA(B) receptors. *J Biol Chem*.

Couve, A., P. Thomas, A.R. Calver, W.D. Hirst, M.N. Pangalos, F.S. Walsh, T.G. Smart, and S.J. Moss. 2002. Cyclic AMP-dependent protein kinase phosphorylation facilitates GABA(B) receptor-effector coupling. *Nat Neurosci*. 5:415-24.

Craig, A.M., and G. Banker. 1994. Neuronal polarity. *Annu Rev Neurosci*. 17:267-310.

Cryan, J.F., and K. Kaupmann. 2005. Don't worry 'B' happy!: a role for GABA(B) receptors in anxiety and depression. *Trends Pharmacol Sci*. 26:36-43.

Cunningham, M.D., and S.J. Enna. 1996. Evidence for pharmacologically distinct GABAB receptors associated with cAMP production in rat brain. *Brain Res*. 720:220-4.

Das, S.S., and G.A. Banker. 2006. The role of protein interaction motifs in regulating the polarity and clustering of the metabotropic glutamate receptor mGluR1a. *J Neurosci*. 26:8115-25.

Davies, C.H., and G.L. Collingridge. 1996. Regulation of EPSPs by the synaptic activation of GABAB autoreceptors in rat hippocampus. *J Physiol*. 496 (Pt 2):451-70.

Davies, C.H., S.J. Starkey, M.F. Pozza, and G.L. Collingridge. 1991. GABA autoreceptors regulate the induction of LTP. *Nature*. 349:609-11.

de Hoop, M., C. von Poser, C. Lange, E. Ikonen, W. Hunziker, and C.G. Dotti. 1995. Intracellular routing of wild-type and mutated polymeric immunoglobulin receptor in hippocampal neurons in culture. *J Cell Biol*. 130:1447-59.

Deisz, R.A., J.M. Billard, and W. Zieglgansberger. 1997. Presynaptic and postsynaptic GABAB receptors of neocortical neurons of the rat in vitro: differences in pharmacology and ionic mechanisms. *Synapse*. 25:62-72.

Deriu, D., M. Gassmann, S. Firbank, D. Ristig, C. Lampert, J. Mosbacher, W. Froestl, K. Kaupmann, B. Bettler, and M.G. Grutter. 2005. Determination of the minimal functional ligand-binding domain of the GABAB1b receptor. *Biochem J*. 386:423-31.

Desai, A., and T.J. Mitchison. 1997. Microtubule polymerization dynamics. *Annu Rev Cell Dev Biol*. 13:83-117.

Dinkel, A., W.K. Aicher, K. Warnatz, K. Burki, H. Eibel, and B. Ledermann. 1999. Efficient generation of transgenic BALB/c mice using BALB/c embryonic stem cells. *J Immunol Methods*. 223:255-60.

Diverse-Pierluissi, M., A.E. Remmers, R.R. Neubig, and K. Dunlap. 1997. Novel form of crosstalk between G protein and tyrosine kinase pathways. *Proc Natl Acad Sci U S A*. 94:5417-21.

Dotti, C.G., C.A. Sullivan, and G.A. Banker. 1988. The establishment of polarity by hippocampal neurons in culture. *J Neurosci*. 8:1454-68.

Drake, C.T., S.B. Bausch, T.A. Milner, and C. Chavkin. 1997. GIRK1 immunoreactivity is present predominantly in dendrites, dendritic spines, and somata in the CA1 region of the hippocampus. *Proc Natl Acad Sci U S A*. 94:1007-12.

Dunlap, K., and G.D. Fischbach. 1981. Neurotransmitters decrease the calcium conductance activated by depolarization of embryonic chick sensory neurones. *J Physiol*. 317:519-35.

Durand, G.M., Y. Kovalchuk, and A. Konnerth. 1996. Long-term potentiation and functional synapse induction in developing hippocampus. *Nature*. 381:71-5.

El-Husseini, A.E., P. Fretier, and S.R. Vincent. 2001. Cloning and characterization of a gene (RNF22) encoding a novel brain expressed ring finger protein (BERP) that maps to human chromosome 11p15.5. *Genomics*. 71:363-7.

Enna, S.J., and N.G. Bowery. 2004. GABA(B) receptor alterations as indicators of physiological and pharmacological function. *Biochem Pharmacol*. 68:1541-8.

Ennaceur, A., and J. Delacour. 1988. A new one-trial test for neurobiological studies of memory in rats. 1: Behavioral data. *Behav Brain Res*. 31:47-59.

Fagni, L., P. Chavis, F. Ango, and J. Bockaert. 2000. Complex interactions between mGluRs, intracellular Ca2+ stores and ion channels in neurons. *Trends in neurosciences*. 23:80-8.

Filippov, A.K., A. Couve, M.N. Pangalos, F.S. Walsh, D.A. Brown, and S.J. Moss. 2000. Heteromeric assembly of GABA(B)R1 and GABA(B)R2 receptor subunits inhibits Ca(2+) current in sympathetic neurons. *The Journal of neuroscience*. 20:2867-74.

Folsch, H., H. Ohno, J.S. Bonifacino, and I. Mellman. 1999. A novel clathrin adaptor complex mediates basolateral targeting in polarized epithelial cells. *Cell*. 99:189-98.

Francesconi, A., and R.M. Duvoisin. 2002. Alternative splicing unmasks dendritic and axonal targeting signals in metabotropic glutamate receptor 1. *J Neurosci*. 22:2196-205.

Fritschy, J.M., C. Sidler, F. Parpan, M. Gassmann, K. Kaupmann, B. Bettler, and D. Benke. 2004. Independent maturation of the GABA(B) receptor subunits GABA(B1) and GABA(B2) during postnatal development in rodent brain. *J Comp Neurol*. 477:235-52.

Froestl, W., M. Gallagher, H. Jenkins, A. Madrid, T. Melcher, S. Teichman, C.G. Mondadori, and R. Pearlman. 2004. SGS742: the first GABA(B) receptor antagonist in clinical trials. *Biochem Pharmacol*. 68:1479-87.

Gally, C., S. Eimer, J.E. Richmond, and J.L. Bessereau. 2004. A transmembrane protein required for acetylcholine receptor clustering in Caenorhabditis elegans. *Nature*. 431:578-82.

Gardiol, A., C. Racca, and A. Triller. 1999. Dendritic and postsynaptic protein synthetic machinery. *J Neurosci*. 19:168-79.

Garrido, J.J., F. Fernandes, P. Giraud, I. Mouret, E. Pasqualini, M.P. Fache, F. Jullien, and B. Dargent. 2001. Identification of an axonal determinant in the C-terminus of the sodium channel Na(v)1.2. *Embo J*. 20:5950-61.

Garrido, J.J., P. Giraud, E. Carlier, F. Fernandes, A. Moussif, M.P. Fache, D. Debanne, and B. Dargent. 2003. A targeting motif involved in sodium channel clustering at the axonal initial segment. *Science*. 300:2091-4.

Gasparini, S., C. Saviane, L.L. Voronin, and E. Cherubini. 2000. Silent synapses in the developing hippocampus: lack of functional AMPA receptors or low probability of glutamate release? *Proc Natl Acad Sci U S A*. 97:9741-6.

Gassmann, M., C. Haller, Y. Stoll, S.A. Aziz, B. Biermann, J. Mosbacher, K. Kaupmann, and B. Bettler. 2005. The RXR-type endoplasmic reticulum-retention/retrieval signal of GABAB1 requires distant spacing from the membrane to function. *Mol Pharmacol*. 68:137-44.

Gassmann, M., H. Shaban, R. Vigot, G. Sansig, C. Haller, S. Barbieri, Y. Humeau, V. Schuler, M. Muller, B. Kinzel, K. Klebs, M. Schmutz, W. Froestl, J. Heid, P.H. Kelly, C. Gentry, A.L. Jaton, H. Van der Putten, C. Mombereau, L. Lecourtier, J. Mosbacher, J.F. Cryan, J.M. Fritschy, A. Luthi, K. Kaupmann, and B. Bettler. 2004. Redistribution of GABAB(1) protein and atypical GABAB responses in GABAB(2)-deficient mice. *J Neurosci*. 24:6086-97.

Gemignani, A., P. Paudice, G. Bonanno, and M. Raiteri. 1994. Pharmacological discrimination between gamma-aminobutyric acid type B receptors regulating cholecystokinin and somatostatin release from rat neocortex synaptosomes. *Mol Pharmacol*. 46:558-62.

Giuditta, A., B.B. Kaplan, J. van Minnen, J. Alvarez, and E. Koenig. 2002. Axonal and presynaptic protein synthesis: new insights into the biology of the neuron. *Trends Neurosci*. 25:400-4.

Goslin K., A.H., Banker G. 1998. Rat hippocampal neurons in low-density culture. *In* Culturing Nerve Cells. G.K. Banker G., editor. MIT Press, Cambridge, MA. 339-370.

Grace, C.R., M.H. Perrin, M.R. DiGruccio, C.L. Miller, J.E. Rivier, W.W. Vale, and R. Riek. 2004. NMR structure and peptide hormone binding site of the first extracellular domain of a type B1 G protein-coupled receptor. *Proc Natl Acad Sci U S A*. 101:12836-41.

Gu, C., Y.N. Jan, and L.Y. Jan. 2003. A conserved domain in axonal targeting of Kv1 (Shaker) voltage-gated potassium channels. *Science*. 301:646-9.

Gu, C., W. Zhou, M.A. Puthenveedu, M. Xu, Y.N. Jan, and L.Y. Jan. 2006. The microtubule plus-end tracking protein EB1 is required for Kv1 voltage-gated K+ channel axonal targeting. *Neuron*. 52:803-16.

Guetg, N., R. Vigot, M. Gassman, H. Bräuner-Osborne, R. Shigemoto, O. Kretz, M. Frotscher, A. Kulik, and B. Bettler. submitted. Differential compartmentalization of GABAB receptor subtypes at mossy fiber-CA3 pyramidal neuron synapses.

Hashiguchi, T., M. Saito, E. Morishita, T. Matsuda, and A. Ichinose. 1993. Two genetic defects in a patient with complete deficiency of the b-subunit for coagulation factor XIII. *Blood*. 82:145-50.

Hawrot, E., Y. Xiao, Q.L. Shi, D. Norman, M. Kirkitadze, and P.N. Barlow. 1998. Demonstration of a tandem pair of complement protein modules in $GABA_B$ receptor 1a. *FEBS Lett*. 432:103-8.

Hill, D.R. 1985. GABAB receptor modulation of adenylate cyclase activity in rat brain slices. *Br J Pharmacol*. 84:249-57.

Hill, D.R., and N.G. Bowery. 1981. 3H-baclofen and 3H-GABA bind to bicuculline-insensitive GABA B sites in rat brain. *Nature*. 290:149-52.

Hirokawa, N. 1998. Kinesin and dynein superfamily proteins and the mechanism of organelle transport. *Science*. 279:519-26.

Hirokawa, N. 2006. mRNA transport in dendrites: RNA granules, motors, and tracks. *J Neurosci*. 26:7139-42.

Hirokawa, N., and R. Takemura. 2005. Molecular motors and mechanisms of directional transport in neurons. *Nat Rev Neurosci*. 6:201-14.

Holter, J., J. Davies, N. Leresche, V. Crunelli, and D.A. Carter. 2005. Identification of two further splice variants of GABABR1 characterizes the conserved micro-exon 4 as a hot spot for regulated splicing in the rat brain. *J Mol Neurosci*. 26:99-108.

Horton, A.C., and M.D. Ehlers. 2003a. Dual modes of endoplasmic reticulum-to-Golgi transport in dendrites revealed by live-cell imaging. *J Neurosci*. 23:6188-99.

Horton, A.C., and M.D. Ehlers. 2003b. Neuronal polarity and trafficking. *Neuron*. 40:277-95.

Horton, A.C., and M.D. Ehlers. 2004. Secretory trafficking in neuronal dendrites. *Nat Cell Biol*. 6:585-91.

Horton, A.C., B. Racz, E.E. Monson, A.L. Lin, R.J. Weinberg, and M.D. Ehlers. 2005. Polarized secretory trafficking directs cargo for asymmetric dendrite growth and morphogenesis. *Neuron*. 48:757-71.

Huang, C.S., S.H. Shi, J. Ule, M. Ruggiu, L.A. Barker, R.B. Darnell, Y.N. Jan, and L.Y. Jan. 2005. Common molecular pathways mediate long-term potentiation of synaptic excitation and slow synaptic inhibition. *Cell*. 123:105-18.

Ichinose, A., R.E. Bottenus, and E.W. Davie. 1990. Structure of transglutaminases. *J Biol Chem*. 265:13411-4.

Isaac, J.T., R.A. Nicoll, and R.C. Malenka. 1995. Evidence for silent synapses: implications for the expression of LTP. *Neuron*. 15:427-34.

Jareb, M., and G. Banker. 1998. The polarized sorting of membrane proteins expressed in cultured hippocampal neurons using viral vectors. *Neuron*. 20:855-67.

Job, C., and J. Eberwine. 2001. Localization and translation of mRNA in dendrites and axons. *Nat Rev Neurosci*. 2:889-98.

Jolimay, N., L. Franck, X. Langlois, M. Hamon, and M. Darmon. 2000. Dominant role of the cytosolic C-terminal domain of the rat 5-HT1B receptor in axonal-apical targeting. *The Journal of neuroscience*. 20:9111-8.

Kanaani, J., D. el-Husseini Ael, A. Aguilera-Moreno, J.M. Diacovo, D.S. Bredt, and S. Baekkeskov. 2002. A combination of three distinct trafficking signals mediates axonal targeting and presynaptic clustering of GAD65. *J Cell Biol*. 158:1229-38.

Kaupmann, K., K. Huggel, J. Heid, P.J. Flor, S. Bischoff, S.J. Mickel, G. McMaster, C. Angst, H. Bittiger, W. Froestl, and B. Bettler. 1997a. Expression cloning of $GABA_B$ receptors uncovers similarity to metabotropic glutamate receptors. *Nature*. 386:239-46.

Kaupmann, K., B. Malitschek, V. Schuler, J. Heid, W. Froestl, P. Beck, J. Mosbacher, S. Bischoff, A. Kulik, R. Shigemoto, A. Karschin, and B. Bettler. 1998a. GABA(B)-receptor subtypes assemble into functional heteromeric complexes. *Nature*. 396:683-7.

Kaupmann, K., J. Mosbacher, V. Schuler, P.J. Flor, W. Froestl, H. Bittiger, B. Sommer, and B. Bettler. 1997b. Structure, pharmacology and chromosomal localization of $GABA_B$ receptors. *Society for Neuroscience*. 23:954.

Kaupmann, K., V. Schuler, J. Mosbacher, S. Bischoff, H. Bittiger, J. Heid, W. Fröstl, T. Leonhardt, T. Pfaff, A. Karschin, and B. Bettler. 1998b. Human $GABA_B$ receptors

are differentially expressed and regulate inwardly rectifying K^+ channels. *Proc Natl Acad Sci USA*. 95:14991-6.

Kerr, D.I., J. Ong, R. Hughes, and R.H. Prager. 1995. 3-amino-2-hydroxy-N-(4-nitrophenyl)-propanesulphonamide, a new class of GABAB receptor antagonist in central and peripheral preparations. *Eur J Pharmacol*. 294:349-52.

Kirkitadze, M.D., and P.N. Barlow. 2001. Structure and flexibility of the multiple domain proteins that regulate complement activation. *Immunol Rev*. 180:146-61.

Kobayashi, T., B. Storrie, K. Simons, and C.G. Dotti. 1992. A functional barrier to movement of lipids in polarized neurons. *Nature*. 359:647-50.

Koyrakh, L., R. Lujan, J. Colon, C. Karschin, Y. Kurachi, A. Karschin, and K. Wickman. 2005. Molecular and cellular diversity of neuronal G-protein-gated potassium channels. *J Neurosci*. 25:11468-78.

Kugler, S., L. Meyn, H. Holzmuller, E. Gerhardt, S. Isenmann, J.B. Schulz, and M. Bahr. 2001. Neuron-specific expression of therapeutic proteins: evaluation of different cellular promoters in recombinant adenoviral vectors. *Mol Cell Neurosci*. 17:78-96.

Kulik, A., K. Nakadate, G. Nyiri, T. Notomi, B. Malitschek, B. Bettler, and R. Shigemoto. 2002. Distinct localization of $GABA_B$ receptors relative to synaptic sites in the rat cerebellum and ventrobasal thalamus. *Eur J Neurosci*. 15:291-307.

Kulik, A., I. Vida, Y. Fukazawa, N. Guetg, Y. Kasugai, C.L. Marker, F. Rigato, B. Bettler, K. Wickman, M. Frotscher, and R. Shigemoto. 2006. Compartment-dependent colocalization of Kir3.2-containing K+ channels and GABAB receptors in hippocampal pyramidal cells. *J Neurosci*. 26:4289-97.

Kulik, A., I. Vida, R. Lujan, C.A. Haas, G. Lopez-Bendito, R. Shigemoto, and M. Frotscher. 2003. Subcellular localization of metabotropic $GABA_B$ receptor subunits $GABA_{B(1a/b)}$ and $GABA_{B(2)}$ in the rat hippocampus. *J Neurosci*. 23:11026-35.

Kullmann, D.M. 1994. Amplitude fluctuations of dual-component EPSCs in hippocampal pyramidal cells: implications for long-term potentiation. *Neuron*. 12:1111-20.

Kyte, J., and R.F. Doolittle. 1982. A simple method for displaying the hydropathic character of a protein. *J Mol Biol*. 157:105-32.

Lehtinen, M.J., S. Meri, and T.S. Jokiranta. 2004. Interdomain contact regions and angles between adjacent short consensus repeat domains. *J Mol Biol*. 344:1385-96.

Lei, S., and C.J. McBain. 2003. GABA B receptor modulation of excitatory and inhibitory synaptic transmission onto rat CA3 hippocampal interneurons. *J Physiol*. 546:439-53.

Leung, L.S., and P. Peloquin. 2006. GABA(B) receptors inhibit backpropagating dendritic spikes in hippocampal CA1 pyramidal cells in vivo. *Hippocampus*. 16:388-407.

Liao, D., N.A. Hessler, and R. Malinow. 1995. Activation of postsynaptically silent synapses during pairing-induced LTP in CA1 region of hippocampal slice. *Nature*. 375:400-4.

Liao, D., X. Zhang, R. O'Brien, M.D. Ehlers, and R.L. Huganir. 1999. Regulation of morphological postsynaptic silent synapses in developing hippocampal neurons. *Nat Neurosci*. 2:37-43.

Lopez-Bendito, G., R. Shigemoto, A. Kulik, O. Paulsen, A. Fairen, and R. Lujan. 2002. Expression and distribution of metabotropic GABA receptor subtypes GABABR1 and GABABR2 during rat neocortical development. *Eur J Neurosci*. 15:1766-78.

Luscher, B., R. Hauselmann, S. Leitgeb, T. Rulicke, and J.M. Fritschy. 1997. Neuronal subtype-specific expression directed by the GABA(A) receptor delta subunit gene promoter/upstream region in transgenic mice and in cultured cells. *Brain Res Mol Brain Res*. 51:197-211.

Lüscher, C., L.Y. Jan, M. Stoffel, R.C. Malenka, and R.A. Nicoll. 1997. G protein-coupled inwardly rectifying K^+ channels (GIRKs) mediate postsynaptic but not presynaptic transmitter actions in hippocampal neurons. *Neuron*. 19:687-95.

Luthi, A., L. Schwyzer, J.M. Mateos, B.H. Gahwiler, and R.A. McKinney. 2001. NMDA receptor activation limits the number of synaptic connections during hippocampal development. *Nat Neurosci*. 4:1102-7.

Malinow, R., and R.C. Malenka. 2002. AMPA receptor trafficking and synaptic plasticity. *Annu Rev Neurosci*. 25:103-26.

Malitschek, B., D. Ruegg, J. Heid, K. Kaupmann, H. Bittiger, W. Frostl, B. Bettler, and R. Kuhn. 1998. Developmental changes of agonist affinity at GABABR1 receptor variants in rat brain. *Mol Cell Neurosci*. 12:56-64.

Margeta-Mitrovic, M., Y.N. Jan, and L.Y. Jan. 2000. A trafficking checkpoint controls $GABA_B$ receptor heterodimerization. *Neuron*. 27:97-106.

Marshall, F.H., K.A. Jones, K. Kaupmann, and B. Bettler. 1999a. $GABA_B$ receptors - the first 7TM heterodimers. *Trends Pharmacol Sci*. 20:396-9.

Marshall, F.H., J. White, M. Main, A. Green, and A. Wise. 1999b. $GABA_B$ receptors function as heterodimers. *Biochem Soc Trans*. 27:530-5.

Martin, S.C., S.J. Russek, and D.H. Farb. 2001. Human GABA(B)R genomic structure: evidence for splice variants in GABA(B)R1 but not GABA(B)R2. *Gene*. 278:63-79.

Masu, M., Y. Tanabe, K. Tsuchida, R. Shigemoto, and S. Nakanishi. 1991. Sequence and expression of a metabotropic glutamate receptor. *Nature*. 349:760-5.

McLatchie, L.M., N.J. Fraser, M.J. Main, A. Wise, J. Brown, N. Thompson, R. Solari, M.G. Lee, and S.M. Foord. 1998. RAMPs regulate the transport and ligand specificity of the calcitonin-receptor-like receptor. *Nature*. 393:333-9.

Mellman, I. 1996. Endocytosis and molecular sorting. *Annu Rev Cell Dev Biol*. 12:575-625.

Mintz, I.M., and B.P. Bean. 1993. GABAB receptor inhibition of P-type Ca2+ channels in central neurons. *Neuron*. 10:889-98.

Mohler, H., and J.M. Fritschy. 1999. GABAB receptors make it to the top--as dimers. *Trends Pharmacol Sci*. 20:87-9.

Morley, B.J., and R.D. Campbell. 1984. Internal homologies of the Ba fragment from human complement component Factor B, a class III MHC antigen. *Embo J*. 3:153-7.

Morrisett, R.A., D.D. Mott, D.V. Lewis, H.S. Swartzwelder, and W.A. Wilson. 1991. GABAB-receptor-mediated inhibition of the N-methyl-D-aspartate component of synaptic transmission in the rat hippocampus. *J Neurosci*. 11:203-9

Mosley, B., M.P. Beckmann, C.J. March, R.L. Idzerda, S.D. Gimpel, T. VandenBos, D. Friend, A. Alpert, D. Anderson, J. Jackson, and et al. 1989. The murine interleukin-4 receptor: molecular cloning and characterization of secreted and membrane bound forms. *Cell*. 59:335-48.

Mostov, K., T. Su, and M. ter Beest. 2003. Polarized epithelial membrane traffic: conservation and plasticity. *Nat Cell Biol*. 5:287-93.

Mostov, K.E., Y. Altschuler, S.J. Chapin, C. Enrich, S.H. Low, F. Luton, J. Richman-Eisenstat, K.L. Singer, K. Tang, and T. Weimbs. 1995. Regulation of protein traffic in polarized epithelial cells: the polymeric immunoglobulin receptor model. *Cold Spring Harb Symp Quant Biol*. 60:775-81.

Nadler, L.S., G. Kumar, and N.M. Nathanson. 2001. Identification of a basolateral sorting signal for the M3 muscarinic acetylcholine receptor in Madin-Darby canine kidney cells. *The Journal of biological chemistry*. 276:10539-47.

Obermair, G.J., W.A. Kaufmann, H.G. Knaus, and B.E. Flucher. 2003. The small conductance Ca2+-activated K+ channel SK3 is localized in nerve terminals of excitatory synapses of cultured mouse hippocampal neurons. *Eur J Neurosci*. 17:721-31.

Ohno, H., J. Stewart, M.C. Fournier, H. Bosshart, I. Rhee, S. Miyatake, T. Saito, A. Gallusser, T. Kirchhausen, and J.S. Bonifacino. 1995. Interaction of tyrosine-based sorting signals with clathrin-associated proteins. *Science*. 269:1872-5.

Pagano, A., G. Rovelli, J. Mosbacher, T. Lohmann, B. Duthey, D. Stauffer, D. Ristig, V. Schuler, I. Meigel, C. Lampert, T. Stein, L. Prezeau, J. Blahos, J. Pin, W. Froestl, R. Kuhn, J. Heid, K. Kaupmann, and B. Bettler. 2001. C-terminal interaction is essential for surface trafficking but not for heteromeric assembly of $GABA_B$ receptors. *J Neurosci*. 21:1189-202.

Palmer, M.J., J.T. Isaac, and G.L. Collingridge. 2004. Multiple, developmentally regulated expression mechanisms of long-term potentiation at CA1 synapses. *J Neurosci*. 24:4903-11.

Patenaude, C., C.A. Chapman, S. Bertrand, P. Congar, and J.C. Lacaille. 2003. GABAB receptor- and metabotropic glutamate receptor-dependent cooperative long-term potentiation of rat hippocampal GABAA synaptic transmission. *J Physiol*. 553:155-67.

Perez-Garci, E., M. Gassmann, B. Bettler, and M.E. Larkum. 2006. The GABA(B1b) Isoform Mediates Long-Lasting Inhibition of Dendritic Ca(2+) Spikes in Layer 5 Somatosensory Pyramidal Neurons. *Neuron*. 50:603-16.

Perrin, M.H., C.R. Grace, R. Riek, and W.W. Vale. 2006. The three-dimensional structure of the N-terminal domain of corticotropin-releasing factor receptors: sushi domains and the B1 family of G protein-coupled receptors. *Ann N Y Acad Sci*. 1070:105-19.

Pin, J.P., J. Kniazeff, C. Goudet, A.S. Bessis, J. Liu, T. Galvez, F. Acher, P. Rondard, and L. Prezeau. 2004. The activation mechanism of class-C G-protein coupled receptors. *Biol Cell*. 96:335-42.

Pineda, V.V., J.I. Athos, H. Wang, J. Celver, D. Ippolito, G. Boulay, L. Birnbaumer, and D.R. Storm. 2004. Removal of G(ialpha1) constraints on adenylyl cyclase in the hippocampus enhances LTP and impairs memory formation. *Neuron*. 41:153-63.

Pologruto, T.A., B.L. Sabatini, and K. Svoboda. 2003. ScanImage: flexible software for operating laser scanning microscopes. *Biomed Eng Online*. 2:13.

Poncer, J.C., R.A. McKinney, B.H. Gahwiler, and S.M. Thompson. 1997. Either N- or P-type calcium channels mediate GABA release at distinct hippocampal inhibitory synapses. *Neuron*. 18:463-72.

Poyatos, I., F. Ruberti, R. Martinez-Maza, C. Gimenez, C.G. Dotti, and F. Zafra. 2000. Polarized distribution of glycine transporter isoforms in epithelial and neuronal cells. *Mol Cell Neurosci*. 15:99-111.

Pozza, M.F., N.A. Manuel, M. Steinmann, W. Froestl, and C.H. Davies. 1999. Comparison of antagonist potencies at pre- and post-synaptic GABA(B) receptors at inhibitory synapses in the CA1 region of the rat hippocampus. *Br J Pharmacol*. 127:211-9.

Prosser, H.M., C.H. Gill, W.D. Hirst, E. Grau, M. Robbins, A. Calver, E.M. Soffin, C.E. Farmer, C. Lanneau, J. Gray, E. Schenck, B.S. Warmerdam, C. Clapham, C.

Reavill, D.C. Rogers, T. Stean, N. Upton, K. Humphreys, A. Randall, M. Geppert, C.H. Davies, and M.N. Pangalos. 2001. Epileptogenesis and enhanced prepulse inhibition in $GABA_{B(1)}$-deficient mice. *Mol Cell Neurosci*. 17:1059-70.

Rapoport, I., Y.C. Chen, P. Cupers, S.E. Shoelson, and T. Kirchhausen. 1998. Dileucine-based sorting signals bind to the beta chain of AP-1 at a site distinct and regulated differently from the tyrosine-based motif-binding site. *Embo J*. 17:2148-55.

Ren, X., and I. Mody. 2003. Gamma-hydroxybutyrate reduces mitogen-activated protein kinase phosphorylation via GABA B receptor activation in mouse frontal cortex and hippocampus. *J Biol Chem*. 278:42006-11.

Restituito, S., A. Couve, H. Bawagan, S. Jourdain, M.N. Pangalos, A.R. Calver, K.B. Freeman, and S.J. Moss. 2005. Multiple motifs regulate the trafficking of GABA(B) receptors at distinct checkpoints within the secretory pathway. *Mol Cell Neurosci*. 28:747-56.

Rivera, J.F., S. Ahmad, M.W. Quick, E.R. Liman, and D.B. Arnold. 2003. An evolutionarily conserved dileucine motif in Shal K+ channels mediates dendritic targeting. *Nat Neurosci*. 6:243-50.

Robbins, T.W., and B.J. Everitt. 1999. Drug addiction: bad habits add up. *Nature*. 398:567-70.

Romano, C., W.-L. Yang, and L. O'Malley. 1996. Metabotropic glutamate receptor 5 is a disulfide-linked dimer. *J Biol Chem*. 271:28612-6.

Roos, J., and R.B. Kelly. 2000. Preassembly and transport of nerve terminals: a new concept of axonal transport. *Nat Neurosci*. 3:415-7.

Saglietti, L., C. Dequidt, K. Kamieniarz, M.C. Rousset, P. Valnegri, O. Thoumine, F. Beretta, L. Fagni, D. Choquet, C. Sala, M. Sheng, and M. Passafaro. 2007. Extracellular interactions between GluR2 and N-cadherin in spine regulation. *Neuron*. 54:461-77.

Sakaba, T., and E. Neher. 2003. Direct modulation of synaptic vesicle priming by GABA(B) receptor activation at a glutamatergic synapse. *Nature*. 424:775-8.

Sampo, B., S. Kaech, S. Kunz, and G. Banker. 2003. Two distinct mechanisms target membrane proteins to the axonal surface. *Neuron*. 37:611-24.

Scanziani, M. 2000. GABA spillover activates postsynaptic GABA(B) receptors to control rhythmic hippocampal activity. *Neuron*. 25:673-81.

Schuler, V., C. Lüscher, C. Blanchet, N. Klix, G. Sansig, K. Klebs, M. Schmutz, J. Heid, C. Gentry, L. Urban, A. Fox, W. Spooren, A.L. Jaton, J.M. Vigouret, M. Pozza, P.H. Kelly, J. Mosbacher, W. Froestl, E. Käslin, R. Korn, S. Bischoff, K. Kaupmann, H. van der Putten, and B. Bettler. 2001. Epilepsy, hyperalgesia,

impaired memory, and loss of pre- and postsynaptic $GABA_B$ responses in mice lacking $GABA_{B(1)}$. *Neuron*. 31:47-58.

Schwarz, D.A., G. Barry, S.D. Eliasof, R.E. Petroski, P.J. Conlon, and R.A. Maki. 2000. Characterization of gamma-aminobutyric acid receptor GABAB(1e), a GABAB(1) splice variant encoding a truncated receptor. *J Biol Chem*. 275:32174-81.

Scimemi, A., A. Fine, D.M. Kullmann, and D.A. Rusakov. 2004. NR2B-containing receptors mediate cross talk among hippocampal synapses. *J Neurosci*. 24:4767-77.

Shaban, H., Y. Humeau, C. Herry, G. Cassasus, R. Shigemoto, S. Ciocchi, S. Barbieri, H. van der Putten, K. Kaupmann, B. Bettler, and A. Luthi. 2006. Generalization of amygdala LTP and conditioned fear in the absence of presynaptic inhibition. *Nat Neurosci*. 9:1028-35.

Sia, G.M., J.C. Beique, G. Rumbaugh, R. Cho, P.F. Worley, and R.L. Huganir. 2007. Interaction of the N-Terminal Domain of the AMPA Receptor GluR4 Subunit with the Neuronal Pentraxin NP1 Mediates GluR4 Synaptic Recruitment. *Neuron*. 55:87-102.

Steiger, J.L., S. Bandyopadhyay, D.H. Farb, and S.J. Russek. 2004. cAMP response element-binding protein, activating transcription factor-4, and upstream stimulatory factor differentially control hippocampal GABABR1a and GABABR1b subunit gene expression through alternative promoters. *J Neurosci*. 24:6115-26.

Stoppini, L., P.A. Buchs, and D. Muller. 1991. A simple method for organotypic cultures of nervous tissue. *J Neurosci Methods*. 37:173-82.

Stowell, J.N., and A.M. Craig. 1999. Axon/dendrite targeting of metabotropic glutamate receptors by their cytoplasmic carboxy-terminal domains. *Neuron*. 22:525-36.

Tabata, T., K. Araishi, K. Hashimoto, Y. Hashimotodani, H. van der Putten, B. Bettler, and M. Kano. 2004. Ca2+ activity at GABAB receptors constitutively promotes metabotropic glutamate signaling in the absence of GABA. *Proceedings of the National Academy of Sciences of the United States of America*. 101:16952-7.

Thompson, S.M., M. Capogna, and M. Scanziani. 1993. Presynaptic inhibition in the hippocampus. *Trends Neurosci*. 16:222-7.

Tienari, P.J., B. De Strooper, E. Ikonen, M. Simons, A. Weidemann, C. Czech, T. Hartmann, N. Ida, G. Multhaup, C.L. Masters, F. Van Leuven, K. Beyreuther, and C.G. Dotti. 1996. The beta-amyloid domain is essential for axonal sorting of amyloid precursor protein. *Embo J*. 15:5218-29.

Tuma, P.L., and A.L. Hubbard. 2003. Transcytosis: crossing cellular barriers. *Physiol Rev*. 83:871-932.

Ulrich, D., V. Besseyrias, and B. Bettler. 2007. Functional mapping of GABAB receptor subtypes in the thalamus.

Ulrich, D., and B. Bettler. 2007. GABA(B) receptors: synaptic functions and mechanisms of diversity. *Curr Opin Neurobiol*. 17:298-303.

Vidal, R.L., O.A. Ramirez, L. Sandoval, R. Koenig-Robert, S. Hartel, and A. Couve. 2007. Marlin-1 and conventional kinesin link GABAB receptors to the cytoskeleton and regulate receptor transport. *Mol Cell Neurosci*. 35:501-12.

Vigot, R., S. Barbieri, H. Brauner-Osborne, R. Turecek, R. Shigemoto, Y.P. Zhang, R. Lujan, L.H. Jacobson, B. Biermann, J.M. Fritschy, C.M. Vacher, M. Muller, G. Sansig, N. Guetg, J.F. Cryan, K. Kaupmann, M. Gassmann, T.G. Oertner, and B. Bettler. 2006. Differential Compartmentalization and Distinct Functions of GABA(B) Receptor Variants. *Neuron*. 50:589-601.

Vogt, K.E., and R.A. Nicoll. 1999. Glutamate and gamma-aminobutyric acid mediate a heterosynaptic depression at mossy fiber synapses in the hippocampus. *Proc Natl Acad Sci U S A*. 96:1118-22.

Wandinger-Ness, A., M.K. Bennett, C. Antony, and K. Simons. 1990. Distinct transport vesicles mediate the delivery of plasma membrane proteins to the apical and basolateral domains of MDCK cells. *J Cell Biol*. 111:987-1000.

Wei, K., Z. Jia, Y.T. Wang, J. Yang, C.C. Liu, and O.C. Snead, 3rd. 2001a. Cloning and characterization of a novel variant of rat $GABA_{B(R1)}$ with a truncated C-terminus. *Brain Res Mol Brain Res*. 89:103-10.

Wei, X., M. Orchardson, J.A. Gracie, B.P. Leung, B. Gao, H. Guan, W. Niedbala, G.K. Paterson, I.B. McInnes, and F.Y. Liew. 2001b. The Sushi domain of soluble IL-15 receptor alpha is essential for binding IL-15 and inhibiting inflammatory and allogenic responses in vitro and in vivo. *J Immunol*. 167:277-82.

West, A.E., E.C. Griffith, and M.E. Greenberg. 2002. Regulation of transcription factors by neuronal activity. *Nat Rev Neurosci*. 3:921-31.

West, A.E., R.L. Neve, and K.M. Buckley. 1997a. Identification of a somatodendritic targeting signal in the cytoplasmic domain of the transferrin receptor. *J Neurosci*. 17:6038-47.

West, A.E., R.L. Neve, and K.M. Buckley. 1997b. Targeting of the synaptic vesicle protein synaptobrevin in the axon of cultured hippocampal neurons: evidence for two distinct sorting steps. *J Cell Biol*. 139:917-27.

Winckler, B., P. Forscher, and I. Mellman. 1999. A diffusion barrier maintains distribution of membrane proteins in polarized neurons. *Nature*. 397:698-701.

Winckler, B., and I. Mellman. 1999. Neuronal polarity: controlling the sorting and diffusion of membrane components. *Neuron*. 23:637-40.

Wisco, D., E.D. Anderson, M.C. Chang, C. Norden, T. Boiko, H. Folsch, and B. Winckler. 2003. Uncovering multiple axonal targeting pathways in hippocampal neurons. *J Cell Biol*. 162:1317-28.

Xiao, M.Y., P. Wasling, E. Hanse, and B. Gustafsson. 2004. Creation of AMPA-silent synapses in the neonatal hippocampus. *Nat Neurosci*. 7:236-43.

Yamada, J., F. Saitow, S. Satake, T. Kiyohara, and S. Konishi. 1999a. GABA(B) receptor-mediated presynaptic inhibition of glutamatergic and GABAergic transmission in the basolateral amygdala. *Neuropharmacology*. 38:1743-53.

Yamada, K., S. Goto, T. Oyama, N. Inoue, S. Nagahiro, and Y. Ushio. 1994. Elevated immunoreactivity for glutamic acid decarboxylase in the rat cerebral cortex following transient middle cerebral artery occlusion. *Acta Neuropathol*. 88:55-9.

Yamada, K., B. Yu, and J.P. Gallagher. 1999b. Different subtypes of GABAB receptors are present at pre- and postsynaptic sites within the rat dorsolateral septal nucleus. *J Neurophysiol*. 81:2875-83.

Zilberter, Y., K.M. Kaiser, and B. Sakmann. 1999. Dendritic GABA release depresses excitatory transmission between layer 2/3 pyramidal and bitufted neurons in rat neocortex. *Neuron*. 24:979-88.

Appendix

Curriculum Vitae

BARBARA BIERMANN
PhD-Student in Neuroscience

Röschenzerstrasse 23
CH-4053 Basel
Switzerland
Email: barbara.biermann@unibas.ch

ACADEMIC EDUCATION

Since 07/2002	PHD-Student in the research group of Prof. Bernhard Bettler, Institute of Physiology, Basel University, Switzerland Topic: *"The sushi domains and their role in $GABA_B$ receptor compartmentalization"*
02/2001-12/2001	"Diplomarbeit" (German equivalent to masters thesis) in the "Protein Function Group" of Prof. R.J. Beynon at Liverpool University, UK under the supervision of Prof. Walter Stöcker Title: "*Analysis of urinary proteins and peptides in autism*"
1998 - 1999	Erasmus exchange programme: Biological studies at Tours University, France
1996 - 2001	Biological studies at Münster University, Germany

LANGUAGES

German (native), English (fluently spoken and written), French (very good spoken and written), Italian (good spoken and written)

MISCELLANEOUS

2004-2005	WIN-Programme at Novartis, Basel, Switzerland Mentoring programme for postgraduate students and postdoctoral fellows to gain insight into the structure of a pharmaceutical company

PUBLICATIONS

Biermann B, Vigot R, Bradaia A, Besseyrias V, Tiao J YH, Abdel Aziz S, Haller C, Kapfhammer JP, Gassmann M, Bettler B (2007) In preparation. *"The sushi domains of metabotropic $GABA_B$ receptors function as a dominant axonal targeting signal."*

Tiao J YH[*], Bradaia A[*], **Biermann B[*]**, Kaupmann K, Gassmann M, Bettler B (2007) In preparation. *"Soluble $GABA_{B1a}$ subunit isoforms interfere with $GABA_B$ heteroreceptor function"*
[*]Equal contribution

Vigot R, Barbieri S, Brauner-Osborne H, Turecek R, Shigemoto R, Zhang YP, Lujan R, Jacobson LH, **Biermann B**, Fritschy JM, Vacher CM, Muller M, Sansig G, Guetg N, Cryan JF, Kaupmann K, Gassmann M, Oertner TG, Bettler B (2006) Neuron 18:50(4):589-601. *"Differential compartmentalization and distinct functions of GABAB receptor variants."*

Gassmann, M., Haller C., Stoll, Y., Aziz, S., **Biermann, B.,** Mosbacher, J. Kaupmann, K. and Bettler, B. (2005) Mol. Pharmacol. 68, 137-144. *"The RXR-type endoplasmic reticulum-retention/retrieval signal of GABAB1 requires distant spacing from the membrane to function."*

TALK

"*Mechanism of $GABA_B$ receptor compartmentalization*", Bench-to-Bedside Symposium, September 9th, 2006, Pharmazentrum Basel, Switzerland

POSTER

"Trafficking of $GABA_{B1}$ subunit isoforms to subcellular compartments"
Biermann B, Vigot R, Bradaia A, Barbieri S, Gassmann M, Kapfhammer JP, Müller M, Bräuner-Osborne H, Kaupmann K, Bettler B.
Federation of Europeen Neuroscience Society, FENS, Vienna July 2007

"Trafficking of $GABA_{B1}$ subunit isoforms in cultured neurons"
Biermann B, Vigot R, Bradaia A, Barbieri S, Gassmann M, Kapfhammer JP, Müller M, Bräuner-Osborne H, Kaupmann K, Bettler B.
Annual Neurex Meeting, March 29th, 2006, Basel, Switzerland
Poster-Prize Winner

"A role for the sushi repeats in $GABA_B$ receptor compartmentalization"
Biermann B, Vigot R, Bradaia A, Barbieri S, Gassmann M, Kapfhammer JP, Müller M, Bräuner-Osborne H, Kaupmann K, Bettler B.
Society for Neuroscience Meeting 2005, Washington DC, USA

Acknowledgement

This doctoral thesis work has been accomplished under the supervision of Prof. Dr. Bernhard Bettler. I would like to thank him for giving me this fascinating project and the great opportunity to do my Ph.D. research work in his lab. It was an important experience in many ways. I am most grateful to him for his support and generosity he offered during the years. I could always find him a ready listener whenever I needed to discuss my project and really appreciated his commitment in my work.

I would like to thank Prof. Thomas G. Oertner from the *Friedrich Miescher Institute* in Basel for accepting to be "Korreferent" on my Ph.D. thesis committee and to Prof. Markus A. Rüegg for being my "Fakultätsverantwortlicher".

Next, I like to express my sincere thanks to our "Underboss" Dr. Martin Gassmann for all the kind assistance constantly rendered, for carefully listening to any kind of problem and his never-ending patience.

I would further like to thank Prof Dr. Josef Kapfhammer for his assistance and cooperative support during the years. His office door was always open both for scientific discussions as well as little chats. I highly acknowledge his great patience all over the years. Especially his efforts teaching me the culturing of organotypic slices and dissociated neurons is deeply appreciated.

I further wish to acknowledge Prof. Dr. Peter Philippsen for his unfailing support with the *Metamoph Imaging* Programm and all the advice he has generously given. I very much enjoyed the warm and funny atmosphere in his research group.

I further like to thank Jim Tiao and Francois Grenier for proof-reading chapters of this manuscript.

In particular I owe a great debt of gratitude to Susanne Blank for organizing the Bettler lab. It was very nice to share the office with you.

Special thanks also go to all the members of the *Bettlerlab* (including the first generation) as well as all the guys on the 7th floor for the funny discussions, jokes and stories making the years pleasant and memorable. I further appreciated everybody's helpfulness and in particular everyone’s encouragement in the last months before printing this thesis.

My sincere thanks are also extended to my parents for their unlimited love and selfless support. I even would like to thank my brothers for their infinite ignorance concerning biology and their persistent efforts to prevent their sister from becoming a science-freak.

Last but not least, I wish to express my thanks to all my close friends for any kind of distraction during my Ph.D. My special thanks further go to the guys from the Schalke supporters clubs *Monasteria* for always reminding me “wo der Hammer hängt”.

Chapter (VI)

THE RXR-TYPE ENDOPLASMIC RETICULUM-RETENTION / RETRIEVAL SIGNAL OF $GABA_{B1}$ REQUIRES DISTANT SPACING FROM THE MEMBRANE TO FUNCTION

Martin Gassmann, Corinne Haller, Yannick Stoll, Said Abdel Aziz, Barbara Biermann, Johannes Mosbacher, Klemens Kaupmann, and Bernhard Bettler

Mol Pharmacol. 2005 Jul; 68(1):137-44 . Epub 2005 Apr 1.

0026-895X/05/6801-137–144$20.00
MOLECULAR PHARMACOLOGY
Vol. 68, No. 1
10256/3037436
Mol Pharmacol 68:137–144, 2005
Printed in U.S.A.

The RXR-Type Endoplasmic Reticulum-Retention/Retrieval Signal of $GABA_{B1}$ Requires Distant Spacing from the Membrane to Function

Martin Gassmann, Corinne Haller, Yanick Stoll, Said Abdel Aziz, Barbara Biermann, Johannes Mosbacher, Klemens Kaupmann, and Bernhard Bettler

Pharmazentrum, University of Basel, Department of Clinical-Biological Sciences, Institute of Physiology, Basel, Switzerland (M.G., C.H., Y.S., B.B., S.A.A., B.B.); and Novartis Institutes for Biomedical Research, Novartis Pharma AG, Basel, Switzerland (J.M., K.K.)

Received December 14, 2004; accepted April 1, 2005

ABSTRACT

Functional γ-aminobutyric acid type B ($GABA_B$) receptors are normally only observed upon coexpression of $GABA_{B1}$ with $GABA_{B2}$ subunits. A C-terminal arginine-based endoplasmic reticulum (ER) retention/retrieval signal, RSRR, prevents escape of unassembled $GABA_{B1}$ subunits from the ER and restricts surface expression to correctly assembled heteromeric receptors. The RSRR signal in $GABA_{B1}$ is proposed to be shielded by C-terminal coiled-coil interaction of the $GABA_{B1}$ with the $GABA_{B2}$ subunit. Here, we investigated whether the RSRR motif in $GABA_{B1}$ remains functional when grafted to ectopic sites. We found that the RSRR signal in $GABA_{B1}$ is inactive in any of the three intracellular loops but remains functional when moved within the distal zone of the C-terminal tail. C-terminal deletions that position the RSRR signal closer to the plasma membrane drastically reduce its effectiveness, supporting that proximity to the membrane restricts access to the RSRR motif. Functional ectopic RSRR signals in $GABA_{B1}$ are efficiently inactivated by the $GABA_{B2}$ subunit in the absence of coiled-coil dimerization, supporting that coiled-coil interaction is not critical for release of the receptor complex from the ER. The data are consistent with a model in which removal of RSRR from its active zone rather than its direct shielding by coiled-coil dimerization triggers forward trafficking. Because arginine-based intracellular retention signals of the type RXR, where X represents any amino acid, are used to regulate assembly and surface transport of several multimeric complexes, such a mechanism may apply to other proteins as well.

$GABA_B$ receptors are the G protein-coupled receptors for GABA, the predominant inhibitory neurotransmitter in the mammalian central nervous system. $GABA_B$ receptors modulate synaptic transmission by controlling neurotransmitter release and by causing postsynaptic hyperpolarization (Bowery et al., 2002; Calver et al., 2002; Bettler et al., 2004). They are broadly expressed in the nervous system and have been implicated in a variety of neurological and psychiatric conditions. In heterologous cells, functional $GABA_B$ receptors are usually only observed upon coexpression of $GABA_{B1}$ with $GABA_{B2}$ subunits, which provided compelling evidence for heteromerization among G protein-coupled receptors (Kaupmann et al., 1997, 1998; Jones et al., 1998; White et al., 1998; Kuner et al., 1999; Marshall et al., 1999; Ng et al., 1999). Two $GABA_{B1}$ subunit isoforms, $GABA_{B1a}$ and $GABA_{B1b}$, arise from the *$GABA_{B1}$* gene by differential promoter use (Kaupmann et al., 1997; Bettler et al., 2004). The data therefore support the existence of two predominant $GABA_B$ receptors in the nervous system, the heteromeric $GABA_{B(1a,2)}$ and $GABA_{B(1b,2)}$ receptors. However, knockout studies also suggest that $GABA_{B1a}$ and $GABA_{B1b}$ could be functional in neurons that naturally lack $GABA_{B2}$ expression (Gassmann et al., 2004).

In the $GABA_B$ heteromer, the $GABA_{B1}$ subunit binds GABA and all competitive $GABA_B$ ligands (Kaupmann et al., 1998), whereas the $GABA_{B2}$ subunit is predominantly responsible for activating the G protein (Galvez et al., 2001; Margeta-Mitrovic et al., 2001; Robbins et al., 2001; Grunewald et al., 2002; Havlickova et al., 2002). Trafficking

This work was supported by Swiss Science Foundation Grant 3100-067100.01 and the Désirée and Niels Yde Foundation (to B.B.).
[1] M.G., C.H., and Y.S. contributed equally to this work.
Article, publication date, and citation information can be found at http://molpharm.aspetjournals.org.
doi:10.1124/mol.104.010256.

ABBREVIATIONS: ER, endoplasmic reticulum; HEK, human embryonic kidney; CGP71872, 3-(1-(*R*)-(3-((4-azido-2-hydroxy-5-iodobenzoylamino)-pentyl) hydroxyphosphoryl)-2-(*S*)-hydroxypropylamino)ethyl)benzoic acid; PAGE, polyacrylamide gel electrophoresis; PBS, phosphate-buffered saline; S, surface, H, homogenate; $\Delta[Ca^{2+}]_i$, change in intracellular calcium concentration; PLC, phospholipase C; PAL, photoaffinity labeling.

of unassembled $GABA_{B1}$ subunits to the plasma membrane is prevented by an arginine-based ER-retention/retrieval signal, the four amino acids RSRR, in the cytoplasmic tail of $GABA_{B1}$ (Couve et al., 1998; Margeta-Mitrovic et al., 2000; Pagano et al., 2001). This ER-retention/retrieval signal is proposed to be shielded by C-terminal coiled-coil interaction of the $GABA_{B1}$ with the $GABA_{B2}$ subunit. Within the RSRR motif the serine residue and the third arginine are not absolutely critical for function, because they can be substituted by other amino acids (Margeta-Mitrovic et al., 2000; Pagano et al., 2001). More recently, it was shown that the sequence context of the RSRR signal in $GABA_{B1}$ influences its function (Grunewald et al., 2002). Thus, the full ER-retention/retrieval motif in $GABA_{B1}$ was extended to the sequence QLQSRQQLRSRR, which includes part of the coiled-coil domain. Arginine-based ER-retention/retrieval signals were observed in a number of other multisubunit proteins [e.g., the K_{ATP} channels (Zerangue et al., 1999) and *N*-methyl-D-aspartate receptors (Scott et al., 2001)], where they control stoichiometry and surface expression of the channel complex. From the available data, it emerges that the core ER-retention/retrieval motif is RXR, consisting of two arginines that are separated by any amino acid (X).

Dilysine ER-retention/retrieval signals require a strict spacing relative to the C terminus. In contrast to KK-signals, functional RXR signals are found in a variety of cytosolic positions, including intracellular loops and the N and C termini in type II and type I membrane proteins, respectively (Schutze et al., 1994; Zerangue et al., 1999). This broad distribution initially suggested that many proteins that harbor the consensus sequence RXR are retained in the ER. This was recently challenged in a study that showed that the RXR-dependent ER-retention/retrieval machinery is sensitive to the length of the spacer that separates the RXR motif and the receptor-anchored membrane (Shikano and Li, 2003). Here, we studied whether the RSRR signal in $GABA_{B1}$ can still function when grafted to ectopic cytoplasmic positions and whether it can be masked by $GABA_{B2}$ regardless of its position. The data let us propose a new mechanism to explain RSRR inactivation upon $GABA_B$ subunit dimerization.

Materials and Methods

Generation of Mutant Expression Plasmids. All constructs were subcloned into the cytomegalovirus-based eukaryotic expression vector pCI (Promega, Madison, WI). Overlap extension polymerase chain reaction (Horton et al., 1990) was used to introduce ectopic RSRR and LRSRR motifs into a $GABA_{B1a}$ mutant (R1[ASAA]) where the endogenous RSRR was inactivated by substitution of arginine with alanine residues (Pagano et al., 2001). Overlap extension polymerase chain reaction was also used to construct $GABA_{B1a}$ deletion mutants, leaving the wild-type RSRR unchanged.

Cell Surface Labeling. HEK293 cells for transient transfection of expression constructs were purchased from the American Type Culture Collection (Manassas, VA) and cultured in Dulbecco's minimum Eagle's medium (Invitrogen, Basel, Switzerland) supplemented with 10% fetal calf serum and 2 mM L-glutamine. The photoaffinity ligand [^{125}I]CGP71872 specifically binds to the GABA-binding site of $GABA_{B1}$ subunits and does not permeate the plasma membrane (Pagano et al., 2001). [^{125}I]CGP71872 labeling of intact cells therefore reveals $GABA_{B1}$ protein at the cell surface, whereas labeling of lysed cells reveals total $GABA_{B1}$ protein, independent of where in the biosynthetic pathway it is present. Six hours after transfection of expression plasmids using Lipofectamine 2000 transfection reagent (Invitrogen), HEK293 cells were transferred to six-well plates. After an additional 24-h incubation, cells were washed twice with ice-cold HEPES, pH 7.6. Half of the cells were then used for photoaffinity labeling of surface receptors (S in Figs. 2, 6, and 7), and the other half were used for labeling of total receptors in the cell homogenates (H in Figs. 2, 6, and 7). For surface labeling, intact cells were incubated in the dark for 1 h at room temperature with 0.8 nM [^{125}I]CGP71872. Thereafter, cells were washed twice with ice-cold Krebs-Tris buffer (118 mM NaCl, 4.7 mM KCl, 1.8 mM $CaCl_2$, 1.2 mM $MgSO_4$, 1.2 mM KH_2PO_4, 5.6 mM glucose, and 20 mM Tris-Cl, pH 7.4) to remove unbound ligand. Bound [^{125}I]CGP71872 was cross-linked to the receptor using UV light (Kaupmann et al., 1997). Photoaffinity-labeled cells were then harvested, and the radioactivity was determined in a gamma counter (PerkinElmer Life and Analytical Sciences, Zurich, Switzerland). For [^{125}I]CGP71872 labeling of total $GABA_{B1}$ protein, cells were harvested and lysed before incubation with the photoaffinity ligand. Preparation of lysates and [^{125}I]CGP71872 binding was as described previously (Kaupmann et al., 1997). For 10% SDS-PAGE, cell pellets and homogenates were resuspended in Krebs-Tris buffer containing 0.1% SDS. An aliquot was used for determination of protein concentration (Micro Protein Assay; Bio-Rad, Munich, Germany). Equal amounts of total protein were used when comparing S receptors and total receptors in cell Hs. We normalized the input of radiolabeled protein in the SDS-PAGE by using equal counts of the H samples for each set of transfections (expression with and without $GABA_{B2}$). Photoaffinity-labeled protein was detected using autoradiography. The S/H ratio of the radioactivity incorporated into the cell surface and the homogenate fraction was determined from the autoradiograms. Because of the differences in the radiolabeling procedure for surface and homogenate receptors, the percentage S/H sometimes exceeds the theoretical value of 100%. Loading was controlled for by Western blot analysis with the polyclonal $GABA_{B1}$ antibody Ab174.1 that is directed against the C-terminal tail of $GABA_{B1}$ (Malitschek et al., 1998). Surface labeling with [^{125}I]CGP71872 was compared with surface biotinylation (Fig. 3). For the biotinylation experiments, we used membrane-impermeable EZ-link Sulfo-NHS-SS-biotin (Pierce Chemical, Rockford IL). Forty-eight hours after transfection, HEK293 cells were washed three times in PBS and then incubated with 1 mg/ml Sulfo-NHS-SS-biotin for 30 min at 4°C on a rocking table. To quench the biotinylation reaction, the cells were then washed in PBS and incubated in 50 mM glycine in PBS for 5 min. After three washes in PBS, the cells were lysed in radioimmunoprecipitation assay buffer (150 mM NaCl, 1% Nonidet-40, 0.5% sodium deoxycholate, 0.1% SDS, and 50 mM Tris-Cl, pH 7.5). The lysates were cleared by centrifugation at 10,000*g* for 10 min. Aliquots were taken and mixed with 2× SDS loading buffer to detect total $GABA_{B1}$ protein expressed. The remaining cleared lysates were incubated with avidin beads (Pierce Chemical) at 4°C overnight. After five washes in radioimmunoprecipitation assay buffer, biotinylated proteins were eluted from the avidin beads using SDS loading buffer. Finally, total and eluted $GABA_{B1}$ proteins were separated on SDS-PAGE and analyzed on Western blots.

Western Blots. After SDS-PAGE, proteins were blotted onto a nitrocellulose membrane (Immobilon-P; Millipore Corporation, Billerica, MA) by standard electrophoretic transfer. After blotting, the membrane was blocked with 5% nonfat milk powder in PBS for 1 h at room temperature. Rabbit antiserum Ab174.1 (1:2500; Malitschek et al., 1998), the monoclonal anti-β-tubulin antibody MAB3408 (1:500; Chemicon International, Temecula, CA), and peroxidase-coupled secondary antibodies (donkey anti-rabbit or anti-mouse conjugates, 1:2500; Amersham Biosciences UK, Ltd., Little Chalfont, Buckinghamshire, UK) were incubated in PBS containing 2.5% nonfat milk powder and 0.1% Tween 20 for 1 h at room temperature. After antibody incubation, three wash steps with PBS containing 0.1% Tween 20 were carried out for 10 min. The blots were developed using the enhanced chemiluminescence chemiluminescent detection

system (Amersham Biosciences UK, Ltd.) and exposed to Kodak Bio-Max maximum resolution X-ray films (Sigma-Aldrich, St. Louis, MO).

Fluorimetric Measurement of Changes in the Intracellular Ca^{2+} Concentration ($\Delta[Ca^{2+}]_i$). For measurement of $\Delta[Ca^{2+}]_i$, all transfections included $G\alpha qz_{IC}$ to artificially couple $GABA_B$ receptors to PLC (Franek et al., 1999). Transfected HEK293 cells were plated into poly-D-lysine-coated 96-well plates (BD Biosciences, Erembodegem, Belgium). After transfection (48–72 h), cells were loaded for 45 min with 2 μM fluo-4 acetoxymethyl ester (Molecular Probes, Leiden, The Netherlands) in Hanks' balanced salt solution (Invitrogen) supplemented with 20 mM HEPES buffer and 50 μM probenecid (Sigma, Buchs, Switzerland). Plates were washed and transferred to a fluorimetric image plate reader (Molecular Devices, Crawley, UK). Fluorescence changes ΔF upon addition of GABA (final concentration of 0.1 mM) were recorded as a function of time, as described previously (Pagano et al., 2001). No quantitative comparison between experiments was made, because the signal amplitude depends on the transfection efficiency.

Results

Generation and Characterization of $GABA_{B1}$ Mutants with Ectopic RSRR Signals. To study whether ectopic RSRR motifs are functional in $GABA_{B1}$, we introduced the RSRR motif into a $GABA_{B1}$ protein where the endogenous RSRR motif is inactivated by substitution of arginine with alanine residues. This protein, R1[ASAA], is efficiently transported to the cell surface in the absence of $GABA_{B2}$ (Pagano et al., 2001). Whenever possible, we inserted the RSRR motif at positions that already harbored an arginine or a serine residue, which is expected to minimize interference with the wild-type amino acid sequence. A scheme depicting the insertion sites of ectopic RSRR motifs in R1[ASAA] is shown in Fig. 1A. The positions of the ectopic RSRR motifs in the primary sequence of $GABA_{B1a}$ are listed in Fig. 1B. We confirmed expression of mutant $GABA_{B1}$ proteins in transiently transfected HEK293 cells by Western blot analysis, using an antibody directed against a C-terminal epitope (Fig. 1C). In general, the expression levels of mutant $GABA_{B1}$ proteins are comparable with those of the wild-type $GABA_{B1a}$ (R1) and R1[ASAA] proteins (Fig. 1C, top). The only exception is R1[R862SRR], which harbors the ectopic RSRR motif in the C-terminal tail and for unknown reasons is poorly expressed. On the other hand, it is also possible that some of the C-terminal epitopes in R1[R862SRR] are affected by the mutation and are no longer recognized by the antibody. Equal loading was controlled for by Western blot analysis with a β-tubulin antibody (Fig. 1C, bottom).

RSRR Remains Functional at the C Terminus but Not in Any of the Intracellular Loops. To examine the functionality of ectopic RSRR motifs, we expressed $GABA_{B1}$ mutants either in isolation or together with $GABA_{B2}$. We determined the ratio of surface and total $GABA_{B1}$ protein levels by photoaffinity labeling of intact and lysed cells, respectively, with the membrane-impermeable antagonist [^{125}I]CGP71872. After SDS-PAGE, labeled proteins were visualized by autoradiography. We consistently observed that wild-type and mutant $GABA_{B1}$ proteins bind significantly more [^{125}I]CGP71872 when coexpressed with $GABA_{B2}$, suggesting that $GABA_{B2}$ assists $GABA_{B1}$ in reaching a binding-competent conformation. To correct for this as well as variability in transfection efficiency, the amount of protein sample subjected to gel electrophoresis was normalized to the respective amount of radioactivity incorporated into the cell Hs. Therefore, for the reason mentioned above, substantially less immunostained $GABA_{B1}$ protein is seen on all Western blots of samples where $GABA_{B2}$ was coexpressed (Fig. 2). For each transfection, photoaffinity-labeled $GABA_{B1}$ protein at the cell S was compared with total $GABA_{B1}$ protein labeled in the cell Hs. We investigated whether the binding-incompetent form of $GABA_{B1}$, which is more abundant in the absence of $GABA_{B2}$, is able to reach the cell surface. We used biotinylation of intact cells and precipitation with avidin-Sepharose as an alternative method to [^{125}I]CGP71872 labeling to detect proteins expressed at the cell surface (Fig. 3). We failed to detect significant amounts of $GABA_{B1}$ protein expressed at the cell surface of HEK293 cells transfected with $GABA_{B1}$ alone (R1), indicating that the binding-incompetent form of $GABA_{B1}$ fails to reach the cell surface in the absence of $GABA_{B2}$. This is also supported by recent studies that show that ligand binding is a critical requirement for plasma membrane expression (Mah et al., 2005; Valluru et al., 2005). In all our experiments, we therefore used photoaffinity labeling with [^{125}I]CGP71872 to quantify $GABA_{B1}$ protein at the cell surface.

As shown in Fig. 2, wild-type $GABA_{B1}$ (R1) is retained in the ER and therefore does not bind the photoaffinity ligand at the cell surface. However, upon coexpression with $GABA_{B2}$ (R1 + R2), or inactivation of the RSRR motif (R1[ASAA]), $GABA_{B1}$ is released to the cell surface, in agreement with previous reports (Margeta-Mitrovic et al., 2000; Pagano et al., 2001). Insertion of RSRR motifs into any of the three intracellular loops (mutant proteins R1[RS616RR], R1[RS624RR], R1[RV690RSRR], R1[E699RSRR], and R1[E796RSRR]) failed to confer detectable intracellular retention in our assay. Likewise, mutants with an ectopic RSRR motif in the C-terminal tail at positions R862 (R1[R862SRR]), S877 (R1[RS877RR]), or S917 (R1[RS917RR]) were efficiently transported to the cell surface, no matter whether they were expressed alone or in combination with $GABA_{B2}$. In contrast, insertion of an ectopic RSRR motif in the C-terminal tail at positions S887 (R1[RS887RR]) and R939 (R1[R939SRR]) resulted in partial intracellular retention. In summary, transposing the RSRR ER-retention/retrieval motif of $GABA_{B1}$ to ectopic positions indicates that it can be functional in preventing transport to the cell surface in the cytoplasmic tail but not in any of the intracellular loops. Functional RSRR signals are efficiently masked at ectopic sites by heterodimerization with $GABA_{B2}$, as shown by the release of the R1[RS887RR] and R1[R939SRR] proteins to the cell surface in the presence of $GABA_{B2}$.

Ectopic RSRR Motifs Do Not Interfere with Receptor Function. The experiments described above show that all $GABA_{B1}$ subunits with ectopic RSRR motifs can reach the cell surface when coexpressed with $GABA_{B2}$. This suggests that the mutated $GABA_{B1}$ proteins fold correctly and assemble into heterodimers. When expressed in heterologous cells, $GABA_{B1}$ is not functional by itself, even when artificially targeted to the cell surface by inactivation of the RSRR signal or by shielding it with a C-terminal $GABA_{B2}$ peptide (Margeta-Mitrovic et al., 2000; Pagano et al., 2001). To confirm heteromeric assembly between mutated $GABA_{B1}$ and wild-type $GABA_{B2}$ subunits, we examined whether coexpression of the subunits yielded functional receptors. Upon transient coexpression of the subunits with a chimeric $G\alpha$ subunit, $G\alpha qz_{IC}$ (Franek et al., 1999), in HEK293 cells, we

measured GABA-induced increases in intracellular Ca^{2+} levels by fluorimetry. As illustrated in Fig. 4, all $GABA_{B1}$ mutants can be activated with 0.1 mM GABA upon coexpression with $GABA_{B2}$, similarly to wild-type $GABA_{B1}$ (R1 + R2). Hence, insertion of ectopic RSRR motifs does not interfere with G protein coupling of the mutant proteins.

Appropriate Spacing to the Plasma Membrane Is Required for ER-Retention/Retrieval of $GABA_{B1}$. RXR-type motifs were proposed to have an operating range and to be sensitive with regard to their spacing from the plasma membrane (Shikano and Li, 2003). This could explain why in $GABA_{B1}$ ectopic RSRR motifs are only functional when located within the distal C-terminal tail (Fig. 2). Conflicting with this explanation, the ectopic RSRR motif at S917, in between the functional motifs at S887 and R939, is unable to confer intracellular retention (Fig. 2, construct R1[RS917RR]). Small changes in the local sequence context can alter the signal strength of arginine-based ER-retention motifs (Zerangue et al., 2001). For example, the functionality of RXR signals is described to improve when a hydrophobic amino acid, in particular leucine, precedes the arginine cluster. We therefore investigated whether insertion of a leucine preceding the RSRR in R1[RS917RR] rescues intracellular retention. We additionally tested whether including a leucine in the R1[RS887RR] and R1[R939SRR] proteins, which are less well retained than R1[ASAA], improves retention. Indeed, insertion of a leucine preceding the RSRR at position S917 renders the otherwise nonfunctional ectopic motif functional (Fig. 5, R1[LRS917RR] versus R1[RS917RR]). In contrast, insertion of leucine in R1[RS887RR] or R1[R939SRR]

A

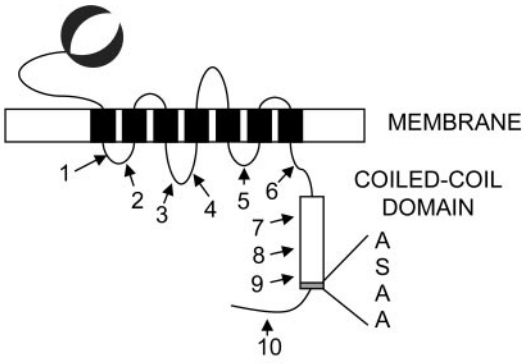

B

Construct	Name	Insertion site of ectopic RSRR	Position
1	R1[RS616RR]	internal loop 1	Ser 616
2	R1[RS624RR]	internal loop 1	Ser 624
3	R1[V690RSRR]	internal loop 2	Val 690 (after)
4	R1[E699RSRR]	internal loop 2	Glu 699 (after)
5	R1[E796RSRR]	internal loop 3	Glu 796 (after)
6	R1[R862SRR]	c-term (proximal of coiled-coil)	Arg 862
7	R1[RS877RR]	c-term (within coiled-coil)	Ser 877
8	R1[RS887RR]	c-term (within coiled-coil)	Ser 887
9	R1[RS917RR]	c-term (within coiled-coil)	Ser 917
10	R1[R939SRR]	c-term (distal of coiled-coil)	Arg 939

C

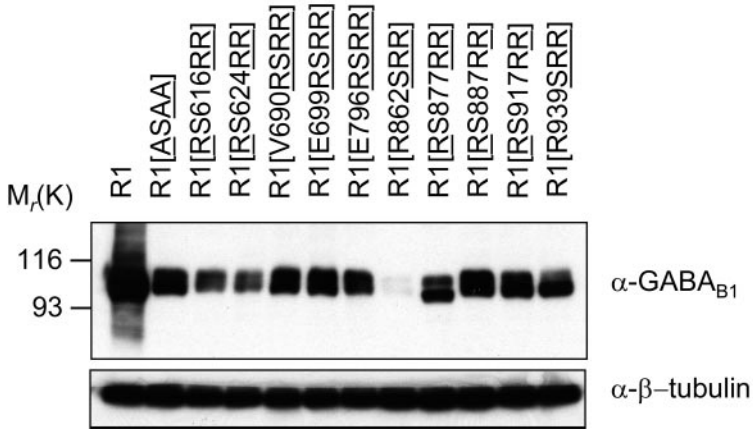

Fig. 1. Description of $GABA_{B1}$ mutants with ectopic RSRR motifs. A, schematic diagram depicting the insertion sites of the ectopic RSRR motifs in a $GABA_{B1a}$ mutant protein where the endogenous RSRR sequence C-terminal to the coiled-coil domain was mutated to ASAA. The seven transmembrane helices are shown as black boxes. B, nomenclature of the $GABA_{B1a}$ constructs used in this study. Residues that were inserted to generate the ectopic RSRR motif are underscored. The positions of the ectopic RSRR motifs are numbered. Residue numbering refers to wild-type $GABA_{B1a}$ protein (GenBank accession no. Y10369). C, Western blot analysis confirming expression of the mutant $GABA_{B1a}$ proteins in HEK293 cells. An antibody specific for the $GABA_{B1}$ C terminus detects a band of approximately 100 kDa (top). A second band is sometimes visible, presumably representing incompletely processed intracellular $GABA_{B1}$ protein. R1[R862SRR], which harbors the ectopic RSRR motif in the C terminus proximal to the coiled-coil domain, is poorly expressed or inefficiently recognized by the antibody. Equal loading of HEK293 cell lysates was controlled for by Western blot analysis with a β-tubulin antibody (bottom).

does not improve intracellular retention of these proteins. Intracellular retention of the R1[LRS917RR] protein further supports that the distal cytoplasmic tail has the potential to harbor functional RSRR signals.

We next tested whether the spacing to the plasma membrane affects the functionality of the ER-retention/retrieval motif in $GABA_{B1}$. To that aim, we constructed three deletion mutants that gradually move the endogenous RSRR motif closer to the plasma membrane (Fig. 6). Deletion of nine amino acid residues has no effect on the functionality of the RSRR motif, whereas deletion of 30 or 52 amino acids increasingly boosts cell surface expression of $GABA_{B1}$. This gradual increase in surface expression clearly shows that the spacing to the plasma membrane is critical for RSRR function.

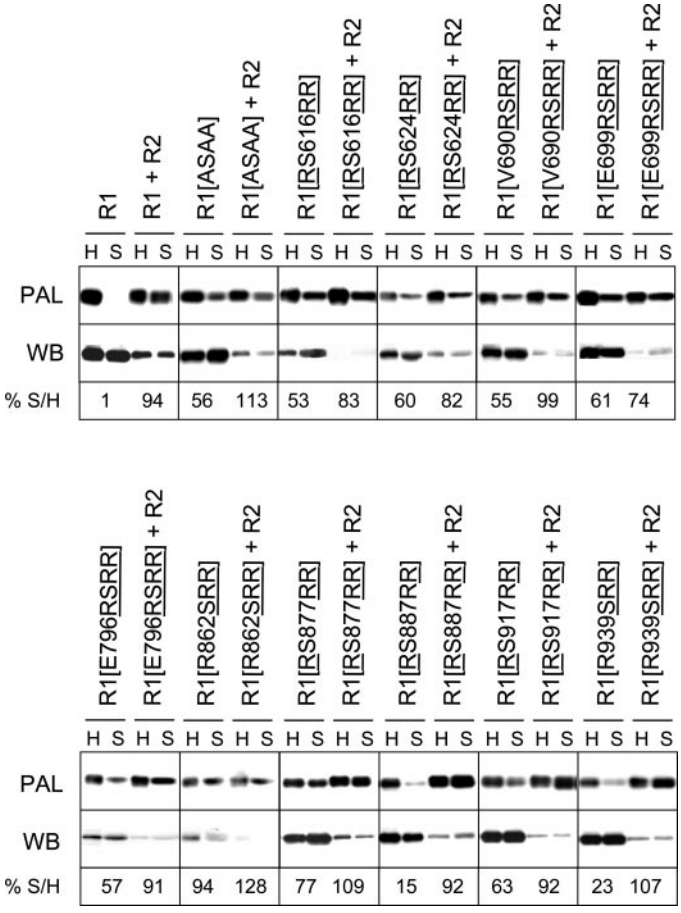

Fig. 2. Surface targeting of wild-type (R1) and mutant $GABA_{B1a}$ proteins expressed individually and in combination with $GABA_{B2}$ (R2). Cell Hs and intact S cells were photoaffinity-labeled with the membrane-impermeable $GABA_{B1}$-specific antagonist [^{125}I]CGP71872 and subjected to SDS-PAGE. To correct for the variability in transfection efficiency, the amount of protein sample subjected to gel electrophoresis was normalized to the respective amount of radioactivity incorporated into the cell Hs for each set of transfection (expression with and without $GABA_{B2}$). Labeled proteins were then visualized by autoradiography (photoaffinity labeling, PAL). Loading was controlled for by Western blot (WB) analysis with a polyclonal antibody raised against $GABA_{B1}$. It is evident that a larger fraction of immunolabeled $GABA_{B1}$ protein binds the photoaffinity ligand when $GABA_{B2}$ is coexpressed (lanes 1 and 2 verus 3 and 4). For each transfection, we compared photoaffinity-labeled $GABA_{B1}$ protein at the cell S to total $GABA_{B1}$ protein labeled in the cell Hs (% S/H). Insertion of an ectopic RSRR motif at positions S887 (R1[RS887RR]) and R939 (R1[R939SRR]) results in partial intracellular retention (lane 2 versus 1), which is overcome by coexpression with $GABA_{B2}$ (lane 4 versus 2). The % S/H values indicated represent the experiment shown in the figure. One-way analysis of variance followed by a pairwise comparison via Tukey's honestly significant difference test confirmed that the % S/H values (mean ± S.D.) for R1[RS887RR] (17.0 ± 10.1; $n = 3$) as well as R1[R939SRR] (26,7 ± 11.9; $n = 3$) differ significantly from the one for R1[ASAA] (57.8 ± 8.7; $n = 4$) ($p < 0.05$ in both cases).

Masking of Ectopic RSRR Signals in $GABA_{B1}$ Does Not Involve C-Terminal Coiled-Coil Domain Interaction. Two reports indicate that surface trafficking is not entirely dependent on coiled-coil domain interaction between the $GABA_{B1}$ and $GABA_{B2}$ subunits (Pagano et al., 2001; Grunewald et al., 2002). For example, $GABA_{B2}$ mutants lacking the C-terminal coiled-coil domain (R2ΔLZ2) are able to traffic $GABA_{B1}$ to the cell surface. We therefore investigated whether coiled-coil interaction is necessary for masking the functional ectopic RSRR motifs in R1[RS887RR] and R1[R939SRR] proteins by cotransfecting them with R2ΔLZ2 (Pagano et al., 2001). As shown in Fig. 7 and in agreement with previous reports, R2ΔLZ2 is able to traffic wild-type $GABA_{B1}$ (R1) to the cell surface, but to a smaller extent than wild-type $GABA_{B2}$ (R2). Both wild-type $GABA_{B2}$ and R2ΔLZ2 are able to traffic the R1[RS887RR] and R1[R939SRR] proteins with functional ectopic RSRR motifs to the cell surface. In addition R1[LRS917RR], which is efficiently retained in the absence of $GABA_{B2}$ (Fig. 5) is translocated to the cell surface by coexpression with R2ΔLZ2 (S/H ratio 69%; not shown). This indicates that coiled-coil domain interaction between the cytoplasmic tails of $GABA_{B1}$ and $GABA_{B2}$ is not crucial for masking the ectopic RSRR motifs in the mutant $GABA_{B1}$ subunits. Additional interaction sites between $GABA_{B1}$ and $GABA_{B2}$ obviously mediate heterodimerization and compensate for the lack of coiled-coil domain interaction, thereby presumably preventing the ectopic RSRR motifs from binding to protein(s) that localize it in the ER.

Discussion

The generic membrane trafficking signals RXR and KK are part of quality control mechanisms that prevent incorrectly folded and/or assembled membrane proteins from reaching the cell surface. Signals of the RXR-type are generally used to control assembly of multimeric protein complexes. It is assumed that the RXR motif is masked upon association with an appropriate partner subunit and consequently only correctly assembled complexes are able to exit the ER. In contrast to the carboxyl-terminal dilysine signal KK, which exhibits a strict spacing relative to the C terminus, RXR-type signals are found in a variety of sequence positions. In octameric K_{ATP} channels they are localized in the cytoplasmic

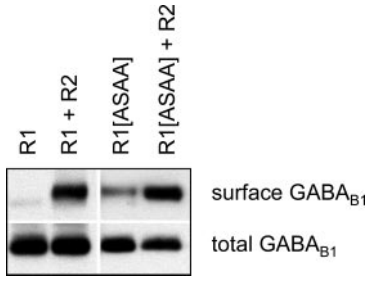

Fig. 3. Surface biotinylation of $GABA_{B1}$ (R1) and R1[ASAA] in the presence and absence of $GABA_{B2}$. The fraction of $GABA_{B1}$ protein at the cell surface is similar when measured with surface biotinylation or with the $GABA_{B1}$-specific antagonist [^{125}I]CGP71872 (Fig. 2), supporting that binding-incompetent $GABA_{B1}$ protein is not delivered to the cell surface.

tail of the pore forming α subunit (Kir6.1/2) as well as in a cytoplasmic loop of the regulatory β subunit SUR1 (Zerangue et al., 1999). In addition, the related ER-retention/retrieval motif RR was identified in the cytosolic N terminus of the myosin heavy chain class II invariant chain isoform lip33, a type II membrane protein (Schutze et al., 1994). In the experiments presented herein, we transposed the RSRR ER-retention/retrieval signal of $GABA_{B1}$ from its normal position adjacent of the coiled-coil domain to ectopic positions within the cytoplasmic tail or within the three intracellular loops. We show that the RSRR motif is not functional in any of the intracellular loops but that it is partially functional at two ectopic positions within the cytoplasmic tail (Fig. 2). A previous study suggested that the functionality of the RSRR motif of $GABA_{B1}$ depends on surrounding sequences (Grunewald et al., 2002). In particular, amino acid residues that are part of the coiled-coil domain and neighbor the RSRR motif N-terminally were proposed to be important for recognition of the RSRR motif. From these previous experiments, it was concluded that the minimal ER retention sequence in $GABA_{B1}$ is comprised of the amino acids QLQXRQQLRSRR, where X can be either S or D (Grunewald et al., 2002). Our data demonstrate that there is not a strict requirement for the RSRR motif to be in its normal sequence context to be functional, because the motif mediates retention when moved N-terminally of QLQXRQQLRSRR to position S887 (R1[RS887RR]) or C-terminally to position R939 (R1[R939SRR]) (Fig. 2). However, the R1[RS917RR] protein, harboring an RSRR motif positioned in between the motifs in R1[RS887RR] and R1[R939SRR], is not retained. This suggests that the sequence environment and/or the secondary structure of the area where the ectopic RSRR motif has been inserted are nevertheless of some influence. It was proposed that small changes in the local sequence context can alter the signal strength of arginine-based ER-retention motifs and that it is favorable when a hydrophobic amino acid, in particular leucine, precedes the arginine cluster (Zerangue et al., 2001). This sequence configuration is also observed for the ER-retention/retrieval signal in wild-type $GABA_{B1}$. R1[RS917RR] and the partly retained R1[RS887RR] and R1[R939SRR] proteins violate this rule. Insertion of a leucine preceding the RSRR rescues intracellular retention of R1[RS917RR] but does not increase retention of R1[RS887RR] and R1[RS939RR] (Fig. 5). This reinforces that the local sequence context can influence RSRR functionality and supports that the distal cytoplasmic tail is accessible for intracellular retention at various sites.

It is emerging that different types of ER-retention/retrieval motifs have characteristic operating ranges with respect to the distance to the plasma membrane. Whereas carboxyl-terminal KK motifs are operational proximal to the membrane, RXR-type motifs are most effective at a certain distance away from the intracellular plasma membrane (Shikano and Li, 2003). In our experiments the ectopic RSRR

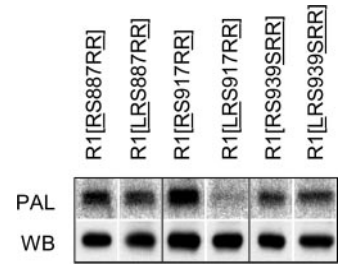

Fig. 5. Intracellular retention of $GABA_{B1}$ protein after insertion of a leucine residue preceding the ectopic RSRR motif at S917. After transfection with the indicated $GABA_{B1}$ expression constructs, intact HEK293 cells were photoaffinity-labeled with the membrane-impermeable $GABA_{B1}$-specific antagonist [^{125}I]CGP71872 and subjected to SDS-PAGE. Labeled proteins were then visualized by autoradiography (PAL). Loading was controlled for by Western blot analysis with a polyclonal antibody raised against $GABA_{B1}$ (WB). Upon insertion of a leucine preceding the ectopic RSRR at S917 (R1[LRS917RR]) no labeled protein is detected indicating that the expressed $GABA_{B1}$ protein fails to be transported to the cell surface. No increased retention is observed with R1[LRS887RR] and R1[LR939SRR] after insertion of a leucine residue.

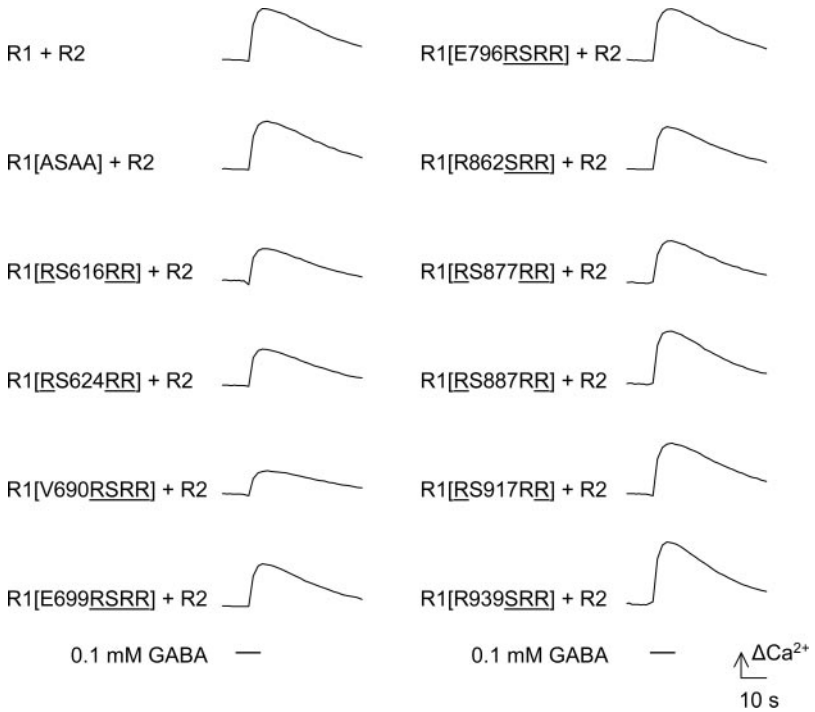

Fig. 4. Functional analysis in HEK293 cells of $GABA_B$ receptors with ectopic RSRR motifs in the $GABA_{B1}$ subunit. Artificial coupling of $GABA_B$ receptors to PLC upon coexpression with a chimeric Gα subunit, Gαqz$_{IC}$ (Franek et al., 1999) results in an intracellular Ca^{2+} transient that is measured by changes in fluo-4 acetoxymethyl ester fluorescence intensity. All $GABA_{B1}$ mutants can be activated by 0.1 mM GABA upon coexpression with $GABA_{B2}$, similarly to wild-type $GABA_{B1}$ (R1 + R2). Representative Ca^{2+} transients of 12 wells are shown. Bars below traces indicate application of GABA.

motifs in the intracellular loops may therefore be positioned too close to the plasma membrane to be in the active zone. It is also conceivable that the binding of a putative RSRR-interacting protein involved in ER retention depends on additional sequence elements within $GABA_{B1}$. Appropriate spacing between the RSRR motif and such additional sequence elements may be lost in $GABA_{B1}$ proteins with mutations in the intracellular loops. On the other hand, in certain ectopic positions the RSRR motif might be inaccessible because of simple steric hindrance. We show that C-terminal deletions that progressively move the wild-type RSRR motif closer to the membrane gradually reduce its signal strength, favoring that primarily the spacing to the plasma membrane is important for RSRR function (Fig. 6).

Functional ectopic RSRR signals in $GABA_{B1}$ are efficiently masked by the $GABA_{B2}$ subunit in the absence of coiled-coil dimerization (Fig. 7). This agrees with previous findings that coiled-coil interaction is not absolutely necessary for shielding (Pagano et al., 2001). The mechanism by which $GABA_{B2}$ prevents intracellular retention of $GABA_{B1}$ therefore remains unclear. The data presented herein suggest a model in which global conformational changes associated with heteromeric assembly remove the RSRR signal from the active zone, thereby restricting its access and triggering surface delivery of the complex. COPI and 14-3-3 are prime candidates for regulating aspects of $GABA_B$ receptor trafficking. COPI components can interact with arginine-based motifs and compete for binding with proteins of the 14-3-3 family (Yuan et al., 2003). It is thought that 14-3-3 binding overcomes ER-retention by preventing recycling of correctly assembled proteins from the ER-Golgi intermediate compartment to the ER via COP1 vesicles (O'Kelly et al., 2002; Nufer and Hauri, 2003). 14-3-3 proteins are known to associate with the C terminus of $GABA_{B1}$ through a domain partially overlapping with the coiled-coil domain (Couve et al., 2001). It is conceivable that COP1 components bind to RSRR when $GABA_{B1}$ in unassembled, which recycles $GABA_{B1}$ back to the ER. After heteromeric assembly and removal of the RSRR motif from its active zone, COP1 could then be replaced by 14-3-3, which avoids recycling and allows for surface trafficking.

In conclusion, our results support that the RSRR ER-retention/retrieval signal of $GABA_{B1}$ is only functional within the distal C-terminal tail. Moreover, coiled-coil interaction is not crucial for inactivation of wild-type (Pagano et al., 2001) and ectopic RSRR motifs. In the light of these data, we propose that removal of the RSRR motif from its active zone rather than direct coiled-coil shielding may trigger surface delivery of the receptor complex. On a broader scope, the data

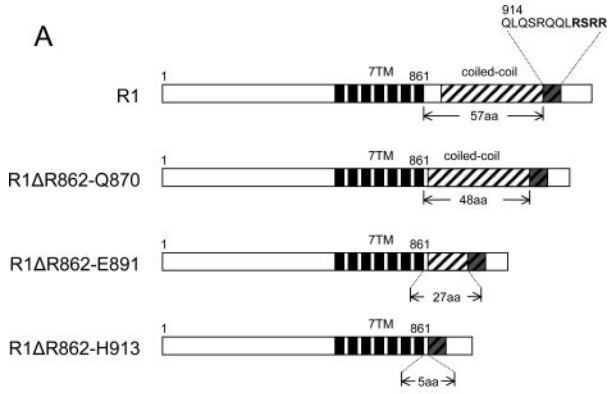

Fig. 6. The RSRR motif is gradually inactivated when positioned closer to the membrane. A, schematic diagram showing the coding regions of different $GABA_{B1}$ expression constructs with deletions of 9 amino acids (R1ΔR862-Q870), 30 amino acids (R1ΔR862-E891) or 52 amino acids (R1ΔR862-H913) between transmembrane domain 7 and the extended ER-retention/retrieval motif QLQSRQQLRSRR. The number of residues that separate the extended ER-retention/retrieval motif from the transmembrane domain is indicated below each construct. B, cell surface targeting of wild-type (R1), R1[ASAA] and deletion mutants in HEK293 cells in the absence of $GABA_{B2}$. Cell homogenates (H) and intact cells (S) were photoaffinity-labeled with the membrane-impermeable $GABA_{B1}$-specific antagonist [^{125}I]CGP71872 and subjected to SDS-PAGE. Labeled proteins were then visualized by autoradiography (PAL). Loading was controlled for by Western blot (WB) analysis with a polyclonal antibody raised against $GABA_{B1}$. For each transfection, photoaffinity-labeled $GABA_{B1}$ protein at the cell S was then compared with total $GABA_{B1}$ protein labeled in the cell Hs (% S/H). A deletion of nine amino acids (R1ΔR862-Q870) has no effect on the functionality of the endogenous ER-retention-retrieval motif. However, deletion of 30 amino acids (R1ΔR862–E891) and 52 amino acids (R1ΔR862–H913) gradually increases cell surface expression of $GABA_{B1}$.

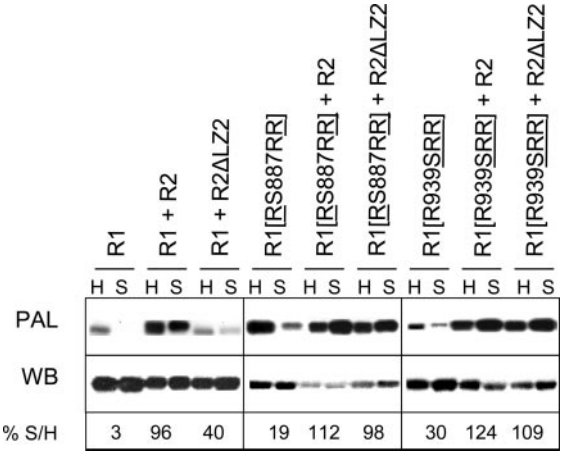

Fig. 7. Coiled-coil domain interaction is not necessary for masking functional ectopic RSRR motifs. Wild-type $GABA_{B1}$ (R1) and the $GABA_{B1}$ mutants with functional ectopic RSRR (constructs R1[RS887RR] and R1[R939SRR]) were expressed alone (lanes 1 and 2) or in combination with wild-type $GABA_{B2}$ (R2) (lanes 3 and 4) or a $GABA_{B2}$ mutant lacking the coiled-coil domain (R2ΔLZ2) (lanes 5 and 6). Cell Hs and intact S cells were photoaffinity-labeled with the membrane-impermeable $GABA_{B1}$-specific antagonist [^{125}I]CGP71872 and subjected to SDS-PAGE. Labeled proteins were then visualized by autoradiography (PAL). Loading was controlled for by Western blot (WB) analysis with a polyclonal antibody raised against $GABA_{B1}$. R2ΔLZ2 is able to traffic wild-type $GABA_{B1}$ to the cell surface, but to a smaller extent than wild-type $GABA_{B2}$ (left, for each transfection compare photoaffinity-labeled $GABA_{B1}$ protein at the cell S to total $GABA_{B1}$ protein labeled in the cell Hs). Both wild-type $GABA_{B2}$ and R2ΔLZ2 are able to traffic the $GABA_{B1}$ mutants R1[RS887RR] and R1[R939SRR] to the cell surface to the same extent (middle and right).

suggest that many proteins featuring the RXR consensus sequence in proximity of the membrane escape intracellular retention because the motif does not reach into its operational zone.

Acknowledgments

We thank Dr. A. Pagano for critical comments on the manuscript and advice for the biotinylation experiments and D. Ristig and C. Lampert for excellent technical assistance.

References

Bettler B, Kaupmann K, Mosbacher J, and Gassmann M (2004) Molecular structure and physiological functions of GABA(B) receptors. *Physiol Rev* **84:**835–867.

Bowery NG, Bettler B, Froestl W, Gallagher JP, Marshall F, Raiteri M, Bonner TI, and Enna SJ (2002) International Union of Pharmacology. XXXIII. Mammalian γ-aminobutyric $acid_B$ receptors: structure and function. *Pharmacol Rev* **54:**247–264.

Calver AR, Davies CH, and Pangalos MN (2002) $GABA_B$ receptors: from monogamy to promiscuity. *Neurosignals* **11:**299–314.

Couve A, Filippov AK, Connolly CN, Bettler B, Brown DA, and Moss SJ (1998) Intracellular retention of recombinant $GABA_B$ receptors. *J Biol Chem* **273:**26361–26367.

Couve A, Kittler JT, Uren JM, Calver AR, Pangalos MN, Walsh FS, and Moss SJ (2001) Association of $GABA_B$ receptors and members of the 14-3-3 family of signaling proteins. *Mol Cell Neurosci* **17:**317–328.

Franek M, Pagano A, Kaupmann K, Bettler B, Pin JP, and Blahos J (1999) The heteromeric $GABA_B$ receptor recognizes G-protein alpha subunit C-termini. *Neuropharmacology* **38:**1657–1666.

Galvez T, Duthey B, Kniazeff J, Blahos J, Rovelli G, Bettler B, Prezeau L, and Pin JP (2001) Allosteric interactions between GB1 and GB2 subunits are required for optimal $GABA_B$ receptor function. *EMBO (Eur Mol Biol Organ) J* **20:**2152–2159.

Gassmann M, Shaban H, Vigot R, Sansig G, Haller C, Barbieri S, Humeau Y, Schuler V, Muller M, Kinzel B, et al. (2004) Redistribution of GABAB(1) protein and atypical GABAB responses in GABAB(2)-deficient mice. *J Neurosci* **24:**6086–6097.

Grunewald S, Schupp BJ, Ikeda SR, Kuner R, Steigerwald F, Kornau HC, and Kohr G (2002) Importance of the gamma-aminobutyric acid(B) receptor C-termini for G-protein coupling. *Mol Pharmacol* **61:**1070–1080.

Havlickova M, Prezeau L, Duthey B, Bettler B, Pin JP, and Blahos J (2002) The intracellular loops of the GB2 subunit are crucial for G-protein coupling of the heteromeric γ-aminobutyrate B receptor. *Mol Pharmacol* **62:**343–350.

Horton RM, Cai ZL, Ho SN, and Pease LR (1990) Gene splicing by overlap extension: tailor-made genes using the polymerase chain reaction. *Biotechniques* **8:**528–535.

Jones KA, Borowsky B, Tamm JA, Craig DA, Durkin MM, Dai M, Yao WJ, Johnson M, Gunwaldsen C, Huang LY, et al. (1998) $GABA_B$ receptors function as a heteromeric assembly of the subunits $GABA_{B(R1)}$ and $GABA_{B(R2)}$. *Nature (Lond)* **396:**674–679.

Kaupmann K, Huggel K, Heid J, Flor PJ, Bischoff S, Mickel SJ, McMaster G, Angst C, Bittiger H, Froestl W, and Bettler B (1997) Expression cloning of $GABA_B$ receptors uncovers similarity to metabotropic glutamate receptors. *Nature (Lond)* **386:**239–246.

Kaupmann K, Malitschek B, Schuler V, Heid J, Froestl W, Beck P, Mosbacher J, Bischoff S, Kulik A, Shigemoto R, et al. (1998) $GABA_B$-receptor subtypes assemble into functional heteromeric complexes. *Nature (Lond)* **396:**683–687.

Kuner R, Kohr G, Grunewald S, Eisenhardt G, Bach A, and Kornau HC (1999) Role of heteromer formation in $GABA_B$ receptor function. *Science (Wash DC)* **283:**74–77.

Mah SJ, Cornell E, Mitchell NA, and Fleck MW (2005) Glutamate receptor trafficking: endoplasmic reticulum quality control involves ligand binding and receptor function. *J Neurosci* **25:**2215–2225.

Malitschek B, Rüegg D, Heid J, Kaupmann K, Bittiger H, Fröstl W, Bettler B, and Kuhn R (1998) Developmental changes in agonist affinity at $GABA_{B(1)}$ receptor variants in rat brain. *Mol Cell Neurosci* **12:**56–64.

Margeta-Mitrovic M, Jan YN, and Jan LY (2000) A trafficking checkpoint controls $GABA_B$ receptor heterodimerization. *Neuron* **27:**97–106.

Margeta-Mitrovic M, Jan YN, and Jan LY (2001) Function of GB1 and GB2 subunits in G protein coupling of $GABA_B$ receptors. *Proc Natl Acad Sci USA* **98:**14649–14654.

Marshall FH, Jones KA, Kaupmann K, and Bettler B (1999) $GABA_B$ receptors - the first 7TM heterodimers. *Trends Pharmacol Sci* **20:**396–399.

Ng GYK, Clark J, Coulombe N, Ethier N, Hebert TE, Sullivan R, Kargman S, Chateauneuf A, Tsukamoto N, McDonald T, et al. (1999) Identification of a $GABA_B$ receptor subunit, gb2, required for functional $GABA_B$ receptor activity. *J Biol Chem* **274:**7607–7610.

Nufer O and Hauri HP (2003) ER export: call 14-3-3. *Curr Biol* **13:**R391–R393.

O'Kelly I, Butler MH, Zilberberg N, and Goldstein SA (2002) Forward transport. 14–3-3 binding overcomes retention in endoplasmic reticulum by dibasic signals. *Cell* **111:**577–588.

Pagano A, Rovelli G, Mosbacher J, Lohmann T, Duthey B, Stauffer D, Ristig D, Schuler V, Meigel I, Lampert C, et al. (2001) C-Terminal interaction is essential for surface trafficking but not for heteromeric assembly of $GABA_B$ receptors. *J Neurosci* **21:**1189–1202.

Robbins MJ, Calver AR, Filippov AK, Hirst WD, Russell RB, Wood MD, Nasir S, Couve A, Brown DA, Moss SJ, et al. (2001) $GABA_{B(2)}$ is essential for G-protein coupling of the $GABA_B$ receptor heterodimer. *J Neurosci* **21:**8043–8052.

Schutze MP, Peterson PA, and Jackson MR (1994) An N-terminal double-arginine motif maintains type II membrane proteins in the endoplasmic reticulum. *EMBO (Eur Mol Biol Organ) J* **13:**1696–1705.

Scott DB, Blanpied TA, Swanson GT, Zhang C, and Ehlers MD (2001) An NMDA receptor ER retention signal regulated by phosphorylation and alternative splicing. *J Neurosci* **21:**3063–3072.

Shikano S and Li M (2003) Membrane receptor trafficking: evidence of proximal and distal zones conferred by two independent endoplasmic reticulum localization signals. *Proc Natl Acad Sci USA* **100:**5783–5788.

Valluru L, Xu J, Zhu Y, Yan S, Contractor A, and Swanson GT (2005) Ligand binding is a critical requirement for plasma membrane expression of heteromeric kainate receptors. *J Biol Chem* **280:**6085–6093.

White JH, Wise A, Main MJ, Green A, Fraser NJ, Disney GH, Barnes AA, Emson P, Foord SM, and Marshall FH (1998) Heterodimerization is required for the formation of a functional $GABA_B$ receptor. *Nature (Lond)* **396:**679–682.

Yuan H, Michelsen K, and Schwappach B (2003) 14-3-3 dimers probe the assembly status of multimeric membrane proteins. *Curr Biol* **13:**638–646.

Zerangue N, Malan MJ, Fried SR, Dazin PF, Jan YN, Jan LY, and Schwappach B (2001) Analysis of endoplasmic reticulum trafficking signals by combinatorial screening in mammalian cells. *Proc Natl Acad Sci USA* **98:**2431–2436.

Zerangue N, Schwappach B, Jan YN, and Jan LY (1999) A new ER trafficking signal regulates the subunit stoichiometry of plasma membrane K(ATP) channels. *Neuron* **22:**537–548.

Address correspondence to: Dr. Bernhard Bettler, Pharmazentrum, University of Basel, Klingelbergstr. 50-70, CH-4056 Basel, Switzerland. E-mail: bernhard.bettler@unibas.ch